

**Neuartige Anwendungen der Thermodesorptions/Pyrolyse-  
Gaschromatographie-Massenspektrometrie mit  
Elektronenstoßionisation und resonanzverstärkter  
Multiphotonenionisation zur Charakterisierung von Rohölen und  
der im Meerwasser gelösten organischen Kohlenstofffraktionen**

**Kumulative Dissertation**

zur Erlangung des akademischen Grades eines  
doctor rerum naturalium (Dr. rer. nat.)  
der Mathematisch-Naturwissenschaftlichen Fakultät  
der Universität Rostock

vorgelegt von

**Stefan Otto**

aus Rostock

geboren am 22. Februar 1983 in Kühlungsborn

Rostock, 2016

Die vorliegende Arbeit entstand in der Zeit von Oktober 2009 bis April 2016 in der Arbeitsgruppe Analytische Chemie des Instituts für Chemie an der Universität Rostock im gemeinsamen Massenspektrometrie-Zentrum der Universität Rostock und des Helmholtz Zentrums München.

**Gutachter:**

1. Gutachter: Prof. Dr. Ralf Zimmermann

Institut für Chemie, Abteilung Technische und Analytische Chemie,  
Universität Rostock

2. Gutachter: Prof. Dr. Gesine Witt

Fakultät Life Sciences, Abteilung Umwettechnik, Hochschule für  
Angewandte Wissenschaften Hamburg

**Datum der Einreichung:** 08. April 2016

**Datum der Verteidigung:** 12. Juli 2016



## Danksagung

Wir sehen es mit viel Verdruss,  
was alles man erleben muss;  
und doch ist jeder darauf scharf,  
dass er noch viel erleben darf.  
Wir alle steigen ziemlich heiter  
empor auf unsrer Lebensleiter:  
Das Gute, das wir gern genossen,  
das sind der Leiter feste Sprossen.  
Das Schlechte – wir bemerken's kaum –  
ist nichts als leerer Zwischenraum.  
(Eugen Roth)

Zunächst gilt mein Dank Prof. Dr. Ralf Zimmermann für die Aufnahme in die Arbeitsgruppe und freundliche Betreuung während der gesamten Promotionszeit. Ich danke zudem Dr. Thorsten Streibel und Dr. Martin Sklorz, die mir immer mit Rat und Tat zur Seite standen.

Weiterhin gilt mein Dank allen aktiven und ehemaligen Mitarbeitern der Arbeitsgruppe, namentlich hervorgehoben Sabrina, Theo, Sven, Jana, Alois, Sophie und Christian.

Dr. Sabine Haack und Frau Petra Sattler danke ich für die Unterstützung bei der Lehrtätigkeit am Institut, die für mich eine willkommende Abwechslung neben der Forschungsarbeit darstellte.

Darüber hinaus bedanke ich mich herzlich bei allen, die mich bei der Anfertigung der Arbeit direkt oder indirekt unterstützt haben. Insbesondere meinen Freunden innigen Dank für die alltägliche Unterstützung und Hilfe während der gesamten Promotionszeit.

Über alles steht natürlich meine Familie. Durch ihre moralische Unterstützung und hilfreichen Ermunterungen konnten sie viel Last von meinen Schultern nehmen.

Herzlichen Dank.

## **Erklärung**

Hiermit versichere ich, dass ich die vorliegende Arbeit selbstständig angefertigt und ohne fremde Hilfe verfasst habe, keine außer den von mir angegebenen Hilfsmitteln und Quellen dazu verwendet habe und die den benutzten Werken inhaltlich und wörtlich entnommenen Stellen als solche kenntlich gemacht habe.

Stefan Otto

Rostock, 08. April 2016

# Inhaltsverzeichnis

1. Einleitung	6
2. Komplexe Umweltproben und Grenzen der Analytik	8
3. Schweröl	10
3.1. Zusammensetzung	10
3.2. Polyzyklische aromatische Kohlenwasserstoffe (PAK) und polyzyklische aromatische schwefelhaltige Heterozyklen (PASH) im Rohöl	12
4. Charakterisierung der gelösten organischen Kohlenstofffraktion im Meerwasser	14
4.1. Das Forschungsobjekt Ostsee	14
4.2. Expedition mit dem Forschungsschiff „FS Meteor“	15
4.3. Gelöster organischer Kohlenstoff (DOM) - Terrigenes DOM und Lignin als Markersubstanz	16
4.4. PAK-Komponenten im marinen System	18
5. Harte und weiche Ionisierung in der Massenspektrometrie	20
6. Pyrolysetechnik und MS-Kopplung	22
7. Ergebnisse und Diskussion	26
7.1. Methodenentwicklung und Anwendung bei Rohölen (Publ. 1)	26
7.2. Charakterisierung und Abbau von terrigenen DOM (Publ. 2)	32
7.3. PAK-Komponenten im marinen System (Publ. 3)	36
8. Zusammenfassung und Aussichten	39
9. Literatur	41
10. Anhang	50
I. Abbildungsverzeichnis	50
II. Abkürzungsverzeichnis	52
III. Liste an Publikationen für den Dokortitel	54
IV. Publikationen	55
Publikation 1	55
Publikation 2	66
Publikation 3	79
V. Wissenschaftlicher Lebenslauf	88

# 1. Einleitung

Hochmolekulare und komplexe Proben, wie sie häufig in der Umwelt vorkommen, bestehen aus einer Vielzahl chemischer Spezies. Deren Erfassung, Identifizierung und Quantifizierung ist oft diffizil, was ein hohes Maß an effizienter Separationstechnik sowie selektiver bzw. sensitiver Detektionsmechanismen voraus setzt. Die Herausforderung besteht darin, leistungsfähige analytische Systeme zu entwickeln, diese zu kombinieren und existierende Methoden effektiver zu gestalten, um insbesondere niedrig konzentrierte Komponenten zu erfassen.

Sowohl Rohöl als auch gelöstes, organisches Material (dissolved organic matter = DOM) zählen zu den komplexesten Probenmatrices (Panda, 2009), deren Aufarbeitung, Anreicherung und Untersuchung sehr hohe Ansprüche an den analytischen Prozess stellen. Die Erfassung spezieller, aus Rohöl generierter, polyzyklischer aromatischer Kohlenwasserstoffe (PAK) dient u.a. dazu, den Verschmutzungsgrad eines Umweltkompartiments und das damit verbundene Gesundheitsrisiko für den Menschen zu beurteilen (Ruczynska, 2011), mögliche Kontaminationswege zu benennen (Tam, 2001; Yunker, 2002) oder deren Abbau in der Umwelt zu verfolgen. (Reunamo, 2013; Thiele-Bruhn, 2005)

Die niederen Molekülfraktionen beider genannten Substanzklassen sind weitestgehend erforscht. Im Gegensatz dazu ist das Wissen zur hochmolekularen Zusammensetzung, auch aufgrund bereits genannter analytischer An- und Herausforderungen noch gering. Laut Mullins et al. (2012) steigen im Schweröl die Anteile insbesondere an hochmolekularen aromatischen Verbindungen, aber auch an schwefelhaltigen Verbindungen wie polyzyklischer, aromatischer, Heterozyklen (PASH), an. Das kann zu Problemen im Raffinerieprozess, bei der Entschwefelung und der Lagerung führen.

PAK und PASH sind sich in den Eigenschaften sehr ähnlich und können die gleiche nominale Masse besitzen. (Nocun, 2012) Daher sind sowohl ein hohes Maß an Massenauflösung und Selektivität zur Analyse als auch zur Unterscheidung dieser Komponenten unerlässlich.

Nicht weniger herausfordernd ist die chemische Charakterisierung von DOM. Vor allem terrigenes gelöstes organisches Material (tDOM) wird infolge der Klimaerwärmung vermehrt in das marine System eingebracht. (Bianchi, 2011) Dessen strukturelle Aufklärung und

Alterung während des fluvialen Transportes in die Ozeane rückt zunehmend in den Fokus der aktuellen Forschung. (Nebbioso, 2013) Ein möglicher abiotischer (Dittmar, 2003; Opsahl and Benner, 1998; Rocker, 2012b; Rosenstock, 2005; Wikner, 1999) und mikrobieller (Herlemann, 2014; Kisand, 2013, 2008) Abbau lässt sich feststellen, jedoch sind die bisherigen Ergebnisse nicht einheitlich. Die Folgen, die sich aus dem vermehrt eingetragenen tDOM für die Umwelt ergeben, sind bis dato nicht abzuschätzen und erfordern weiterführende Forschung. Die Anwendung und Kopplung selektiver, hochauflösender Analysemethoden könnte einen entscheidenden Beitrag dazu leisten.

Die Pyrolysetechnik (Py) in Verbindung mit der Gaschromatographie (GC) ermöglicht die Untersuchung und Trennung von hochmolekularen Bestandteilen anhand ihrer thermischen Abbauprodukte. Die Detektion muss zum Einen universell sein, um das breite Substanzspektrum der jeweiligen Probe zu erfassen und qualitativ abzubilden. Zum Anderen sollte eine hochselektive und sensitive Erfassung von aromatischen Strukturen ermöglicht werden. Beide Voraussetzungen werden durch den Einsatz eines Elektronenstoß-Quadrupol-Massenspektrometers (EI-QMS) und der Resonanzverstärkten-Multiphotonionisation-Flugzeit-Massenspektrometrie (REMPI-ToFMS), bei gleichzeitiger Anbindung an das Py/GC-System, erfüllt. Dadurch eröffnen sich neue Möglichkeiten für die chemische Charakterisierung komplexer und hochmolekularer Proben. (Otto, 2015a, 2015b, 2016)

## 2. Komplexe Umweltproben und Grenzen der Analytik

Mit den stetig steigenden Anforderungen im Hinblick auf die chemisch-strukturelle Charakterisierung von komplexen Umweltproben geht eine rasante Weiterentwicklung der instrumentellen Analytik einher. Die bestehenden Analysemethoden werden zunehmend verfeinert, neue Systeme und Methoden entwickelt sowie moderne Gerätetechniken miteinander kombiniert, um innerhalb kürzester Zeit spezifische Informationen über die Zusammensetzung einer Probe zu generieren. Dabei müssen Probennahme, -vorbereitung und Analytik gezielt aufeinander abgestimmt werden.

Ein besonderes Augenmerk ist auf die Probenvorbereitung zu richten, die bei unzureichender Anpassung an die Zielsubstanzen und / oder Analysenmethode zu nennenswerten Fehlerquoten bei der Interpretation der erhaltenen Messwerte führen kann. Bei der hier durchgeführten Untersuchung von DOM muss die Probe in einem mehrstufigen Verfahren vorbereitet, angereichert und aufgeschlossen werden (Dittmar, 2008), um es gaschromatographisch bzw. massenspektrometrisch vermessen zu können. Ein Aufschluss hochmolekularer Bestandteile gelingt u.a. durch die Pyrolysetechnik, die speziell bei der DOM-Analytik das zeitlich aufwendige nass-chemische Verfahren des basischen Kupferoxidaufschlusses erfolgreich (Hedges and Ertel, 1982; Hernes and Benner, 2006; Miltner and Emeis, 2001) ersetzen könnte. Das freigesetzte Spektrum an Pyrolyseprodukten gilt es durch nachgeschaltete, hochauflösende analytische Systeme zu erfassen. Dazu sind die klassische Gaschromatographie und Massenspektrometrie einzeln betrachtet kaum noch in der Lage, da hohe Ansprüche an die Selektivität und Sensitivität bestehen, um ein möglichst breites Substanzspektrum, meist niedrig konzentrierter Stoffe, zu ermitteln. Eine Übersicht über klassische, bestehende Methoden gibt Herod et al. (2007).

Durch die Kopplung analytischer Methoden sollen somit möglichst viele Informationen in einem Messzyklus aufgenommen werden. Dabei wird auf spezielle Methoden der hochauflösenden Massenspektrometrie (MS) in Verbindung mit selektiven Photoionisationstechniken (PI) zurückgegriffen, die durchaus ohne chromatographischen Separationsschritt auskommen. Diese können, in Verbindung mit der MS, direkt mit einem Pyrolyseofen als Injektorsystem gekoppelt werden. (Adam, 2012; Fendt, 2011; Geissler, 2009a, 2009b) Auch die etablierte Methodik der Ionen-Zyklotron-Resonanz-Massenspektrometrie (Fourier transform ion cyclotron resonance mass spectrometry = FT-ICRMS), die sich durch eine sehr hohe Auflösung auszeichnet, kommt ohne

chromatographischen Zwischenschritt aus und wird meistens mit dem Elektronenstoß oder der Elektronensprayionisation kombiniert. (Panda, 2009; Miyabayashi, 2009; Smith, 2009; Teravainen, 2007)

Speziell in Verbindung mit der Pyrolysetechnik kann auf eine chromatographische Trennung oft nicht verzichtet werden, insbesondere dann, wenn MS Techniken mit geringer Selektivität und/oder Auflösung verwendet werden. Hierfür kann neben der eindimensionalen auf die multidimensionale GC (GCxGC) zurückgegriffen werden, die eine deutlich höhere Auflösung ermöglicht. (Edam, 2005; Hao, 2005) In Verbindung mit dem Flugzeit-MS als massenselektive Detektionseinheit konnten bereits Rohöle und ölähnliche Proben erfolgreich analysiert werden. (Eschner, 2010; Welthagen, 2007)

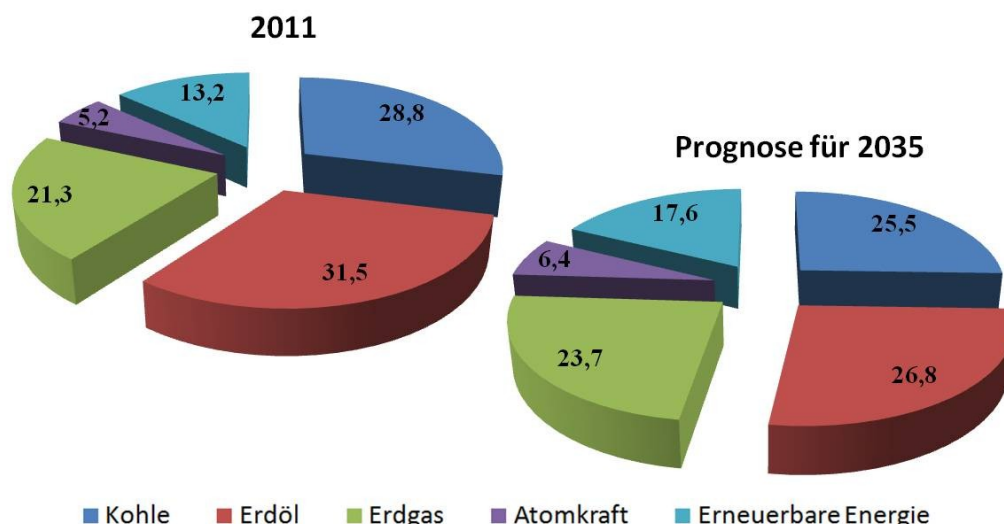
Das hier entwickelte System zeichnet sich durch die pyrolytische Zersetzung von hochmolekularen Strukturen, hohe Trennkapazitäten mittels Gaschromatographie (GC) sowie durch eine sowohl universelle, selektive und sensitive Detektion innerhalb eines Messzyklus aus. Letzteres wird durch die gleichzeitige Anbindung der Elektronenstoßionisation in Verbindung mit der Quadrupolmassenspektrometrie (EI-QMS), sowie der (1+1)-Resonanzverstärkten-Multiphotonenionisation in Kombination mit einem Flugzeitmassenspektrometer (REMPI-ToFMS), gewährleistet. Durch REMPI werden aromatische Verbindungen zugänglich, die oft niedrig konzentriert vorliegen. Zugleich sind durch die EI-QMS-Analyse mittels Datenbankabgleich Strukturvorschläge zugänglich und somit die Unterscheidung einzelner Komponenten und Isomere möglich. Das wäre durch eine direkte Kopplung zwischen Pyrolysator und MS kaum möglich.

Zusammenfassend kann das vorliegende System einen entscheidenden Beitrag zur Strukturaufklärung komplexer Umweltproben leisten. Insbesondere durch die Pyrolysetechnik werden hochmolekulare Bestandteile in separierbare und detektierbare Fragmente zerlegt, ohne zeitlich aufwendige nass-chemische Aufschlusstechniken anwenden zu müssen.

### 3. Schweröl

Die Verbrennung von fossilen Brennstoffen wie Kohle, Erdöl und Erdgas treibt den Klimawandel voran. Trotzdem werden in Zukunft voraussichtlich weiterhin drei Viertel des Energiebedarfes damit abgedeckt werden (Abb. 1). Mit rund 32 % Primärverbrauch ist Erdöl heutzutage der wichtigste Energieträger weltweit. Allerdings sind ca. 44 % der seit Beginn der industriellen Förderung bekannten Erdölreserven bereits verbraucht. (Energiestudie 2012) Nicht zuletzt deshalb wird die Gewinnung aus immer schwerer zugänglichen Lagerstätten zunehmend attraktiver und erfordert zugleich eine fortschreitende Technik der Förderung und Aufarbeitung. Dabei werden auch potentiell nicht-konventionelle Rohöle mit höher siedenden Fraktionen erschlossen und genutzt. Diese sind in ihrer Zusammensetzung komplexer und unterscheiden sich dadurch vom traditionellen Rohöl. (Panda, 2008, 2009; Teravainen 2007)

**Verteilung (in %) des Primärenergiebedarfs in den Jahren 2011 und 2035**



*Abbildung 1: Verteilung (in %) des Primärenergiebedarfs in den Jahren 2011 und 2035 gemäß des Ausblicks der ICA (International Energy Agency) 2011.*

#### 3.1. Zusammensetzung

Die Rohöle verschiedener Lagerstätten zeigen keine einheitliche Zusammensetzung. Es sind komplexe Mischungen, in denen der Anteil an Kohlenwasserstoffen überwiegt. Die Ausbeute an Komponententypen variiert deutlich, dennoch existiert eine enge Spanne im Elementgehalt (Abb. 2).



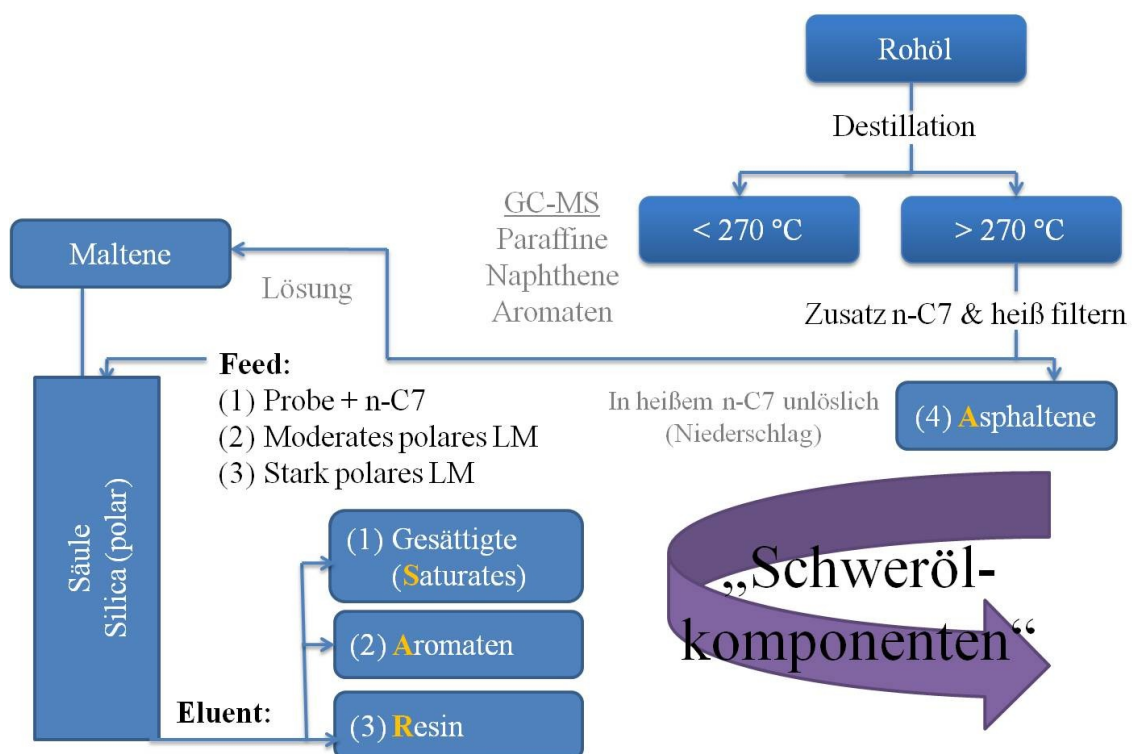
**Elementare Zusammensetzung:**

Kohlenstoff	83 – 87 %
Wasserstoff	10 – 14 %
Stickstoff	0,1 – 2 %
Sauerstoff	0,05 – 1,5 %
Schwefel	0,05 – 6 %
Metalle	< 1000 ppm

*Abbildung 2: Elementare Zusammensetzung von konventionellem Rohöl (Enhanced Oil Recovery I)*

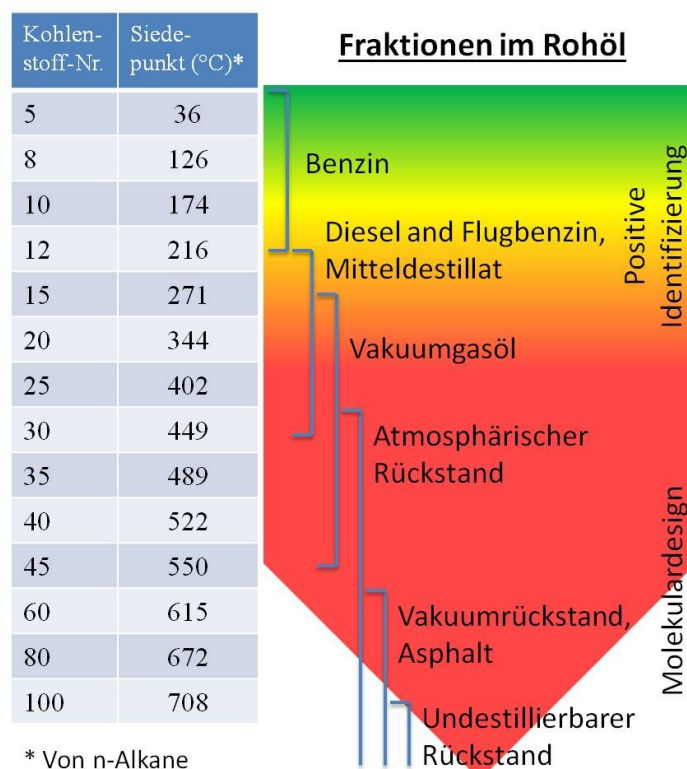
Die strukturelle Vielfalt im Rohöl ist groß und steigt zu höher siedenden Fraktionen extrem an. Die SARA-Trennung ermöglicht die Unterscheidung zwischen gesättigten (**saturated**) Verbindungen, Aromaten (**aromatics**), Harzen (**resins**) und Asphaltenen (**asphaltenes**), wie es vereinfacht die Abb. 3 zeigt. (Fan, 2002)

Die Trennung der vier chemischen Klassen basiert auf Löslichkeitseffekten und Polaritäten. Eine Separation nach Siedepunkten zeigt vereinfacht die Abb. 4. Die Struktur hochmolekularer Fraktionen, speziell der der Asphaltene, ist weitestgehend ungeklärt. Die Asphaltene sollen einen aromatischen Grundkörper besitzen, an dem sich Alkylketten befinden und azyklische Systeme mit Heteroatomen integriert sind. (Groenzin, 2000)



*Abbildung 3: Trennung von Komponenten im Rohöl*

**Abbildung 4:** Fraktionen im Rohöl  
(Abb. Entwickelt nach K. H. Altgelt & M. M. Boduszynski, *Composition and analysis of heavy petroleum fractions*, New York, 1994, Chapter 2: *Compositional Analysis*)

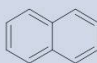


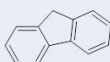
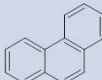



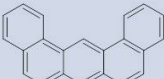



### 3.2. PAK und PASH im Rohöl

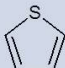
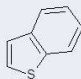
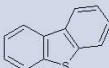
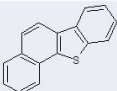
Innerhalb des großen Spektrums an Inhaltsstoffen gelten besonders die PAK als Umweltschadstoffe, da sie eine Gefährdung für die menschliche Gesundheit darstellen (Brody, 2007; Kim, 2013). In alkylierter und unalkylierter Form sind sie persistent und annähernd resistent gegen biologische Alterungsprozesse. Das gilt vor allem für hochmolekulare Komponenten. (Gagni, 2007; Thiele-Bruhn, 2005) Nach Mullins et al. (2007) steigt im schweren Rohöl sowohl der Anteil an hochmolekularen und aromatischen Verbindungen enorm, als auch der Anteil an schwefelhaltigen Komponenten an. Das führt im Vergleich zum konventionellen Rohöl zu Problemen im Raffinerie- bzw. Entschwefelungsprozess und der nachfolgenden Lagerung.

Die PAK und PASH sind im strukturellen Aufbau analog und zeigen demzufolge ähnliche Eigenschaften. Einige Vertreter besitzen sogar die gleichen nominalen Massen, wie z.B. das Dibenzothiophen (DBT) und das vierfach alkylierte Naphthalin (NAP) mit  $m/z$  184. (Nocun, 2012) Das stellt die Analytik vor großen Herausforderungen hinsichtlich der Auflösung und Selektivität, um diese Vertreter getrennt voneinander zu erfassen (Andersson, 2006; Panda, 2008; Stader, 2013). Die für diese Arbeit relevanten Grundkörper der PAK und PASH sind in der Abb. 5 zusammengestellt.

**PAK Vertreter**

Elutions- reihenfolge*	Substanz	Struktur	Nominale Masse
1	NAP		128
2	ACY		152
3	ACE		154
4	FLO		166
5	PHE		178
6	PYR		202
7	BaANT		228
8	BaPYR		252
9	DBaHANT		278
10	BghiPER		276

**PASH Vertreter**

Elutions- reihenfolge*	Substanz	Struktur	Nominale Masse
1	Thiophen		84
2	BT		134
3	DBT		184
4	BNT		234

**Abbildung 5:** PAK- und PASH-Strukturen (\* Elutionsreihenfolge beim verwendeten unpolaren Säulentyp „SGB-BPX5“)

## 4. Charakterisierung der gelösten organischen

### Kohlenstofffraktion im Meerwasser

Die Verbrennung fossiler Rohstoffe führt neben der Emission von PAK auch zur vermehrten Freisetzung klimarelevanter Gase wie z.B. Kohlenstoffdioxid, die zur globalen Klimaveränderung beitragen. Insbesondere in den arktischen Zonen kommt es durch den Effekt der globalen Erwärmung zu einer gesteigerten Mobilisierung von organischem Material (Zuidhoff, 2000), wobei zu berücksichtigen ist, dass in den Permafrostböden von Tundra und Taiga bis zu 60 % des weltweiten gebundenen organischen Kohlenstoffs lagern. (Dixon, 1994; Tamocai, 2009) Die Flusssysteme der arktischen Breiten führen nicht zuletzt deshalb die größten Mengen an organischem Material mit sich. (Dittmar, 2003) Zudem kommt es zur Zunahme von Verwitterungsprozessen und einem vermehrten Eintrag an Spurenelementen in die Rand- und Küstenmeere. (Humborg, 2004) Das Zusammenspiel von zunehmenden Flusslasten und sich verändernder temperatursensibler Prozesse wie z.B. der mikrobiellen Aktivität wird zu einer Veränderung der Produktions-Abbau-Gleichgewichte führen und den Kohlenstoffkreislauf in den Randmeeren zusätzlich beeinflussen. So führt eine steigende mikrobielle Aktivität zur vermehrten Produktion von Kohlenstoffdioxid, welches wiederum den Treibhauseffekt verstärkt. Zudem fehlen Studien zur Interaktion von Mikroorganismen mit dem terrigenen, eingetragenen Material und zum Einfluss von abiotischen Faktoren auf die mikrobielle Degradation. Zur Klärung dieser Zusammenhänge wurde das interdisziplinäre Forschungsprojekt „ATKiM“ (Abbaubarkeit von Arktischem Terrigenem Kohlenstoff im Meer) initiiert.

#### 4.1. Das Forschungsobjekt Ostsee

Die nördlichen Becken der Ostsee stellen ein ideales Modellsystem dar, um Vorhersagen über die zu erwartenden Klimaszenarien und insbesondere deren Einfluss auf das marine System der Ozeane abzuleiten. Durch die Beckenstruktur ergeben sich lange Wasserresidenzzeiten und ein stufenweiser Übergang zu marinen Lebensräumen. Neben der Änderung abiotischer Faktoren, d.h. von physikalisch-chemischen Bedingungen wie Temperatur oder Salzgehalt zeigen sich auch Änderungen biotischer Parameter, z.B. in der mikrobiellen Gemeinschaftstruktur. (Herlemann, 2011) Zudem dürfte der Salzgehalt, der in der Ostsee als deutlicher Gradient ausgebildet ist, erheblichen Einfluss auf die Abbaubarkeit des DOM haben. (Sholkovitz, 1976)

Das in der Ostsee über Flusssysteme eingetragene terrigene gelöste organische Material (tDOM) soll strukturell analysiert und in Abhängigkeit des Salzgradienten halbquantitativ verfolgt werden. Neben diesem abiotischen Aspekt, wird das Potential der mikrobiellen Gemeinschaften zum Abbau des DOM in den Untersuchungen herangezogen. In dieser Arbeit stehen aber die eingehende Charakterisierung des organischen Materials und die Verfolgung der Veränderung der chemischen Struktur bzw. Zusammensetzung während des mikrobiellen Abbaus im Vordergrund.

## 4.2. Expedition mit dem Forschungsschiff „Meteor“

Ziel der vom 29.05. bis 10.06.2012 durchgeführten Expedition war es, die mikrobielle Abbaubarkeit des gelösten organischen Materials in der Ostsee zu untersuchen und dessen veränderte Zusammensetzung entlang des Salzgradienten zu beurteilen. Die Abb. 6 und 7 zeigen das Forschungsschiff Meteor sowie die relevanten, beprobten Stationen.



Abbildung 6: Meteor (Foto privat)



Abbildung 7: Stationsplan der Expedition

Auf der Expedition 87/3a wurde Oberflächenwasser entlang des Salzgradienten, von S1 bis At4, beprobt. Nähere Details sind in der Abb. 8 vermerkt. Das Wasser vom nordschwedischen Fluss „Kalix“ wurde im Mai 2011 entnommen (steril gefiltert, bei - 20 °C gelagert). Es stellt den Ausgangspool an tDOM dar und wurde für die später durchgeführten Inkubationsansätze benötigt. (Herlemann, 2014)



Station	Tag	GPS-Position		Tiefe [m]	T [°C]	S [PSU]
S1	2012-05-30	57 00.0995N	006 55.1060E	2.85	11.61	32.06
At1	2012-06-01	58 07.9991N	010 00.0005E	1.70	12.16	30.38
Mo5	2012-05-31	54 42.0068N	010 56.0121E	1.59	12.88	11.68
S6	2012-06-01	55 33.9834N	016 22.0539E	2.70	9.83	7.47
At3	2012-06-02	57 18.3467N	020 04.6968E	3.75	9.07	7.19
S8	2012-06-04	59 21.4864N	020 06.0728E	1.35	6.93	6.31
S10	2012-06-06	61 46.9808N	19 17.6021E	2.33	5.77	5.47
At4	2012-06-05	65 26.7066N	023 17.9074E	1.79	4.32	2.66

*Abbildung 8: Details zu den Probestandorten*

### 4.3. Gelöster organischer Kohlenstoff (DOM) – Terrigenes DOM und Lignin als Markersubstanz

Die Ostsee als Forschungsobjekt eignet sich hervorragend, um eine Verbindung zwischen Frischwasserbedingungen (nördliche Ostsee) und marinen Verhältnissen (südwestliche Ostsee) herzustellen. Die Ostsee ist über Skagerrak und Kattegat mit der Nordsee verbunden. Aus diesen hydrographischen Bedingungen resultiert ein ausgeprägter Salzgradient von 2 (Bottenwiek mit geringem Salzgehalt) bis 25-32 (hoher Salzgehalt) in der südwestlichen Ostsee. (Miltner, 2001). Über v.a. die skandinavischen Flusssysteme kommt es zum Eintrag von organischem Material. Definitionsgemäß kann zwischen partikulären (POM) und gelöstem, organischen (DOM) Material unterschieden werden. Letzteres passiert einen 0,45 µm Filter, wohingegen das POM zurückgehalten wird. Beim DOM ist wiederum eine Unterleilung in marin gebildete oder durch Frischwasser zugeführte (terrigenes) Komponenten möglich. Eine klare Trennung zwischen marinen und terrestrischen Komponenten gelingt allerdings nicht. Das marine, gelöste, organische Material ist durch kleinere Substanzen und größere Biomoleküle gekennzeichnet. Es handelt sich um biochemische Produkte der Lebensformen im Meer. Komponenten im Frischwasser-DOM hingegen haben ihren Ursprung im terrigenen, organischen Material und leiten sich zumeist von pflanzlichen Produkten ab. Dazu gehören Lipide, Zucker, Terpendervative und Ligninkomponenten.

Das organische Material, dass durch Flüsse eingebracht wird, ist größtenteils terrigenen Ursprungs. (Dittmar, 2003) Das tDOM ist sowohl ubiquitär als auch eine dynamische Komponente mit charakteristischer, chemischer Signatur für eine bestimmte Region. (Ertel,

1984) Der Eintrag an terrigenem Material durch Frischwasser ist zwar hoch (Rocker, 2012b; Sleighter, 2008), allerdings lassen sich nur kleine Anteile von 0,7-2,4 % des theoretischen Gesamteintrags von terrigenen Tracern in den Ozeanen detektieren. (Opsahl, 1997)

Lignin ist ein zuverlässiger Marker für terrigenes, organisches Material und wird durch vaskuläre Pflanzen gebildet. (Ertel, 1984; Miltner, 2001; Nebbioso, 2013) Der klassische basische Kupfer(II)-Oxidaufschluss produziert in erster Linie phenolische Monomere, die in strukturelle Gruppen (siehe Abb. 9) unterteilt werden können: p-Hydroxybenzene (H-Bausteine), Syringyl- (S-Bausteine), Vanillin- und Cinnamylphenole. (Hedges, 1982) Zur Vereinfachung, werden die Beiden letztgenannten zur Gruppe der V-Bausteine zusammengefasst. Die drei daraus resultierenden phenolischen Klassen unterscheiden sich in der Anzahl der Methoxygruppen in Nachbarstellung zur Hydroxylgruppe und tragen einen individuellen Rest. Das S/V-Verhältnis wird oft genutzt, um zwischen Angiospermen (blühende Gefäßpflanzen) und Gymnospermen (nichtblühende Gefäßpflanzen) zu unterscheiden und somit eine Aussage über den Eintragungsort zu treffen. (Hedges, 1982; Miltner, 2001) H-Bausteine sind oft Bestandteil von Gräsern. (Kisand, 2013) Allerdings können diese Bausteine auch einen marinen Ursprung besitzen (Goni, 1995) und sind daher als tDOM-Tracer ungeeignet.

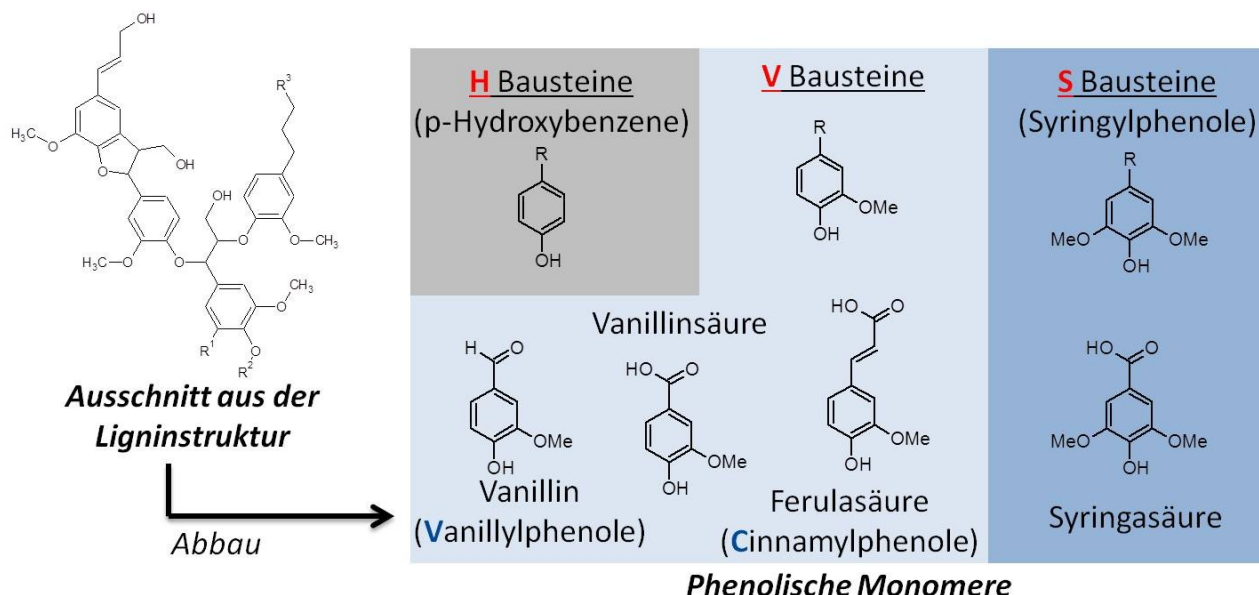


Abbildung 9: Lignin und phenolische Abbauprodukte

Die mit der steigenden Salinität verbundene Ausfällung hochmolekularer DOM-Spezies sowie die Adsorption an Partikeln (Sholkovitz, 1976), deren photochemische Transformation (Dittmar, 2007; Opsahl, 1998; Rosenstock, 2005) und der mikrobielle Abbau (Wikner, 1999), sind wichtige Mechanismen, um deren Anteil auf dem Weg von der Flussmündung in die Ozeane zu verringern. In Abhängigkeit von den vorherrschenden Umweltbedingungen wurden mikrobiell bedingte Abbauraten zwischen 6-70 % beobachtet. (Benner, 2011; Bianchi, 2011; Fellman, 2010; Rocker, 2012a) Oft stehen dabei die abiotischen und biotischen Faktoren im unmittelbaren Zusammenhang und beeinflussen sich gegenseitig. (Rosenstock, 2005; Shiah, 1994)

#### 4.4. PAK-Komponenten im marinen System

PAK-Vertreter können assoziiert mit dem DOM vorliegen und werden vorwiegend anthropogen in das marine System eingebracht. (Schwarzenbach, 2003) Die Zuordnung von anthropogenen oder natürlichen Quellen ist schwierig und daher Gegenstand der aktuellen Forschung. (Motelay-Massei, 2006; Pazdro, 2004; Rogowska, 2010; Ruczynska, 2011; Stader, 2013; Witt, 2009; Wu, 2011) Aufgrund der hydrophoben Natur, adsorbieren PAK relativ schnell an partikulärem Material (Chiou, 1998) und reichern sich im Sediment an. (Neff, 1979) Die Ozeane stellen daher eine enorme Senke für diese Umweltschadstoffe dar. (Wang, 2007) In diesem Zusammenhang sind die PAK-Konzentrationen im Oberflächenwasser sehr gering, wodurch sich ein besonderer Anspruch an die Analytik ergibt.

Für den anthropogenen Eintrag von PAK kommt u.a. die unvollständige Verbrennung von fossilen Brennstoffen in Betracht. Sie entstehen oftmals als Nebenprodukt vieler chemischer Prozesse, aber auch die Verschmutzung durch Ölbohrungen und durch Schiffe können ursächlich sein. (Pazdro, 2005; Witt, 1995) Daneben haben ebenfalls natürliche Prozesse, wie z.B. Waldbrände, einen Einfluss. (Wu, 2011) Allgemein kann zwischen pyrolytischer, diagenetischer und petrogener Herkunft unterschieden werden. (Lubecki, 2012) Das Aufstellen bestimmter Isomerenverhältnisse, wie das zwischen Phenanthren (PHE) und Anthracen (ANT) mit  $m/z$  178 oder Fluoranthren (FLU) und Pyren (PYR) mit  $m/z$  202 kann genutzt werden, um die Kontaminationsquellen zu lokalisieren. (Tam, 2001) Ebenso können PAK und ihre alkylierten homologen Serien herangezogen werden, um auf einen Eintrag durch Erdöl oder Erdölprodukte zu schließen. (Yunker, 2002)

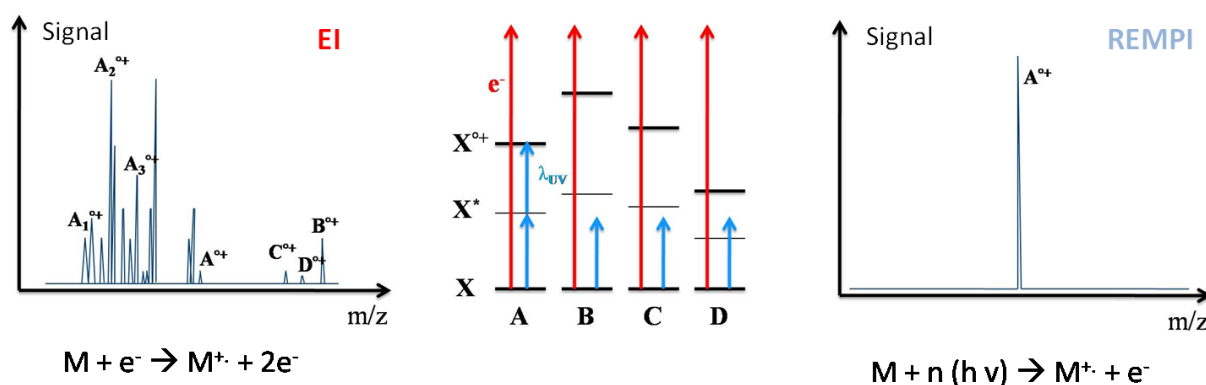


Auch in diesem Zusammenhang stellt die Ostsee ein ideales Forschungsobjekt dar. Durch die quasi umschlossene geologische Struktur und die angrenzenden hochentwickelten Länder mit ihrer vielseitigen Industrie, modernen Landwirtschaft und hoch frequentierten Schifffahrtswegen erfolgt ein hoher Eintrag an Schadstoffen. Laut Lipiatou et al. (1997), Moore et al. (1984) und Motelay-Massei et al. (2006) erfolgt dieser hauptsächlich über Flüsse und die Atmosphäre. Im Allgemeinen ist die PAK-Konzentration in der Ostsee 2- bis 10-mal höher als in der Nordsee, wobei sich die höchsten Konzentrationen nahe den Küsten wiederfinden. (Witt, 1995)

## 5. Harte und weiche Ionisierung in der Massenspektrometrie

Die Ionisationstechniken in der Massenspektrometrie sind vielfältig und reichen vom klassischen Elektronenstoß und der chemischen Ionisierung bis hin zu speziellen LASER-basierten Ionisationstechniken. In dieser Applikation werden die Vorteile der EI- und REMPI-Technik in einem Messsystem vereint und ermöglichen dadurch neue Ansätze der Datenerfassung und -analyse.

EI in Kombination mit der Chromatographie ist eine sehr leistungsstarke Methode und noch immer weitverbreitet. Diese Art der Ionisierung wird als „hart“ bezeichnet, da die kinetische Energie der Elektronen weit über der Ionisierungsenergie der meisten organischen Moleküle liegt. Folglich resultiert eine Fragmentierung, wobei die Molekülinformation weitestgehend verloren geht. Allerdings stellt das Fragmentierungsmuster einen Vorteil im Hinblick auf die Charakterisierung der Substanzen dar, da dieses sehr spezifisch ist und durch MS-Datenbankabgleich Strukturvorschläge zur Identifizierung der Stoffe zur Verfügung stehen. Zum Erhalt der Molekülinformation kann auf die sogenannte „weiche“ Ionisierung, z.B. mittels Photoionisation, zurückgegriffen werden. Dazu zählt u.a. die REMPI-Technik. Speziell für die Multiphotonionisations-Massenspektrometrie existieren vielversprechende Entwicklungen in der Hinsicht auf Selektivität und Sensitivität. (Imasaka, 2013; Li, 2010, 2011a, 2011b) Erstere ist abhängig von der Wellenlänge der generierten Photonen, von den UV-Absorptionsbanden sowie der Ionisierungsgrenze der Moleküle. Die Anregung eines Elektrons erfolgt beim (1+1)-REMPI durch zwei Photonen über einen angeregten Zwischenzustand, wie in der Abb. 10 dargestellt.



**Abbildung 10:** Schema der "harten" (EI) und der "weichen" (REMPI) Ionisierung im Vergleich [X: Elektronischer Grundzustand; X\*: angeregter Zwischenzustand; X<sup>+</sup>: Ionisationskontinuum]

REMPI in Kombination mit einem ToFMS ist im Bereich der Spurenanalytik einsetzbar, hoch selektiv und sensitiv für PAK. (Fendt, 2012; Geissler, 2009b; Haefliger, 1998; Li, 2010; Stader, 2013; Zimmermann, 1995) Für das hier verwendete REMPI-System wurde ein Nd:YAG-LASER (BIG SKY ULTRA, Quantel, Les Ulis Cedex, France) unter Verwendung einer Wellenlänge von 266 nm genutzt, was einer Photonenergie von 4,11 eV entspricht. Bei diesem LASER-Typ sind weitere Wellenlängen durch Frequenzvervielfachung zugänglich (1064, 532, 355 und 213 nm). Der LASER arbeitet bei einer Pulsrate von 10 ns mit einer maximalen Frequenz von 20 Hz. Die Energiedichte betrug  $7 \times 10^6 \text{ W cm}^{-2}$ . Detaillierte Informationen zum genutzten REMPI-ToFMS-System sind in der Applikation von Fendt et. al. (2012) beschrieben.

## 6. Pyrolysetechnik und MS-Kopplung

Der pyrolytische Prozess umfasst die thermische Zersetzung unter Luftausschluss. (Bayerbach, 2006) Im Gegensatz zur Verbrennung findet keine vollständige Umsetzung des Materials zu Kohlendioxid und Wasser statt. Bei diesem Hochtemperaturprozess zwischen 300 und 700 °C kommt es innerhalb polymerer Strukturen zu Bindungsbrüchen und in Abhängigkeit vom Probenmaterial zu Fragmenten geringeren Molekulargewichts. (Cammann, 2001) Die resultierenden Pyrolyseprodukte können aufgrund ihrer Flüchtigkeit über ein angeschlossenes GC- und MS-System analysiert werden. (Heidenreich, 2005)

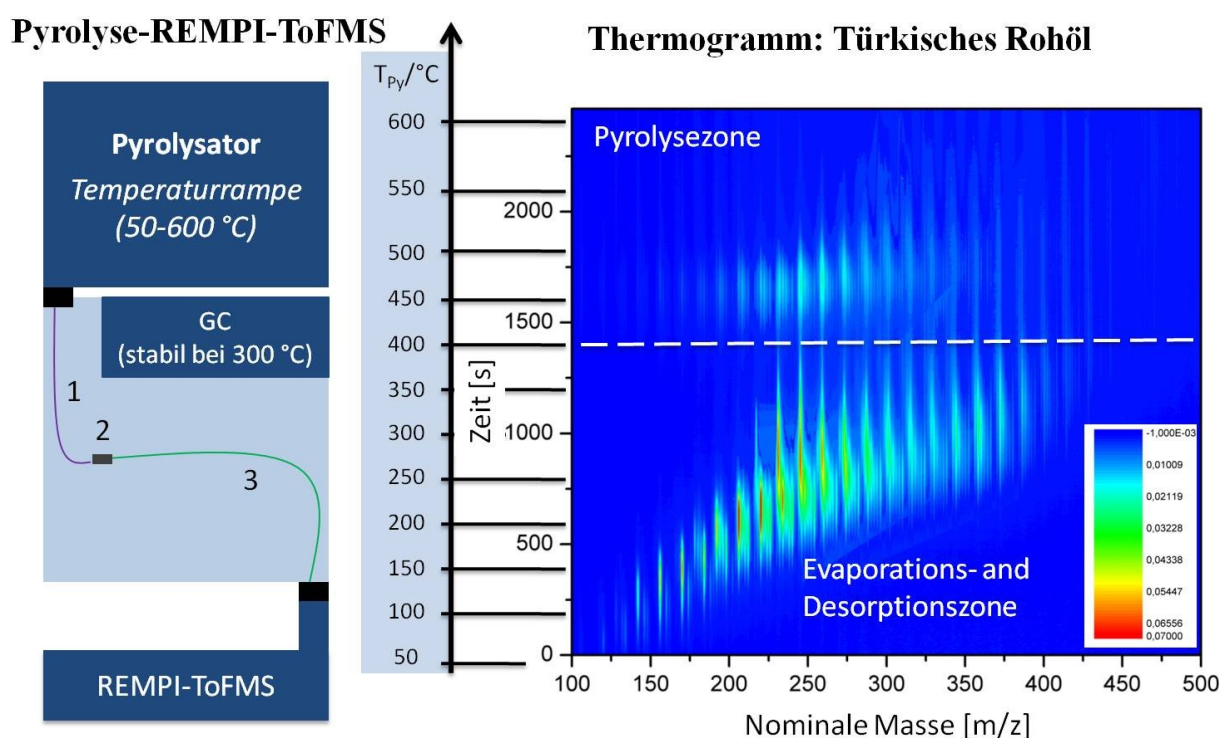
Neben der relativ einfachen Kopplungsmöglichkeit kommerzieller GC- oder MS-Systeme besteht die analytische Stärke darin, dass die Strukturinformation erhalten bleibt, um folglich einen Rückschluss auf das Ausgangsmolekül ziehen zu können. Hervorzuheben ist der vergleichbar geringe Präparationsaufwand im Vergleich zu klassischen Extraktionsprozessen, ein kleiner Probenbedarf ( $\leq$  ein Mikrogramm) und die Analyse von hochmolekularen Bestandteilen, deren Analyse der kommerziellen Analytik (z.B. GC) verwehrt bleibt.

### Thermoanalyse / REMPI-ToFMS

Bei der Pyrolyse haben sich im Wesentlichen zwei Verfahren etabliert, die Thermoanalyse und die Flash-Pyrolyse, wobei letztere auch stufenweise erfolgen kann (fraktionierte Thermoanalyse). Bei Ersterem, analog der Thermogravimetrie, wird die Probe in einem Ofen entlang einer Temperaturrampe erhitzt. (Adam, 2012; Geissler, 2009a, 2009b; Fendt, 2011) In Abhängigkeit der erreichten Temperatur finden Thermodesorptions- oder Pyrolyseprozesse statt. Die Abb. 11 zeigt schematisch die Direktanbindung zwischen Pyrolysesystem und MS, sowie das resultierende Thermogramm eines Schweröls, indem der Evaporations- und Pyrolysebereich deutlich zu erkennen sind. (Otto, 2015a) FT-ICRMS, meist in Kombination mit EI oder ESI (electrospray ionisation), lässt sich ebenfalls sinnvoll anwenden. (Panda, 2008; Teravainen, 2007; Miyabayashi, 2009; Smith, 2009)

Aus dem Thermogramm, welches aus Direktkopplung zwischen Pyrolysator und REMPI-ToFMS zugänglich wird, resultiert ein aromatischer Fingerprint der Probe und es ergibt sich ein erster Überblick zur strukturellen Beschaffenheit. Es sind neben frei verdampfenden Verbindungen, auch hochmolekulare Bestandteile vorhanden, die nur durch die Pyrolyseanwendung detektiert werden können. Ein weiterer Vorteil ist, dass zu jeder Pyrolysetemperatur ein komplettes Massenspektrum vorliegt. In der Veröffentlichung Otto et al. (2015a) sind das Thermogramm für die Ionenspur 178 und ein Ausschnitt aus dem aktuell

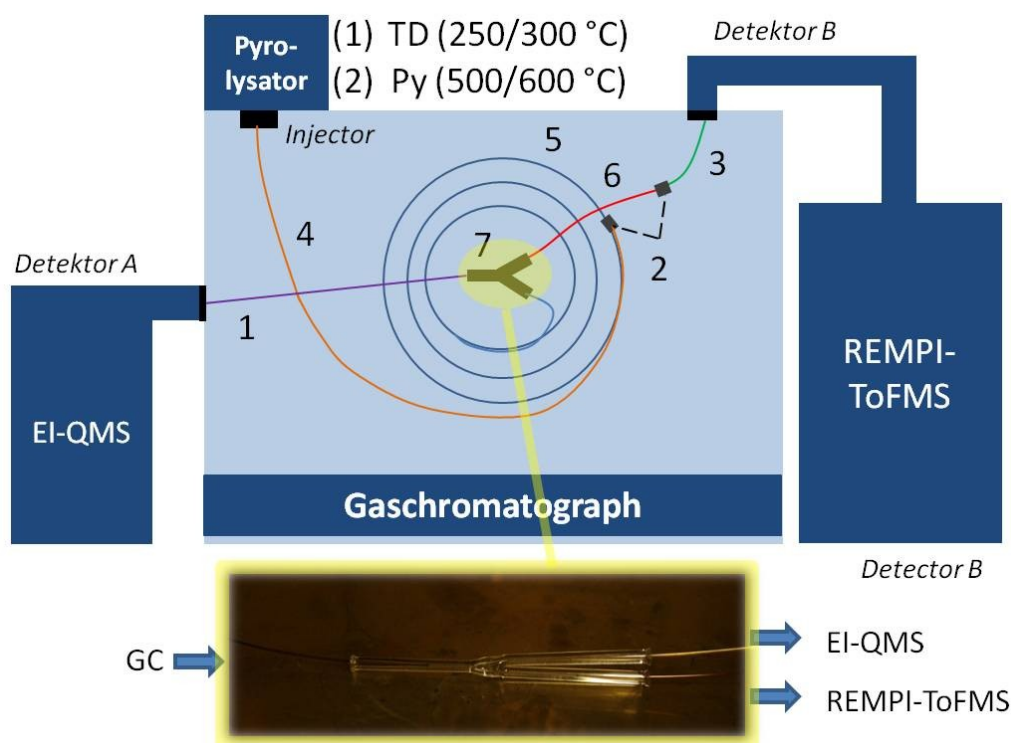
resultierenden Massenspektrum dargestellt. Letzteres zeigt die periodische Verteilung von Signalen, die als alkylierte Phenanthrenderivate (PHE-Derivate) interpretierbar sind. Allerdings gelangen keine Aussagen über die isomere Verteilung. Zudem sind Verbindungen mit gleicher nominaler Masse wie z.B. C4-NAP ( $m/z$  184) und DBT ( $m/z$  184), nicht voneinander zu unterscheiden. Zugleich ist noch umstritten, ob sich unter Pyrolysebedingungen neben den Aromaten auch längere Alkylseitenketten, die dann abgespalten vorliegen, parallel nachweisen lassen. Zur Klärung dieser Zusammenhänge ist eine Erweiterung des Systems, durch eine vorgeschaltete, leistungsstarke Chromatographie und eine zusätzliche universelle Detektion notwendig.



**Abbildung 11:** Thermische Analyse von Rohöl in direkter Anbindung zum REMPI-ToFMS. Der schematische Aufbau (links), in dem der Gaschromatograph als kontinuierliches Heizsystem genutzt wird und nicht zur Trennung der Komponenten beiträgt. Folgende Bestandteile sind im GC verbaut: (1) Phenyl/Methyl desaktivierte TSP Standard FS Verbinder, 250  $\mu\text{m}$  ID, 375  $\mu\text{m}$  OD, 1 m; (2) SS Union, 250  $\mu\text{m}$  Bohrung; (3) P/M desaktivierte TSP Standard FS Vubing, 200  $\mu\text{m}$  ID, 375  $\mu\text{m}$  OD, 2,5 m. Das resultierende Thermogramm (rechts) zeigt den Desorptions- und Pyrolysebereich.

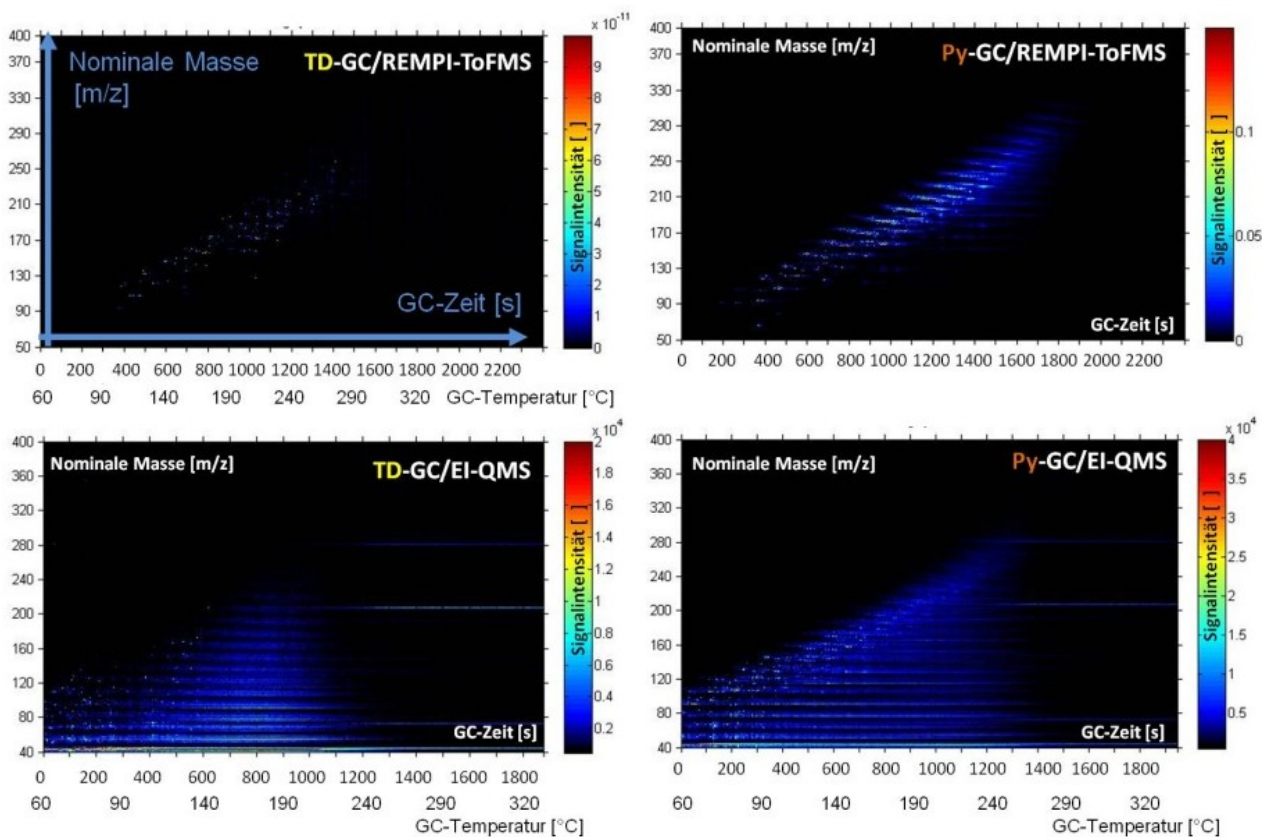
### Fraktionierte Thermoanalyse / GC/MS (EI-QMS und REMPI-ToFMS)

Eine zweite pyrolytische Technik ist die sogenannte Flashpyrolyse, bei der die Erwärmung und somit Zersetzung der Probe augenblicklich erfolgt. Zudem kann die Probe verschiedenen Temperaturstufen ausgesetzt werden (fraktionierte Thermoanalyse). Es wird schlagartig ein breites Substanzspektrum emittiert, dass eine anschließende, hochauflösende Separationstechnik zur Trennung der Komponenten voraussetzt. Die in dieser Arbeit verwendete Art der gleichzeitigen Einkopplung von massenselektiven Detektoren eröffnet neue Möglichkeiten zur Erfassung hochmolekularer Strukturen in komplexen Probenmatrizes sowie deren Trennung und bietet zudem Zugang zu neuen Interpretationsansätzen. Zusammenfassend besteht das Gesamtsystem aus Flash-Pyrolysator, eindimensionaler GC und zwei Massenspektrometern und ist der Abb. 12 zu entnehmen.



**Abbildung 12:** Aufbau Pyrolysator-GC/MS (EI-QMS und REMPI-ToFMS). Im GC sind folgende Komponenten verbaut: (1) Phenyl/Methyl (P/M) deaktivierte TSP Standard FS Verbinder, 250  $\mu\text{m}$  ID, 375  $\mu\text{m}$  OD, 1 m; (2) SS Union, 250  $\mu\text{m}$  Bohrung; (3) P/M deaktivierte TSP Standard FS Verbinder, 200  $\mu\text{m}$  ID, 375  $\mu\text{m}$  OD, 2.5 m; (4) Vorsäule: P/M deaktiviert TSP Standard FS Verbinder, 250  $\mu\text{m}$  ID, 375  $\mu\text{m}$  OD, 4 m; (5) Trennsäule: SGB-BPX5, 250  $\mu\text{m}$  ID, 250  $\mu\text{m}$  Film, 375  $\mu\text{m}$  OD, 30 m; (6) P/M deaktivierte TSP Standard FS Verbinder, 100  $\mu\text{m}$  ID, 375  $\mu\text{m}$  OD, 0.3 m; (7) deaktivierte PressFit 3-Wege Y-Splitter für FS Verbindung mit 0.20 bis 0.75 mm OD

Beispielchromatogramme unter Thermodesorptions- (TD) und Pyrolysebedingungen sind im direkten Vergleich zwischen EI-QMS und REMPI-ToFMS in der Abb. 13 für DOM dargestellt. Das Substanzspektrum und die Signalverteilung im EI-Chromatogramm ergeben einen universellen Fingerprint. Dieser ist zwar charakteristisch, allerdings auch sehr komplex, d.h. mehrere Peaks sind überlagert, die jeweils für eine oder mehr Komponenten stehen. Die EI-Daten allein sind v.a. hinsichtlich des Aromatengehaltes nur schwer interpretierbar. REMPI wirkt dem entgegen, indem die Fragmentierung unterdrückt wird und selektiv Aromaten detektiert werden. Es wird ein „aromatischer Fingerprint“ der Probe erhalten, welcher im Vergleich zum EI-Spektrum deutliche Molekülpeaks aromatischen Ursprungs zeigt.



**Abbildung 13:** Direkter Vergleich der Chromatogramme die aus den REMPI-ToFMS (oben) und EI-QMS-Messungen (unten) für die DOM-Zusammensetzung in der nördlichen Ostsee (At4-Station) resultieren. Links sind der TD- und rechts der Pyrolyseschritt dargestellt. Die GC-Zeit bzw. GC-Temperatur (Abszisse) ist gegen die nominale Masse (Ordinate) aufgetragen. Die Signalintensitäten entsprechen der Farbskala.

## 7. Ergebnisse und Diskussion

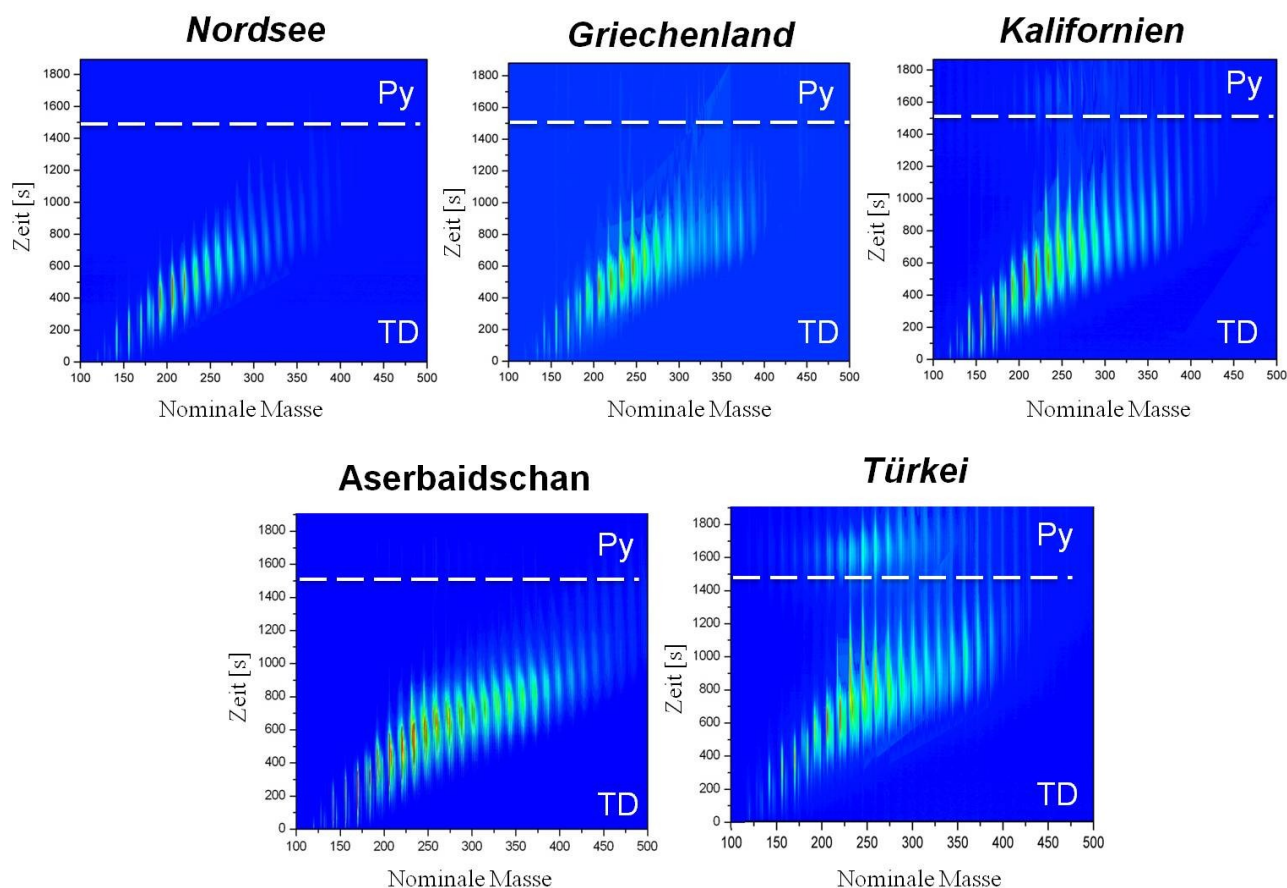
### 7.1. Methodenentwicklung und Anwendung am schweren Rohöl (Publikation 1)

Für die höher siedenden Fraktionen werden neue Analysetechniken und -methoden benötigt, um die Trennung (meist basierend auf GC Technik) und Detektion von Komponenten nebeneinander zu ermöglichen. Herausfordernd ist v. a. die Erfassung von niedrig konzentrierten Verbindungen und die Separation isomerer Strukturen. In dieser Applikation wurden kommerzielle (Pyrolysator, GC, EI-QMS) und in der Arbeitsgruppe entwickelte LASER basierende Systeme (siehe oben) kombiniert und somit die Vorteile leistungsstarker analytischer Methoden vereint, um den Informationsgehalt, insbesondere zu hochmolekularen Strukturen, zu erweitern. Die Probenaufgabe erfolgt stufenweise (TD/Pyrolyse), über die angebundene GC findet die Haupttrennung der verdampften bzw. der pyrolytisch freigesetzten Komponenten statt und speziell über das angebundene ToF werden Molekülonen mit gleicher Retentionszeit, aber unterschiedlichem  $m/z$ -Verhältnis, nachträglich separiert und detektiert. Letztlich wird ein universelles (EI) neben einem aromatischen (REMPI) Chromatogramm erhalten, welche für jede Probe eine individuelle Verteilung der chemischen Spezies aufzeigen. Das verwendete System wurde anhand von PAK-Standards getestet und bewertet und ist erstmals bei schweren Rohölproben zur Anwendung gekommen.

#### Thermolyse von Rohöl (Py-MS)

Bei direkter Kopplung zwischen Pyrolysator- und REMPI-ToFMS-System, ohne GC-Zwischenschritt, werden Thermogramme in Form eines aromatischen Fingerprints (Abb. 14) erhalten. Der Evaporationsbereich ist bei allen fünf Rohölen deutlich ausgeprägt und endet bei einer Pyrolysatortemperatur von 350 – 400 °C. Es liegt ein individuell verteiltes Muster an Signalintensitäten vor, entsprechend dem unterschiedlichen geologischen Ursprung. Bei türkischem Rohöl kommt ein ausgeprägter Pyrolysebereich oberhalb von 400 °C hinzu. Es handelt sich um Pyrolysefragmente, die zuvor in hochmolekularen Strukturen gebunden vorlagen. Diese Ergebnisse korrelieren mit denen von Geissler et al. (2009a), wobei die dort untersuchten Rohöle dem gleichen Trend im Evaporations- und Pyrolysebereich folgen.





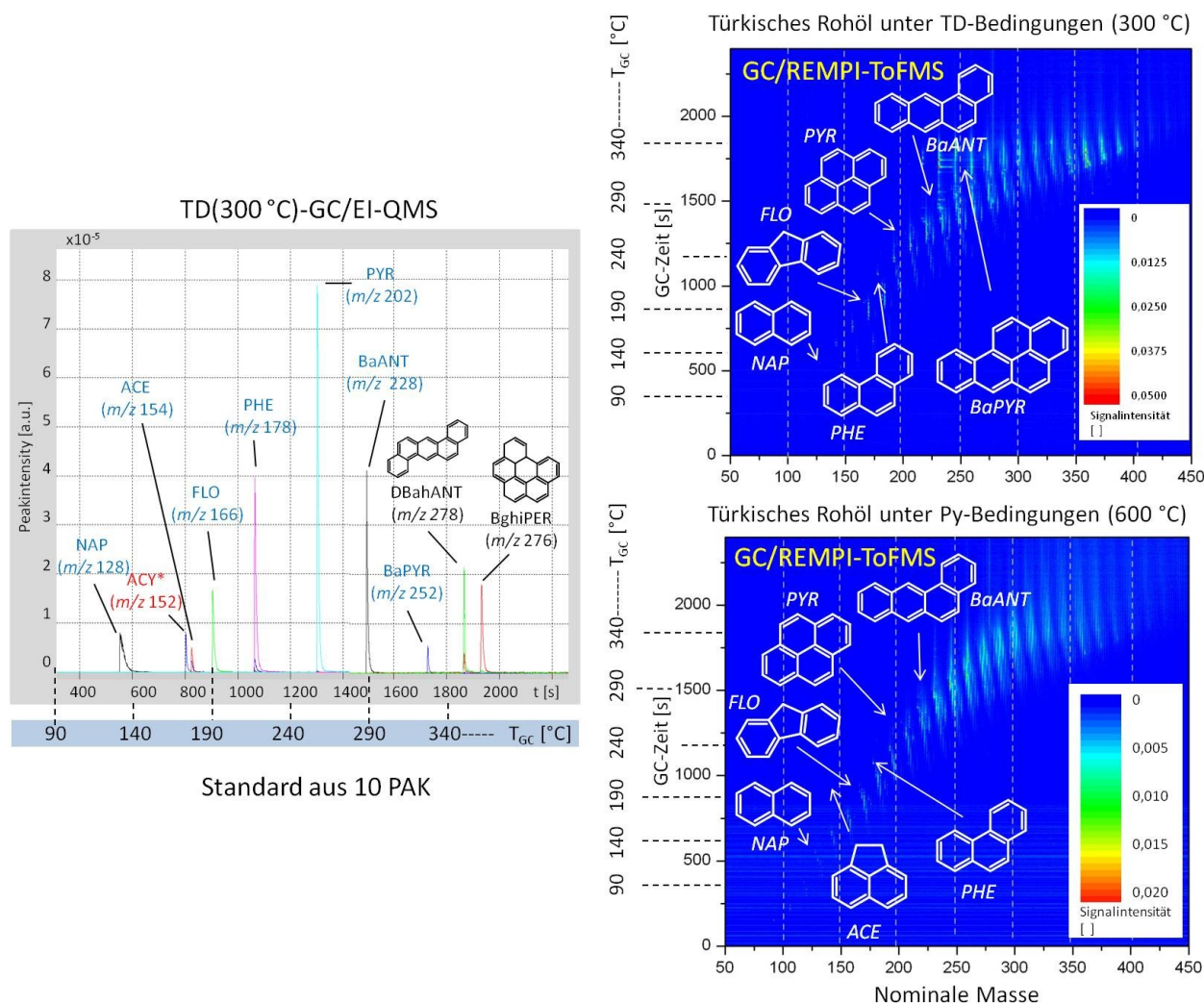
**Abbildung 14:** Thermogramme zu 5 Rohölen durch direkte Kopplung von Pyrolysator und REMPI-ToFMS.

In den dargestellten Thermogrammen kann eine periodische Verteilung der Signale in festen Abständen beobachtet werden, denn zu jedem aromatischen Grundkörper existieren alkylierte Derivate. Jeder Grad der Alkylierung verschiebt das detektierte Signal um 14 nominale Massen (je Methylgruppensubstitution). Dabei dominieren die alkylierten Spezies oftmals gegenüber den Kernaromaten. (Otto, 2015a) Die verwendete Pyrolyse-MS-Kopplung ist hervorragend geeignet, um einen Überblick über das vermessene Probenmaterial zu erhalten und schwere Komponentenfraktionen nachzuweisen. Allerdings ist keine Trennung zwischen Molekülen mit gleicher nominaler Masse möglich und es gelingt somit keine Aussage zu einer möglichen Isomerenverteilung.

### Fraktionierte Thermolyse von Rohöl (Py-GC/MS)

Das gekoppelte System, bestehend aus Pyrolysator, GC und zwei massenselektiven Detektoren (Abb. 12) konnte erfolgreich auf Funktionalität an zehn PAK-Standardsubstanzen (siehe Abb. 5) getestet werden. In dem EI-Chromatogramm (Abb. 15, links) sind die zehn PAK-Vertreter dargestellt. In den Chromatogrammen für Türkisches Rohöl (Abb. 15, rechts),

welche auf die REMPI-ToFMS-Detektion basieren, können neun der zehn PAK deutlich lokalisiert werden. ACY ( $m/z$  152) ist bei dem verwendeten Lasertyp und der genutzten Wellenlänge von 266 nm nicht detektierbar. Die möglichen Ursachen sind in den Publikationen Otto et al. (2015a) und Li et al. (2010) genannt.



**Abbildung 15:** Links: PAH-Standard gemessen durch das Py-GC/MS-System. Dargestellt ist der SIM-Modus (single ion monitoring) unter EI-Bedingungen. Rechts: Chromatogramm (REMPI-ToFMS) von Türkisches Rohöl mit identifizierten PAK-Komponenten bei 300 °C (oben) und 600 °C (unten) Injektionstemperatur.

Es ist erstmals möglich die Sensitivität zwei massenselektiver Detektoren direkt miteinander zu vergleichen, beruhend auf derselben Messung (siehe Otto et al., 2015a, Bild 5). Im türkischen Rohöl können aromatische Verbindungen in einem Massenbereich von 100 bis 450 erfasst werden. Dabei steigt die Signalverteilung von Verbindungen mit dem gleichen  $m/z$ -

Verhältnis oberhalb von 230 extrem an, was die Zunahme an Varianten der alkylierten Spezies widerspiegelt.

Eine Vielzahl von PAK-Vertretern konnte mit Hilfe der Retentionszeit identifiziert und durch Standardaddition in den Rohölen verifiziert werden. Die Thermodesorption zeigt ein intensiveres Substanzspektrum mit höheren Peakintensitäten. Unter Pyrolysebedingungen ist die Substanzvielfalt zwar durchaus größer, aber die Peakintensitäten sind merklich geringer (siehe Abb. 15 für Türkisches Rohöl). Allgemein betrachtet sind die Signalintensitäten für den zweiten bis dritten Alkylierungsgrad am höchsten und nehmen dann deutlich ab.

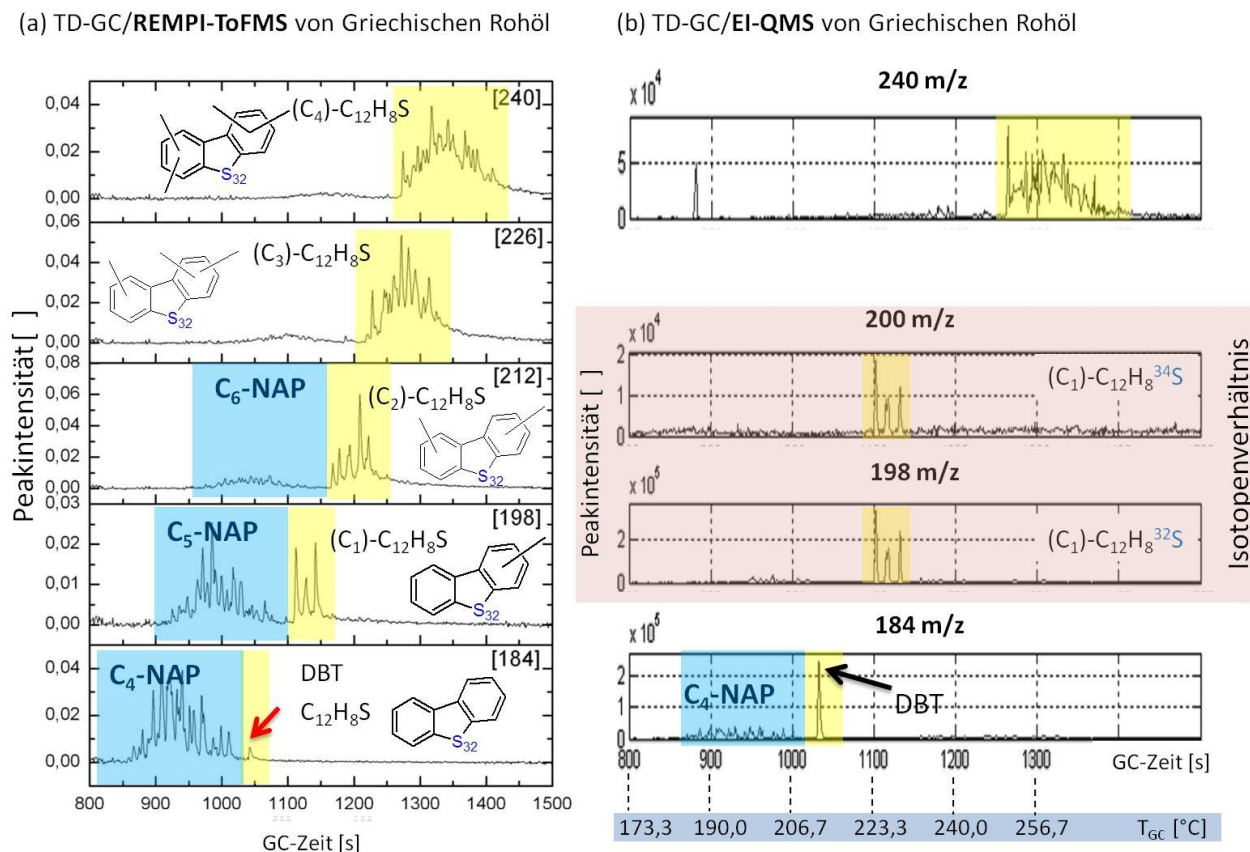
Die Verteilung einiger PAK-Vertreter ist bis zum vierten Alkylierungsgrad in Abb. 16 zusammengefasst. Es wird ersichtlich, dass sie in Abhängigkeit vom Rohöltyp nur geringfügig variiert.

Rohöl	Türkei					Aserbaidschan					Griechenland					Nordsee					Kalifornien				
C <sub>x</sub> -PAK	0	1	2	3	4	0	1	2	3	4	0	1	2	3	4	0	1	2	3	4	0	1	2	3	4
NAP [m/z 128]	X	X	X	X	X	X	X	X	X	X	-	X	X	X	X	X	X	X	X	X	X	X	X	X	X
ACE [m/z 154]	R	R	R	R	R	X	X	X	X	X	-	-	-	-	-	-	-	-	-	-	R	-	-	-	-
FLU [m/z 166]	X	X	X	R	R	X	X	X	X	X	X	X	X	R	R	X	X	X	X	R	X	X	X	X	X
PHE [m/z 178]	X	X	X	X	X	X	X	X	X	X	X	X	X	X	R	X	X	X	X	X	X	X	X	X	X
PYR [m/z 202]	X	X	X	R	-	X	X	X	X	X	X	X	X	X	-	X	X	X	R	R	X	X	X	-	-
Ba-ANT [m/z 228]	R	-	-	-	-	X	X	X	X	-	-	-	-	-	-	X	X	-	-	-	X	X	-	-	-

**Abbildung 16:** Verteilung von PAK-Vertretern in fünf Rohölproben bis zum vierten Alkylierungsgrad (C<sub>4</sub>). Einige Verbindungen können nur durch REMPI (R) erfasst werden.

Herausfordernd und neuartig in dieser Applikation ist die Erfassung von PAK neben PASH mit gleicher nominaler Masse ohne großen präparativen Aufwand. Die Abb. 17 zeigt bei einer Retentionszeit von 1030 s, für den vierten Grad der Alkylierung von NAP (*m/z* 184) einen Peak im EI-Chromatogramm, der in der Intensität deutlich über denen der übrigen C<sub>4</sub>-NAP-

Isomere liegt. Nach einem Datenbankabgleich, der Einbindung von Literatur (Andersson, 2006) und dem Heranziehen der Isotopenverhältnisse für Schwefel ( $^{32}\text{S}$  (96 %) und  $^{34}\text{S}$  (4 %)), handelt es sich mit hoher Wahrscheinlichkeit um DBT.



**Abbildung 17:** DBT und seine alkylierten Vertreter ( $\text{C}_x$ ) in Griechischen Rohöl. Direkter Vergleich relevanter Ionenspuren zwischen EI-QMS und REMPI-ToFMS unter TD-Bedingungen. Die Ionenspuren  $m/z$  212 und  $m/z$  226 der EI-Daten sind aus Gründen der Übersichtlichkeit nicht dargestellt.

Bei Betrachtung des REMPI-Chromatogramms kehren sich die Verhältnisse, gemessen an der Peakhöhe, vom  $\text{C}_4\text{-NAP}$  gegenüber DBT um. Dafür ist es bei REMPI möglich, NAP bis zum fünf- und sechsfachen Alkylierungsgrad zu detektieren, was mit dem EI-Setup nicht gelingt. Bei REMPI (266 nm) kann DBT anscheinend nicht so effizient ionisiert werden wie NAP bzw. deren Derivate, was auf einen ungünstigen Wirkungsquerschnitt schließen lässt. Dies kann auf einen zu kurzlebigen angeregten Zwischenzustand zurückgeführt werden. Hingegen kann postuliert werden, dass alkylierte DBT besser ionisierbar sind, da die Alkylgruppen den angeregten Zwischenzustand besser stabilisieren.

DBT ist in allen fünf Rohöltypen sowohl als aromatischer Grundkörper als auch in alkylierter Form präsent. BT kann nur im türkischen und griechischen Rohöl gefunden werden. Dagegen ist BNT mit kleinen Peakintensitäten im aserbaidischen und griechischen Öl detektierbar.

Werden ausschließlich diese drei PASH-Vertreter zur Beschreibung der Schwefelbelastung in den Rohölen herangezogen, sind kalifornisches Öl und Nordseeöl am wenigsten belastet. Indessen zeigt griechisches Rohöl den höchsten Schwefelgehalt. Allerdings sind zur Untermauerung dieser Aussage weiterführende Messungen unter Einbeziehung weiterer Schwefelverbindungen notwendig.



## 7.2. Charakterisierung und Abbau von tDOM (Publikation 2)

In der folgenden Betrachtung wurde das Py-GC/MS-System auf eine Umweltstudie zur Erfassung terrigener, geochemischer Tracer (phenolische Ligninabbauprodukte) im marinen System angewendet. Die Applikation nach Otto et al. (2016) befasst sich mit der strukturellen Charakterisierung von tDOM und deren halbquantitative Veränderungen in Abhängigkeit vom Salinitätsgradienten. Zudem soll in Inkubationsexperimenten ein möglicher Abbau von Ligninkomponenten durch Mikroorganismen untersucht werden.

Zur Untersuchung der Einflussnahme des Salzgehaltes auf die DOM-Zusammensetzung, wurde Oberflächenwasser entlang des dargestellten Salzgradienten (Abb. 7) beprobt. Die Probenaufarbeitung erfolgte direkt an Bord nach dem Protokoll von Dittmar et al. (2008) und ist schematisch in der Abb. 18 dargestellt. Details zur Probenaufarbeitung sowie spezifische Geräteparameter für die chemische Analyse sind in Otto et al. (2016) genannt.

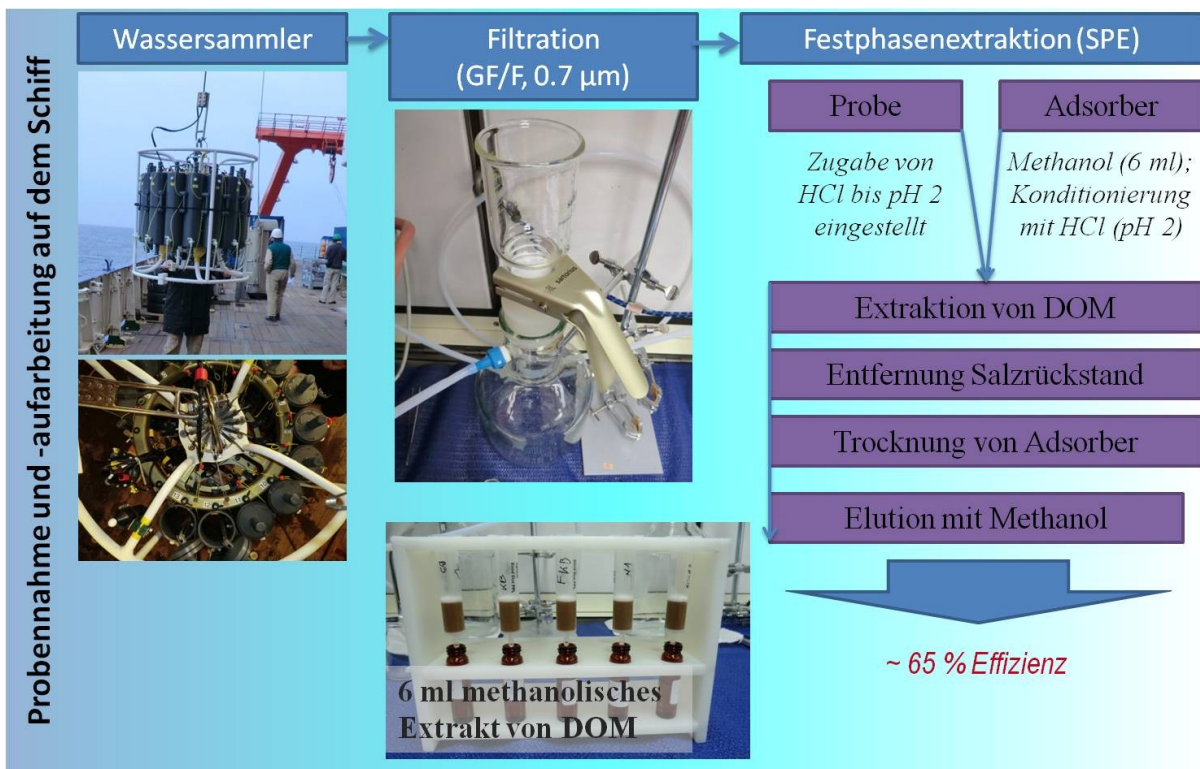
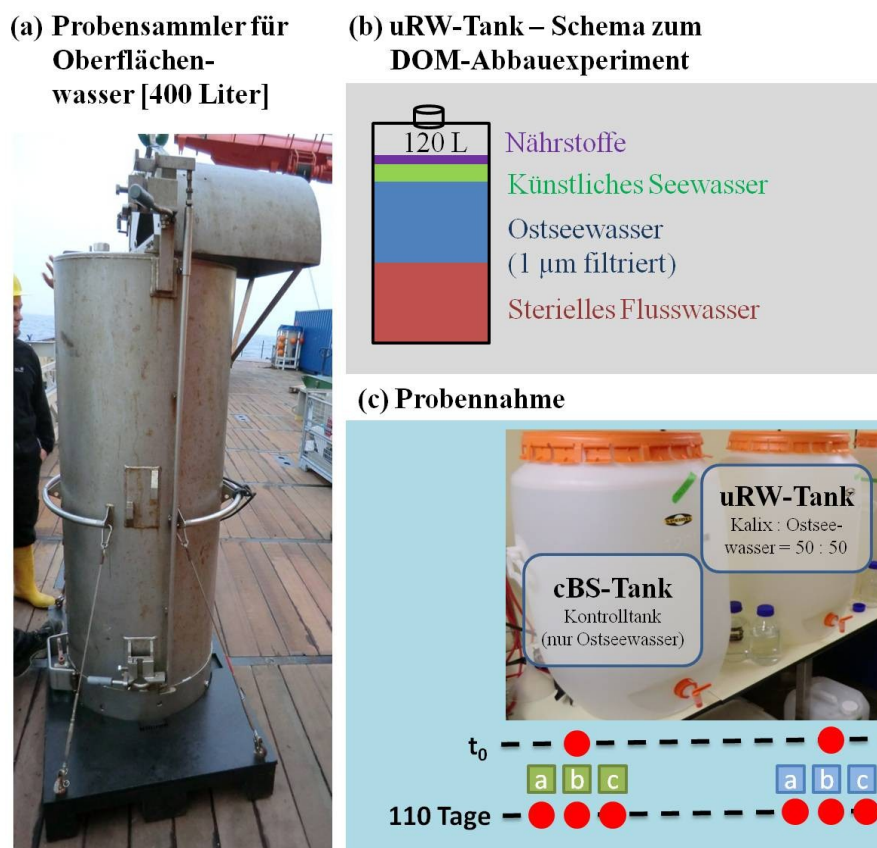


Abbildung 18: Probenaufarbeitung durch Filtration und Festphasenextraktion.

Neben dem Einfluss des abiotischen Faktors Salz, sollte in Inkubationsversuchen ein möglicher Abbau von tDOM durch Mikroorganismen verfolgt werden. Diese Experimente wurden an drei Stationen durchgeführt (At-Stationen in der Abb. 7). Das dazu benötigte Oberflächenwasser wurde mit dem Probensammler in Abb. 19a genommen. Die Auswahl der Stationen erfolgte in Anlehnung an die Publikation von Herlemann et al. (2011), da dort

aufgrund der Salinitätsverhältnisse unterschiedliche Gruppen von Mikroorganismen anzutreffen sind, die das DOM als Kohlenstoffquelle nutzen könnten. Zum Ansetzen der Inkubationsexperimente wurde Flusswasser vom Kalix (Ortsangabe), dass zuvor aufgesalzen und mit Nährstoffen versetzt wurde, mit dem Ostseewasser 1:1 gemischt (uRW-Tank; Vgl. Abb.19b), um den Einfluss des vermehrt ins Gewässer eingetragenen DOM auf die Mikroorganismen zu untersuchen, wurde ein Kontrolltank cBS mit reinem Ostseewasser der aktuellen Station angesetzt, in dem ebenfalls Veränderungen aufgrund des natürlich vorkommenden DOM-Gehaltes zu erwarten waren. Eine Probennahme erfolgte direkt nach der Inkubation der beiden Wassermassen ( $t = 0$  s) und aus organisatorischen Gründen nach 110 Tagen, wobei zu beachten ist, dass die jeweilige Probe zuvor in 3 Parallelen aufgeteilt wurde (Abb. 19c).

Stellvertretend für das tDOM sollten spezifische Ligninbausteine (H-, G- und S-Bausteine) herangezogen werden, um zum Einen Veränderungen entlang des Salzgradienten zu verfolgen und zum Anderen einen möglichen Abbau durch Mikroorganismen halbquantitativ zu diskutieren. Zur Darstellung des Konzentrationsverlaufes von der Flussmündung (niedriger



**Abbildung 19:** (a) Probensammler, (b) Experimentelles Design und (c) zeitliche Abfolge der Probennahme mit drei biologischen Replikaten nach 110 Tagen Inkubation.

Salzgehalt) bis zur S1-Station (höchster Salzgehalt) wurden je Station drei technische Replikate vermessen (siehe Otto et al., 2016).

Für das Phenol ( $m/z$  94,  $t(R) = 370$  s), als Vertreter für die H-Bausteine, zeigt sich unter TD-Bedingungen (250 °C Injektionstemperatur) ein abnehmender Trend im halbquantitativ betrachteten Konzentrationsverlauf vom niedrigen zum hohen Salzgehalt (Otto, 2016). Der Konzentrationsverlauf unter Pyrolysebedingungen (500 °C) zeigt einen ähnlichen Trend. Dementsprechend wird Phenol in freier oder gebundener Form (möglicher Ligninbaustein) zur Nordsee hin aus dem marinen System entfernt.

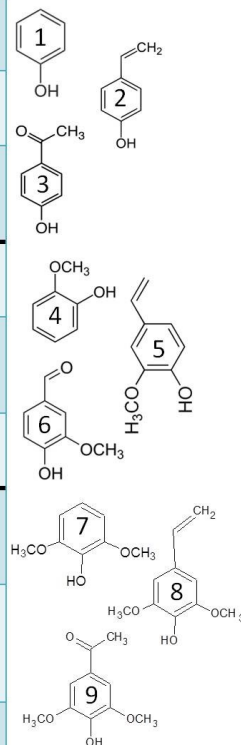
In den Inkubationsversuchen (M1, M2, M3 mit den Salinitäten  $S = 32, 7, 3$ ) wird der Kontrolltank (cBS) mit dem Mischtank (uRW) verglichen, um ein abweichendes Verhalten durch den zusätzlichen tDOM-Eintrag festzustellen. Der direkte Vergleich zwischen cBS- und uRW-Tank, bei  $t = 0$ , zeigt einen deutlichen Anstieg der Phenolkonzentration bei der Zugabe von Flusswasser, sowohl unter TD- als auch unter Pyrolysebedingungen. Die zeitlichen Verläufe beim cBS- und uRW-Tank zeigen nach 110 Tagen eine deutliche Konzentrationszunahme der freien Phenolkomponenten unter TD-Bedingungen. Bei der Pyrolyse hingegen stagniert die Konzentration an Phenolbruchstücken, was wiederum bedeuten könnte, dass das hochmolekulare Lignin nicht durch Mikroorganismen verstoffwechselt wird. Ähnliche Ergebnisse ergeben sich für weitere herangezogene Ligninkomponenten, die in der Abb. 20 zusammengefasst aufgeführt sind. Die H- und V-Bausteine verhalten sich ähnlich und sinken in ihrer Konzentration hin zum höheren Salzgehalt. Es ist bekannt, dass mit zunehmendem Salzgehalt sich DOM-Bestandteile partikulär zusammenballen und als partikuläres organisches Material ausfallen. (Sholkovitz, 1976) Daran könnten auch Ligninkomponenten beteiligt sein. Eine Ausnahme stellt das p-Hydroxyacetophenon dar, das bis zur S6-Station (TD-Bedingungen) in seiner Konzentration zunimmt und zur Nordsee hin (S1-Station) wieder abfällt. Eine Erklärung für das Verhalten der Komponente konnte durch keine Literatur belegt werden.

Die S-Bausteine zeigen einen stagnierenden bis leicht zunehmenden Trend mit ansteigendem Salzgehalt. Aus den Inkubationsexperimenten ist ersichtlich, dass die Ligninstruktur nicht abgebaut wird. Allerdings kann nicht ausgeschlossen werden, dass bei Veränderung der Reaktionsbedingungen und Betrachtung größerer Zeitskalen die Mikroorganismen durchaus



in der Lage sind, diese aufzubrechen und das tDOM zu verstoffwechseln, was mit einem Response für die Klimaveränderung einhergeht und die Erderwärmung verstärken könnte.

	Molekül	Salzlinie	Inkubation: TD-Bedingungen						Inkubation: Pyrolyse-Bedingungen					
			M1		M2		M3		M1		M2		M3	
			cBS	uRW	cBS	uRW	cBS	uRW	cBS	uRW	cBS	uRW	cBS	uRW
H	(1) Phenol [m/z 94] t(R) = 370 s	↓ ↓	↑	↓	↗	↗	↑	↗	→	→	→	↓	↗	→
	(2) Vinylphenol [m/z 120] t(R) = 610 s	↘ ↓	↑	↓	↘	↗	↑	↘	→	↗	↓	→	↗	→
	(3) p-Hydroxy-acetophenon [m/z 136] t(R) = 698 s	↑ <sub>s6</sub> ↓ <sub>s1</sub>	↑	↑	→	↑	↑	↑	→	↓	↓	→	↗	↗
V	(4) Guaiacol [m/z 124] t(R) = 468 s	↘ ↓	↑	↘	→	↘	↑	↓	→	↓	→	↓	↗	↓
	(5) 4-Vinyl-2-methoxyphenol [m/z 150] t(R) = 680 s	↓ ↓	↑	↓	→	→	↑	↘	→	→	→	↓	→	→
	(6) Vanillin [m/z 152] t(R) = 644 s	- ↓	-	-	-	-	-	-	→	↓	↓	→	→	↓
S	(7) 2,6-Dimethoxyphenol [m/z 154] t(R) = 800 s	- ↗	-	-	-	-	-	-	↓	→	↓	→	↗	→
	(8) 4-Vinyl-2,6-dimethoxyphenol [m/z 180] t(R) = 1010 s	→ ↗	↑	↓	↑	↓	↑	↓	→	→	→	→	→	→
	(9) Acetosyringon [m/z 196] t(R) = 1050 s	→ ↗	↑	↓	↑	↘	↑	↘	→	→	↓	→	→	→



**Abbildung 20:** Trendverlauf für einzelne Moleküle entlang der Salzlinie (salzarm zu salzreich) und während der Inkubation (↑ starke Zunahme, ↓ starke Abnahme, ↗ leichte Zunahme, ↘ leichte Abnahme, → Stagnation).

### 7.3. PAK-Komponenten im marinen System (Publikation 3)

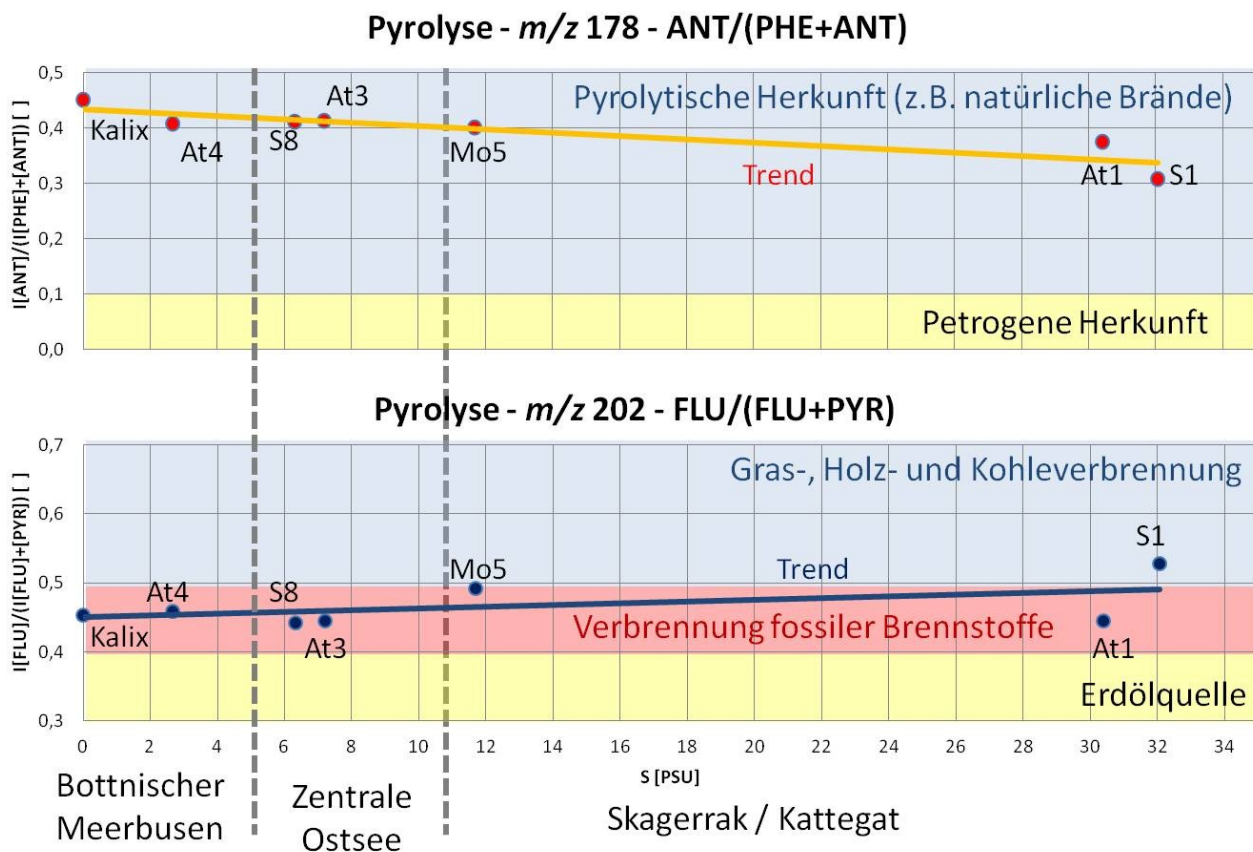
In diesem Abschnitt soll mit dem Analysesystem die PAK-Signatur entlang des Salinitätsgradienten der Ostsee verfolgt werden. Unter Pyrolysebedingungen sind indirekt auch hochmolekulare PAK zugänglich, die durch einen anthropogenen Eintrag (z.B. Schiffsverkehr unter Schwerölnutzung) in das Umweltkompartiment gelangen und bislang wenig untersucht sind. Für die halbquantitative Analyse, ähnlich der für die Ligninfragmente aus dem vorhergehenden Abschnitt, wurden NAP, FLO, PHE und PYR herangezogen, die auch in der Literatur häufig beschrieben werden. (u.a. Tam, 2001)

Die halbquantitativen Veränderungen der PAK als Funktion des Salzgradienten werden in der Publikation Otto et al. (2015b, Bild 3) diskutiert. Hier wurden die Peakintensitäten aus den REMPI-ToFMS-Messungen der Molekülonen herangezogen. Im REMPI-Chromatogramm konnten NAP, FLO, PHE und PYR eindeutig unter Pyrolysebedingungen identifiziert werden. Unter TD-Bedingungen sind die Peakintensitäten mit zunehmendem Salzgehalt oftmals zu gering. Ergänzend werden Isomere wie ANT ( $m/z$  178) und PHE ( $m/z$  178) sowie FLU ( $m/z$  202) und PYR ( $m/z$  202) herausgegriffen. Für PHE und PYR sind dabei die Wirkungsquerschnitte bei REMPI (266nm) um zwei Zehnerpotenzen höher (Otto, 2015a), als bei ihren Isomeren ANT bzw. FLU. Die letztgenannten PAK werden im weiteren Verlauf ausschließlich für die Aufstellung von Isomerenverhältnissen herangezogen (Abb. 21), um wiederum eine Emissionsquelle postulieren zu können.

Vom Fluss Kalix ausgehend bis hin zur Nordsee (S1-Station) wurden drei technische Replikate des Oberflächenwassers analysiert. Für NAP ( $m/z$  128,  $t(R) = 580$  s) kann eine geringe Zunahme der Konzentration von der Flussmündung bis zur Mo5-Station festgestellt werden. Zwischen der Mo5- und S1-Station (Nordseewassereinstrom) stagniert die Konzentration. Allgemein ist für FLO, PHE, PYR ein fast unveränderter, tendenziell leicht ansteigender Trend entlang des zunehmenden Salzgehaltes feststellbar. Die Ergebnisse stimmen dabei gut mit denen von Broman et al. (1991) überein.

Die anthropogen eingetragenen PAK können nach Wu et al. (2011) pyrolytischen oder petrogenen Ursprungs sein. Nach Tam (2001) und Yunker (2002) bietet die Aufstellung von Isomerenverhältnissen eine Möglichkeit der Unterscheidung zwischen natürlichen und anthropogenen Quellen sowie zwischen einem pyrolytisch- oder petrogen-anthropogenen Eintragungsmechanismus. In diesem Zusammenhang wurden die Verhältnisse

$ANT/(ANT+PHE)$  und  $FLU/(FLU+PYR)$  aufgestellt (siehe Abb. 21). Im Fluss- und Oberflächenwasser der At4-Station ergibt sich für  $ANT/(ANT+PHE)$  ein Verhältnis von 0,45-0,41 und für  $FLU/(FLU+PYR)$  von 0,45. Bei  $ANT/(ANT+PHE)$  wird im weiteren Verlauf bis zur S1-Station (Norseezugang) ein leicht fallender Trend bis 0,31 verzeichnet, was für einen pyrolytischen Ursprung sprechen würde. (Yunker, 2002; Tam, 2001) Hingegen stagniert das  $FLU/(FLU+PYR)$ -Verhältnis zwischen einem Bereich von 0,4 bis 0,5, dass auf eine unvollständige Verbrennung von fossilen Brennstoffen hindeutet. (Wu, 2011)



**Abbildung 21:** Darstellung der Iosomenverhältnisse (EI-Daten, Pyrolysebedingungen) von  $ANT/(ANT+PHE)$  und  $FLU/(FLU+PYR)$  gegen den Salzgradienten der Ostsee. Die farbigen Bereiche stehen für eine spezifische Eintragsquelle in das marine System (Yunker, 2002; Tam, 2001).

Alkylierte PAK werden ebenfalls als potentielle Indikatoren für einen anthropogenen Eintrag genannt (Wang, 2007). Insbesondere NAP und seine alkylierten Vertreter können auf einen petrogenen Ursprung hindeuten (Tam, 2001) und bilden eine bedeutende Fraktion im Rohöl oder Erdölprodukten (Mullins, 2007; Otto, 2015a). Bei der Thermodesorption (siehe Otto et al., 2015b) lassen sich in den einzelnen Proben (S1 bis At4) und im Flusswasser alkyliertes NAP nachweisen, allerdings sind die Intensitäten sehr gering. Unter Pyrolysebedingungen

wiederum ergeben sich deutliche Signale über den gesamten Salzgradienten für Substanzen bis zu einem Alkylierungsgrad von sechs. Das bedeutet, dass höher molekulare, aromatische Strukturen einen bedeutenden Anteil des Ostseewassers, wahrscheinlich assoziiert mit dem DOM (Schwarzenbach, 2003), darstellen. Die Peakintensitäten für NAP steigen bis zu einem Alkylierungsgrad von zwei an und sinken daraufhin stark ab, was laut Yunker (2002) auf einen anthropogenen Eintrag durch Erdöl hinweist. Ähnliche Ergebnisse konnten für die PAK FLO, PHE und PYR festgestellt werden.

In Kombination mit den zuvor berechneten Isomerenverhältnissen kann eine pyrolytische Quelle, die unvollständige Verbrennung fossiler Brennstoffe wie Erdöl, über den gesamten Salzgradienten postuliert werden. In Richtung der zentralen und südlichen Ostsee gewinnt dieser Trend sogar an Bedeutung, in guter Übereinstimmung mit der industriellen Entwicklung und dem zunehmenden Schiffsverkehr zur Nordsee hin. (Helcom, 2010) Dabei ist anzunehmen, dass organische Stoffe, die durch unvollständige Verbrennung gebildet werden, größtenteils über die Atmosphäre in das marine System eingetragen werden. (Pazdro, 2004; Motelay-Massei, 2006)

## 8. Zusammenfassung und Ausblick

In dieser Arbeit konnte erfolgreich ein analytisches System bestehend aus Pyrolysator, Gaschromatograph und zwei selektiven Massenspektrometern konzipiert und angewendet werden. Ziel war es, in einem direkten Vergleich zwischen REMPI-ToFMS und EI-QMS die unterschiedliche Selektivität zur Charakterisierung von Komponenten zu nutzen und hochmolekulare Strukturen zu erfassen, um diese getrennt voneinander zu charakterisieren. Mit der leistungsstarken GC-Trennung und einer Kombination aus universeller (EI) sowie selektiver und sensitiver (REMPI) Detektion von Aromaten, ist eine verbesserte Strukturaufklärung von hochkomplexen Proben möglich. Die erhaltenen Peakintensitäten in den Chromatogrammen durch EI und REMPI (266 nm) sind substanzspezifisch für die hier genutzte Wellenlänge von 266 nm. (Muller, 2012; Haeffliger, 1998)

Rohöl zeichnet sich durch eine nahezu unüberschaubare Komponentenvielfalt aus und stellt ein ideales Forschungsobjekt für die Erprobung des gekoppelten Systems dar. Speziell die Identifizierung von niedrig konzentrierten Spezies wie den PAK und PASH gestaltet sich oft schwierig, gelingt aber mit dem neuen System. Durch REMPI werden aromatische Strukturen zugänglich, die sich aufgrund der niedrigen Konzentrationen beim EI-QMS nur bei genauerer, gezielter Betrachtung der Chromatogramme zeigen. Allerdings werden Strukturvorschläge mittels Datenbankenabgleich aus der EI-QMS-Analyse benötigt, um Komponenten und sofern möglich Isomere zu unterscheiden. Die erhaltenen Informationen spielen eine entscheidende Rolle und können den Prozess der Rohölaufarbeitung verbessern.

Die Effizienz der Kopplung zeigt sich bei einer weiterführenden Umweltstudie, die sich mit der Charakterisierung und der Abbaubarkeit von terrigenem eingetragenen, gelösten organischen Material im marinen System befasst, welches vermehrt infolge der Klimaerwärmung mit ungeklärten Folgen für das Ökosystem eingebracht wird. Die Ostsee stellt in diesem Zusammenhang ein ideales Forschungsobjekt dar. Dabei wird der Einfluss von biotischen und abiotischen Faktoren auf das tDOM untersucht. Für diese Studie werden spezielle Ligninmarker herausgegriffen und der Einfluss von Salzgehalt sowie eines möglichen mikrobiellen Abbaus untersucht. Es zeigt sich, dass ersterer einen großen Einfluss auf die DOM-Zusammensetzung hat. Zudem liegt der Hauptanteil der Komponenten in Form hochmolekularer Verbindungen vor. Aus den Inkubationsversuchen wird deutlich, dass sich die Zusammensetzung von niedermolekularen DOM kaum ändert. Auch im hochmolekularen

Bereich werden jedoch keine nennenswerten Veränderungen festgestellt. Daher hat der vermehrte Eintrag von terrigenem Material in die Ozeane laut dieser Studie innerhalb der betrachteten Zeitskala von 110 Tagen und der vorherrschenden mikrobiellen Artenvielfalt in der Ostsee keinen Einfluss auf deren Verstoffwechselung zu Kohlenstoffdioxid. Dies müsste allerdings in weiterführenden Studien diskutiert werden, zu denen diese Arbeit einen Ausgangspunkt darstellen kann.

Die strukturelle Charakterisierung von hochmolekularen PAK und deren anthropogener Eintrag sowie Verteilung entlang des Ostseetransektes wurden abschließend untersucht. Dazu konnten spezifische PAK-Marker herausgegriffen und deren Alkylierungsverhalten aufgezeigt werden. Über spezielle Isomerenverhältnisse wird die unvollständige Verbrennung von fossilen Brennstoffen als Haupteintragsquelle postuliert. Die Ostsee (Bottnischer Meerbusen, Zentrale Ostsee und Skagerrak/Kattegat) zeigt halbquantitativ betrachtet durchaus einen Trend im PAK-Profil, der mit der Zivilisations- und Industriedichte korreliert.

Es konnte anhand der drei Applikationen gezeigt werden, dass das entwickelte System sehr effizient sowie universell einsetzbar ist und für weiterführende Umweltstudien hilfreiche Dienste leisten kann. Neben einer möglichen Probenaufgabe mit festen und flüssigen Matrices sind auch klassisch nicht GC-gängige Komponenten mit hohem Molekulargewicht als Pyrolysefragmente zugänglich. Die Messanordnung könnte durch die Verwendung anderer weicher Ionisierungstechniken, wie der „Single-Photon-Ionisierung“ (Fendt, 2011) erweitert werden. Um eine höhere Trennkapazität zu gewährleisten, könnte ein mehrdimensionales GCxGC-System zum Einsatz kommen. (Edam, 2005; Miyabayashi, 2009) Bei der Verwendung anderer Wellenlängen für das REMPI-System oder eine Erhöhung der LASER-Frequenz, könnte das Substanzspektrum verändert und zusätzlich erweitert werden (Smith, 2009; Li, 2011).

Die erhaltenen Informationen wie Isomerenverteilung, Kettenlängen und die Größe von aromatischen Strukturen oder der Anteil an Substanzen mit Heteroatomen sind wichtige Parameter, um die Effizienz der Rohölaufarbeitung zu verbessern oder Kontaminationen eines Umweltkompartiments zu beschreiben, so dass mögliche Eintragsquellen zu ermitteln sind. Die Quantifizierung zumeist aromatischer Strukturen, in Verbindung mit der Ermittlung von Wirkungsquerschnitten, ist eine vielversprechende Einsatzmöglichkeit und zugleich ein wichtiger, zukunftsweisender Forschungsschwerpunkt.

## 9. Literatur

- Adam, T. W.; Clairotte, M.; Streibel, T.; Elsasser, M.; Pommeres, A.; Manfredi, U.; Carriero, M.; Martini, G.; Sklorz, M.; Krasenbrink, A.; Astorga, C.; Zimmermann, R., Real-time analysis of aromatics in combustion engine exhaust by resonance-enhanced multiphoton ionisation time-of-flight mass spectrometry (REMPI-TOF-MS): a robust tool for chassis dynamometer testing. *Analytical and Bioanalytical Chemistry* 2012, 404, (1), 273-276.
- Andersson, J.T., Hegazi, A.H. and Roberz, B., 2006. Polycyclic aromatic sulfur heterocycles as information carriers in environmental studies. *Analytical and Bioanalytical Chemistry*, 386(4): 891-905.
- Bayerbach, D.-H. R., 2006. Über die Struktur der oligomeren Bestandteile von Flash-Pyrolyseölen aus Biomasse; Dissertationsarbeit zur Erlangung des Doktorgrades im Department Biologie der Fakultät Mathematik, Informatik und Naturwissenschaften an der Universität Hamburg
- Benner, R. and Kaiser, K., 2011. Biological and photochemical transformations of amino acids and lignin phenols in riverine dissolved organic matter. *Biogeochemistry*, 102(1-3): 209-222.
- Bianchi, T.S., 2011. The role of terrestrially derived organic carbon in the coastal ocean: A changing paradigm and the priming effect (vol 108, pg 19473, 2011). *Proceedings of the National Academy of Sciences of the United States of America*, 109(13).
- Brody, J. G.; Moysich, K. B.; Humblet, O.; Attfield, K. R.; Beehler, G. P.; Rudel, R. A., 2007. Environmental pollutants and breast cancer - Epidemiologic studies. *Cancer*, 109(12): 2667-2711.
- Broman, D.; Naf, C.; Rolff, C.; Zebuhr, Y., 1991. Occurrence and dynamics of polychlorinated dibenzo-para-dioxins and dibenzofurans and polycyclic aromatic-hydrocarbons in the mixed surface-layer of remote coastal and offshore waters of the Baltic. *Environmental science & technology*, 25(11): 1850-1864.
- Bundesanstalt für Geowissenschaften und Rohstoffe (BGR) für die Deutsche Rohstoffagentur (DERA) in der Reihe DERA Rohstoffinformationen, Hannover, 2011; [http://www.bgr.bund.de/DE/Themen/Energie/energie\\_node.html](http://www.bgr.bund.de/DE/Themen/Energie/energie_node.html)
- Cammann, Karl, 2001. Instrumentelle Analytische Chemie: Verfahren, Anwendung und Qualitätssicherung; Spektrum Akademischer Verlag GmbH Heidelberg – Berlin.
- Chiou, C.T., McGroddy, S.E. and Kile, D.E., 1998. Partition characteristics of polycyclic aromatic hydrocarbons on soils and sediments. *Environmental Science and Technology*, 32(2): 264-269.

- Dittmar, T. and Kattner, G., 2003. The biogeochemistry of the river and shelf ecosystem of the Arctic Ocean: a review. *Marine Chemistry*, 83(3-4): 103-120.
- Dittmar, T., Whitehead, K., Minor, E.C. and Koch, B.P., 2007. Tracing terrigenous dissolved organic matter and its photochemical decay in the ocean by using liquid chromatography/mass spectrometry. *Marine Chemistry*, 107(3): 378-387.
- Dittmar, T., Koch, B., Hertkorn, N. and Kattner, G., 2008. A simple and efficient method for the solid-phase extraction of dissolved organic matter (SPE-DOM) from seawater, *Limnology and Oceanography-Methods*, 6: 230-235.
- Dixon, R. K., Brown S., Houghton, R. A., Solomon, A. M., Trexler, M. C., Wisniewski, J., 1994. Carbon pools and flux of global forest ecosystems. *Science* 263(5144): 185-190.
- Donaldson, E. C., G. V. Chilingsrian, 1985. Enhanced Oil Recovery I - Fundamentals and Analyses. Elsevier Science Publishers B. V., New York.
- Edam, R., Blomberg, J., Janssen, H.G. and Schoenmakers, P.J., 2005. Comprehensive multi-dimensional chromatographic studies on the separation of saturated hydrocarbon ring structures in petrochemical samples. *Journal of Chromatography A*, 1086(1-2): 12-20.
- Energiestudie 2012 – Reserven, Ressourcen und Verfügbarkeit von Energierohstoffen; Bundesanstalt für Geowissenschaften und Rohstoffe (BGR) für die Deutsche Rohstoffagentur (DERA) in der Reihe DERA Rohstoffinformationen; Hannover 2011; [http://www.bgr.bund.de/DE/Themen/Energie/energie\\_node.html](http://www.bgr.bund.de/DE/Themen/Energie/energie_node.html)
- Ertel, J.R., Hedges, J.I. and Perdue, E.M., 1984. Lignin signature of aquatic humic substances. *Science*, 223(4635): 485-487.
- Eschner, M. S.; Welthagen, W.; Groger, T. M.; Gonin, M.; Fuhrer, K.; Zimmermann, R., Comprehensive multidimensional separation methods by hyphenation of single-photon ionization time-of-flight mass spectrometry (SPI-TOF-MS) with GC and GCxGC. *Anal. and Bioanal. Chem.* 2010, 398, (3), 1435-1445.
- Fan, T.G. and Buckley, J.S., 2002. Rapid and accurate SARA analysis of medium gravity crude oils. *Energy & Fuels*, 16(6): 1571-1575.
- Fellman, J. B.; Spencer, R. G. M.; Hernes, P. J.; Edwards, R. T.; D'Amore, D. V.; Hood, E., 2010. The impact of glacier runoff on the biodegradability and biochemical composition of terrigenous dissolved organic matter in near-shore marine ecosystems. *Marine Chemistry*, 121(1-4): 112-122.



- Fendt, A., Streibel, T., Sklorz, M., Richter, D., Dahmen, N., Zimmermann, R., 2011. On-Line Process Analysis of Biomass Flash Pyrolysis Gases Enabled by Soft Photoionization Mass Spectrometry. *Energy & Fuels*, 26(1): 701-711.
- Fendt, A., Geissler, R., Streibel, T., Sklorz, M. and Zimmermann, R., 2012. Hyphenation of two simultaneously employed soft photo ionization mass spectrometers with thermal analysis of biomass and biochar. *Thermochimica Acta*, 551: 155-163.
- Gagni, S. and Cam, D., 2007. Stigmastane and hopanes as conserved biomarkers for estimating oil biodegradation in a former refinery plant-contaminated soil. *Chemosphere*, 67(10): 1975-1981.
- Geissler, R., Saraji-Bozorgzad, M., Streibel, T., Kaisersberger, E., Denner, T., Zimmermann, R., 2009a. Investigation of different crude oils applying thermal analysis/mass spectrometry with soft photoionisation. *Journal of Thermal Analysis and Calorimetry*, 96(3): 813-820.
- Geissler, R., Saraji-Bozorgzad, M. R., Groger, T., Fendt, A., Streibel, T., Sklorz, M., Krooss, B. M., Fuhrer, K., Gonin, M., Kaisersberger, E., Denner, T., Zimmermann, R., 2009b. Single Photon Ionization Orthogonal Acceleration Time-of-Flight Mass Spectrometry and Resonance Enhanced Multiphoton Ionization Time-of-Flight Mass Spectrometry for Evolved Gas Analysis in Thermogravimetry: Comparative Analysis of Crude Oils. *Analytical Chemistry*, 81(15): 6038-6048.
- Goni, M. A. and Hedges, J. I., 1995. Sources and reactivities of marine-derived organic-matter in coastal sediments as determined by alkaline CuO oxidation, *Geochimica Et Cosmochimica Acta*, 59(14): 2965-2981.
- Groenzin, H., Mullins, O. C., 2000. Molecular size and structure of asphaltenes from various sources, *Energy Fuels*, 14(3): 677-684.
- Haefliger, O.P. and Zenobi, R., 1998. Laser mass spectrometric analysis of polycyclic aromatic hydrocarbons with wide wavelength range laser multiphoton ionization spectroscopy. *Analytical Chemistry*, 70(13): 2660-2665.
- Hao, C. Y.; Headley, J. V.; Peru, K. A.; Frank, R.; Yang, P.; Solomon, K. R., Characterization and pattern recognition of oil-sand naphthenic acids using comprehensive two-dimensional gas chromatography/time-of-flight mass spectrometry. *J. Chromatog. A* 2005, 1067, (1-2), 277-284.
- Hedges, J.I. and Ertel, J.R., 1982. Characterisation of lignin by gas capillary chromatography of cupric oxide oxidation-products. *Analytical Chemistry*, 54(2), 174-178

- Heidenreich, A., 2005. Methodenentwicklung zur Charakterisierung und Quantifizierung von kosmetiktypischen Polymeren mittels Pyrolyse-Gaschromatographie / Massenspektrometrie; Dissertationsarbeit zur Erlangung des Doktorgrades im Fachbereich Chemie - Universität Hamburg.
- HELCOM, 2010. Report on Shipping Accidents in the Baltic Sea Area for the Year.
- Herlemann, D. P. R.; Labrenz, M.; Juergens, K.; Bertilsson, S.; Waniek, J. J.; Andersson, A. F., 2011. Transitions in bacterial communities along the 2000 km salinity gradient of the Baltic Sea. *Isme Journal*, 5(10): 1571-1579.
- Herlemann, D. P. R.; Manecki, M.; Meeske, C.; Pollehne, F.; Labrenz, M.; Schulz-Bull, D.; Dittmar, T.; Juergens, K., 2014. Uncoupling of bacterial and terrigenous dissolved organic matter dynamics in decomposition experiments, *PloS one*, 9(4): e93945-e93945.
- Hernes, P.J. and Benner, R., 2006, Terrigenous organic matter sources and reactivity in the North Atlantic Ocean and a comparison to the Arctic and Pacific oceans, *Marine Chemistry*, 100(1-2), 66-79
- Herod, A. A.; Bartle, K. D.; Kandiyoti, R., Characterization of heavy hydrocarbons by chromatographic and mass spectrometric methods: An overview. *Energy Fuels* 2007, 21, (4), 2176-2203.
- Humborg, C.; Smedberg E.; Blomqvist S.; Mörtz C. M.; Brink J.; Rahm L.; Danielsson Å.; Sahlberg J., 2004. Nutrient variations in boreal and subarctic Swedish rivers: Landscape control of land-sea fluxes. *Limnology and Oceanography*, 49(5): 1871-1883.
- Imasaka, T., 2013. Gas chromatography/multiphoton ionization/time-of-flight mass spectrometry using a femtosecond laser. *Analytical and Bioanalytical Chemistry*, 405(22): 6907-6912.
- Kim, K.-H., Jahan, S.A., Kabir, E. and Brown, R.J.C., 2013. A review of airborne polycyclic aromatic hydrocarbons (PAHs) and their human health effects. *Environment International*, 60: 71-80.
- Kisand, V., Rocker D., Simon M., 2008. Significant decomposition of riverine humic-rich DOC by marine but not estuarine bacteria assessed in sequential chemostat experiments. *Aquatic Microbial Ecology*, 53: 151-160
- Kisand, V., Gebhardt, S., Rullkotter, J. and Simon, M., 2013. Significant bacterial transformation of riverine humic matter detected by pyrolysis GC-MS in serial chemostat experiments. *Marine Chemistry*, 149: 23-31.

- Li, A., Uchimura, T., Tsukatani, H. and Imasaka, T., 2010. Trace Analysis of Polycyclic Aromatic Hydrocarbons Using Gas Chromatography-Mass Spectrometry Based on Nanosecond Multiphoton Ionization. *Analytical Sciences*, 26(8): 841-846.
- Li, A., Uchimura, T., Watanabe-Ezoe, Y. and Imasaka, T., 2011a. Analysis of Dioxins by Gas Chromatography/Resonance-Enhanced Multiphoton Ionization/Mass Spectrometry Using Nanosecond and Picosecond Lasers. *Analytical Chemistry*, 83(1): 60-66.
- Li, A., Imasaka, T. and Uchimura, T., 2011b. Analysis of pesticides by gas chromatography/multiphoton ionization/mass spectrometry using a femtosecond laser. *Analytica Chimica Acta*, 701(1): 52-59.
- Lipiatou, E.; Tolosa, I.; Simó, R.; Bouloubassi, I.; Dachs, J.; Marti, S.; Sicre, M.-A.; Bayona, J.M.; Grimalt, J.O.; Salot, A.; Albaigés, J., 1997. Mass budget and dynamics of polycyclic aromatic hydrocarbons in the Mediterranean Sea. *Deep-Sea Research Part II: Topical Studies in Oceanography*, 44(3-4): 881-905.
- Lubecki, L. and Kowalewska, G., 2012. Indices of PAH Origin-A Case Study of the Gulf of Gdansk (SE Baltic) Sediments. *Polycyclic Aromatic Compounds*, 32(3): 335-363.
- Miltner, A. and Emeis, K.C., 2001, Terrestrial organic matter in surface sediments of the Baltic Sea, Northwest Europe, as determined by CuO oxidation, *Geochimica Et Cosmochimica Acta*, 65(8), 1285-1299
- Miyabayashi, K., Naito, Y. and Miyake, M., 2009. Characterization of Heavy Oil by FT-ICR MS Coupled with Various Ionization Techniques. *Journal of the Japan Petroleum Institute*, 52(4): 159-171.
- Motelay-Massei, A., Garban, B., Tiphagne-larcher, K., Chevreuil, M. and Ollivon, D., 2006. Mass balance for polycyclic aromatic hydrocarbons in the urban watershed of Le Havre (France): Transport and fate of PAHs from the atmosphere to the outlet. *Water Research*, 40(10): 1995-2006.
- Moore, S. W.; Ramamoorthy, S., 1984. *Organic Chemicals in Natural Water*. Springer-Verlag, New York.
- Motelay-Massei, A., Garban, B., Tiphagne-larcher, K., Chevreuil, M. and Ollivon, D., 2006. Mass balance for polycyclic aromatic hydrocarbons in the urban watershed of Le Havre (France): Transport and fate of PAHs from the atmosphere to the outlet. *Water Research*, 40(10): 1995-2006.

- Muller, H., Adam, F.M., Panda, S.K., Al-Jawad, H.H. and Al-Hajji, A.A., 2012. Evaluation of Quantitative Sulfur Speciation in Gas Oils by Fourier Transform Ion Cyclotron Resonance Mass Spectrometry: Validation by Comprehensive Two-Dimensional Gas Chromatography. *Journal of the American Society for Mass Spectrometry*, 23(5): 806-815.
- Mullins, O.C., Sheu, E.Y., Hammami, A. and Marshall, A.G., 2007. *Asphaltenes, Heavy Oils, and Petroleomics*. Springer Science+Business Media, New York.
- Nebbioso, A. and Piccolo, A., 2013. Molecular characterization of dissolved organic matter (DOM): a critical review. *Analytical and bioanalytical chemistry*, 405(1): 109-24.
- Neff, J. M., 1979. *Polycyclic aromatic hydrocarbons in the aquatic environment*; Applied Science Publishers Ltd., London.
- Nocun, M. and Andersson, J.T., 2012. Argentation chromatography for the separation of polycyclic aromatic compounds according to ring number. *Journal of Chromatography A*, 1219: 47-53.
- Opsahl, S. and Benner, R., 1997. Distribution and cycling of terrigenous dissolved organic matter in the ocean. *Nature*, 386(6624): 480-482.
- Opsahl, S. and Benner, R., 1998. Photochemical reactivity of dissolved lignin in river and ocean waters. *Limnology and Oceanography*, 43(6): 1297-1304.
- Panda, S.K., Schrader, W. and Andersson, J.T., 2008. Fourier transform ion cyclotron resonance mass spectrometry in the speciation of high molecular weight sulfur heterocycles in vacuum gas oils of different boiling ranges. *Analytical and Bioanalytical Chemistry*, 392(5): 839-848.
- Panda, S.K., Andersson, J.T. and Schrader, W., 2009. Characterization of Supercomplex Crude Oil Mixtures: What Is Really in There? *Angewandte Chemie-International Edition*, 48(10): 1788-1791.
- Pazdro, K., 2004. Persistent Organic Pollutants in Sediments from the Gulf of Gdansk. *Ann Set Environ Prot.* 6: 63-76
- Reunamo, A., Riemann, L., Leskinen, P. and Jorgensen, K.S., 2013. Dominant petroleum hydrocarbon-degrading bacteria in the Archipelago Sea in South-West Finland (Baltic Sea) belong to different taxonomic groups than hydrocarbon degraders in the oceans. *Marine Pollution Bulletin*, 72(1): 174-180.
- Rocker, D., Brinkhoff, T., Gruener, N., Dogs, M. and Simon, M., 2012a. Composition of humic acid-degrading estuarine and marine bacterial communities. *Fems Microbiology Ecology*, 80(1): 45-63.

- Rocker, D., Kisand V., Scholz-Böttcher B., Kneib T., Lemke A., Rullkötter J., Simon M., 2012b. Differential decomposition of humic acids by marine and estuarine bacterial communities at varying salinities. *Biogeochemistry*, 111(1-3): 331-346.
- Rogowska, J., Wolska, L. and Namiesnik, J., 2010. Impacts of pollution derived from ship wrecks on the marine environment on the basis of s/s "Stuttgart" (Polish coast, Europe). *Science of the Total Environment*, 408(23): 5775-5783.
- Rosenstock, B., Zwisler, W. and Simon, M., 2005. Bacterial consumption of humic and non-humic low and high molecular weight DOM and the effect of solar irradiation on the turnover of labile DOM in the Southern Ocean. *Microbial Ecology*, 50(1): 90-101.
- Ruczynska, W.M., Szlinder-Richert, J., Malesa-Ciecwierz, M. and Warzocha, J., 2011. Assessment of PAH pollution in the southern Baltic Sea through the analysis of sediment, mussels and fish bile. *Journal of Environmental Monitoring*, 13(9): 2535-2542.
- Schwarzenbach, R. P., Gschwend, P. M., Imboden, D. M., 2003. Sorption of Natural Compounds to "Dissolved" Organic Matter (DOM). *Environmental Organic Chemistry* (second edition), 9.4: 314-321.
- Shiah, F. and Ducklow, H. W., 1995. Multiscale variability in bacterioplankton abundance, production, and specific growth rate in a temperate salt-marsh tidal creek. *Limnology and Oceanography*, 40(1): 55-66.
- Sholkovitz, E. R., 1976. Flocculation of dissolved organic and inorganic matter during mixing of river water and sea water. *Geochimica Et Cosmochimica Acta*, 40(7): 831-845.
- Sleighter, R. L. and P. G. Hatcher, 2008. Molecular characterization of dissolved organic matter (DOM) along a river to ocean transect of the lower Chesapeake Bay by ultrahigh resolution electrospray ionization Fourier transform ion cyclotron resonance mass spectrometry. *Marine Chemistry*, 110(3-4): 140-152.
- Smith, D.F., Rodgers, R.P., Rahimi, P., Teclemariam, A. and Marshall, A.G., 2009. Effect of Thermal Treatment on Acidic Organic Species from Athabasca Bitumen Heavy Vacuum Gas Oil, Analyzed by Negative-Ion Electrospray Fourier Transform Ion Cyclotron Resonance (FT-ICR) Mass Spectrometry. *Energy & Fuels*, 23(1): 314-319.
- Stader, C., Beer, F.T. and Achten, C., 2013. Environmental PAH analysis by gas chromatography-atmospheric pressure laser ionization-time-of-flight-mass spectrometry (GC-APLI-MS). *Analytical and Bioanalytical Chemistry*, 405(22): 7041-7052.
- Tam, N.F.Y., Ke, L., Wang, X.H. and Wong, Y.S., 2001. Contamination of polycyclic aromatic hydrocarbons in surface sediments of mangrove swamps. *Environmental Pollution*, 114(2): 255-263.

- Tamocai, C., J. G. Canadell, Schuur, E. A. G., Kuhry, P., Mazhitova, G., Zimov, S., 2009. Soil organic carbon pools in the northern circumpolar permafrost region. *Global Biogeochemical Cycles*, 23(2).
- Teravainen, M.J., Pakarinen, J.M.H., Wickstrom, K. and Vainiotalo, P., 2007. Comparison of the composition of Russian and North Sea crude oils and their eight distillation fractions studied by negative-ion electrospray ionization Fourier transform ion cyclotron resonance mass spectrometry: The effect of suppression. *Energy & Fuels*, 21(1): 266-273.
- Thiele-Bruhn, S. and Brummer, G.W., 2005. Kinetics of polycyclic aromatic hydrocarbon (PAH) degradation in long-term polluted soils during bioremediation. *Plant and Soil*, 275(1-2): 31-42.
- Wang, J.Z., Guan, Y.F., Ni, H.G., Luo, X.L. and Zeng, E.Y., 2007. Polycyclic aromatic hydrocarbons in riverine runoff of the pearl river delta (China): Concentrations, fluxes, and fate. *Environmental science & technology*, 41(16): 5614-5619.
- Welthagen, W., Mitschke, S., Muhlberger, F., Zimmermann, R., 2007. One-dimensional and comprehensive two-dimensional gas chromatography coupled to soft photo ionization time-of-flight mass spectrometry: A two- and three-dimensional separation approach. *J. Chromatog. A*, 1150(1-2): 54-61.
- Wikner, J., Cuadros, R. and Jansson, M., 1999. Differences in consumption of allochthonous DOC under limnic and estuarine conditions in a watershed. *Aquatic Microbial Ecology*, 17(3): 289-299.
- Witt, G., 1995. Polycyclic aromatic hydrocarbons in water and sediment of the Baltic Sea. *Marine Pollution Bulletin*, 31(4-12): 237-248.
- Witt, G., Liehr, G.A., Borck, D. and Mayer, P., 2009. Matrix solid-phase microextraction for measuring freely dissolved concentrations and chemical activities of PAHs in sediment cores from the western Baltic Sea. *Chemosphere*, 74(4): 522-529.
- World Energy Outlook 2011. International Energy Agency; Paris.
- Wu, Y.-L., Wang, X.-H., Li, Y.-Y. and Hong, H.-S., 2011. Occurrence of polycyclic aromatic hydrocarbons (PAHs) in seawater from the Western Taiwan Strait, China. *Marine Pollution Bulletin*, 63(5-12): 459-463.
- Yunker, M. B.; Macdonald, R. W.; Vingarzan, R.; Mitchell, R. H.; Goyette, D.; Sylvestre, S., 2002. PAHs in the Fraser River basin: a critical appraisal of PAH ratios as indicators of PAH source and composition. *Organic Geochemistry*, 33(4): 489-515.

- Zimmermann, R., Lerner, C., Schramm, K.W., Kettrup, A. and Boesl, U., 1995. 3-dimensional trace analysis-combination of gas-chromatography, supersonic beam UV spectroscopy and Time-of-Flight mass-spectrometry. *European Mass Spectrometry*, 1(4): 341-351.
- Zuidhoff, F.S. and Kolstrup, E., 2000. Changes in palsa distribution in relation to climate change in Laivadalen, northern Sweden, especially 1960-1997. *Permafrost and Periglacial Processes*, 11(1): 55-69.



## 10. Anhang

### I. Abbildungsverzeichnis

Abb. 1:	Verteilung (in %) des Primärenergiebedarfs in den Jahren 2011 und 2035 gemäß des Ausblicks der ICA 2011.....	10
Abb. 2:	Elementare Zusammensetzung von konventionellem Rohöl.....	11
Abb. 3:	Trennung von Komponenten im Rohöl.....	11
Abb. 4:	Fraktionen im Rohöl.....	12
Abb. 5:	PAK- und PASH-Strukturen.....	13
Abb. 6:	Meteor.....	15
Abb. 7:	Stationsplan der Expedition.....	15
Abb. 8:	Details zu den Probestandorten.....	16
Abb. 9:	Lignin und phenolische Abbauprodukte.....	17
Abb. 10:	Schema der "harten" (EI) und der "weichen" (REMPI) Ionisierung im Vergleich [X: Elektronischer Grundzustand; X*: angeregter Zwischenzustand; $X^+$ : Ionisationskontinuum].....	20
Abb. 11:	Thermische Analyse von Rohöl in direkter Anbindung zum REMPI-ToFMS. Der schematische Aufbau (links), in dem der Gaschromatograph als kontinuierliches Heizsystem genutzt wird und nicht zur Trennung der Komponenten beiträgt.....	23
Abb. 12:	Aufbau Pyrolysator-GC/MS (EI-QMS und REMPI-ToFMS).....	24
Abb. 13:	Direkter Vergleich der Chromatogramme die aus den REMPI-ToFMS (oben) und EI-QMS-Messungen (unten) für die DOM-Zusammensetzung in der nördlichen Ostsee (At4-Station) resultieren.....	25
Abb. 14:	Thermogramme zu 5 Rohölen durch direkte Kopplung von Pyrolysator und REMPI-ToFMS.....	27
Abb. 15:	Links: PAH-Standard gemessen durch das Py-GC/MS-System. Dargestellt ist der SIM-Modus unter EI-Bedingungen. Rechts: Chromatogramm (REMPI-ToFMS) von Türkischen Rohöl mit identifizierten PAK-Komponenten bei 300 °C (oben) und 600 °C (unten) Injektionstemperatur....	28
Abb. 16:	Verteilung von PAK-Vertretern in fünf Rohölproben bis zum vierten Alkylierungsgrad (C <sub>4</sub> ).....	29

Abb. 17:	DBT und seine alkylierten Vertreter ( $C_x$ ) in Griechischen Rohöl. Direkter Vergleich relevanter Ionenspuren zwischen EI-QMS und REMPI-ToFMS unter TD-Bedingungen.....	30
Abb. 18:	Probenaufarbeitung durch Filtration und Festphasenextraktion.....	32
Abb. 19:	(a) Probensammler, (b) Experimentelles Design und (c) zeitliche Abfolge der Probennahme mit drei biologischen Replikaten nach 110 Tagen Inkubation.....	33
Abb. 20:	Trendverlauf für einzelne Moleküle entlang der Salzlinie (salzarm zu salzreich) und während der Inkubation.....	35
Abb. 21:	Darstellung der Iosomenverhältnisse (EI-Daten, Pyrolysebedingungen) von ANT/(ANT+PHE) und FLU/(FLU+PYR) gegen den Salzgradienten der Ostsee. Die farbigen Bereiche stehen für eine spezifische Eintragsquelle in das marine System.....	37

## II. Abkürzungsverzeichnis

ACE	Acenaphthen
ACY	Acenaphthylen
AG	Arbeitsgruppe
ANT	Anthracen
BaANT	Benz(a)anthracen
BaPYR	Benz(a)pyren
BghiPER	Benz(ghi)perylene
BNT	Benzonaphtothiophen
BT	Benzothiophen
C <sub>x</sub>	Alkylierungsgrad (x.. Anzahl der –CH <sub>2</sub> - Anbindungen)
DBahANT	Dibenz(ah)anthracen
DBT	Dibenzothiophen
DSMZ	Leibniz-Institut Deutsche Sammlung von Mikroorganismen und Zellkulturen GmbH
DOM	Gelöstes organisches Material (dissolved organic matter)
EI	Elektronenstoßionisation (electron impact)
FLO	Fluoren
FLU	Fluoranthren
FT-ICRMS	Ionen-Zyklotron-Resonanz-Massenspektrometrie (Fourier transform ion cyclotron resonance mass spectrometry)
GC	Gaschromatografie (gas chromatography)
IGB	Leibniz-Institut für Gewässerökologie und Binnenfischerei
ICA	International Energy Agency
ICBM	Institut für Chemie und Biologie des Meeres (Universität Oldenburg)
MfN	Museum für Naturkunde
MPI	Max-Planck-Institut
MS	Massenspektrometrie

NAP	Naphthalin
PHE	Phenanthren
PYR	Pyren
QMS	Quadrupolmassenspektrometrie (quadrupole mass spectrometry)
REMPI	Resonanzverstärkte-Multiphotonionisation (resonance-enhanced-multi-photonionisation)
SIM	Single Ion Monitoring
tDOM	Terrigen gelöstes organisches Material
TD	Thermodesorption
ToFMS	Flugzeitmassenspektrometrie (time-of-flight mass spectrometry)

### III. Liste an Publikationen für den Dokortitel

1. Otto, S.; Streibel T.; Erdmann S.; Sklorz M.; Schulz-Bull D.; Zimmermann R., 2015. Application of pyrolysis-mass spectrometry and pyrolysis-gas chromatography-mass spectrometry with electron-ionization or resonance-enhanced-multi-photon-ionization for characterization of crude oils. *Analytica Chimica Acta* 855: 60-69.
2. Otto, S.; Erdmann, S.; Streibel, T.; Herlemann, PR D.; Schulz-Bull, D.; Zimmermann, R., 2016. Pyrolysis-gas chromatography-mass spectrometry with electron-ionization and resonance-enhanced-multi-photon-ionization for characterization of terrestrial dissolved organic matter in the Baltic Sea. *Analytical Methods* 8: 2592-2603.
3. Otto, S.; Streibel, T.; Erdmann, S.; Klingbeil, S.; Schulz-Bull, D.; Zimmermann, R., 2015. Pyrolysis-gas chromatography-mass spectrometry with electron-ionization or resonance-enhanced-multi-photon-ionization for characterization of polycyclic aromatic hydrocarbons in the Baltic Sea. *Marine Pollution Bulletin* 99: 35-42.

#### Darlegung des persönlichen Beitrages:

Publikation	Persönlicher Beitrag:
1	<ul style="list-style-type: none"> <li>• Entwicklung und Optimierung der Kopplungsmethode</li> <li>• Wartung der verbauten Analysesysteme</li> <li>• Probenaufarbeitung und -vermessung der Rohöle</li> <li>• Auswertung der Messergebnisse</li> </ul>
2	<ul style="list-style-type: none"> <li>• Planung und Expeditionsmitglied auf dem Forschungsschiff „Meteor“</li> <li>• Konzeption und Durchführung der Probennahme zur Salzlinie und Inkubationsexperimenten</li> <li>• Durchführung der Probenaufarbeitung auf dem Schiff</li> <li>• Messung der Proben</li> <li>• Datenauswertung und Präsentation in Projektmeetings</li> </ul>
3	<ul style="list-style-type: none"> <li>• Analyse der Proben</li> <li>• Datenauswertung</li> </ul>

## IV. Publikationen

### Publikation 1

Otto, S.; Streibel, T.; Erdmann S.; Sklorz, M.; Schulz-Bull, D.; Zimmermann, R., 2015. Application of pyrolysis-mass spectrometry and pyrolysis-gas chromatography-mass spectrometry with electron-ionization or resonance-enhanced-multi-photon-ionization for characterization of crude oils. *Analytica Chimica Acta* 855: 60-69.  
(DOI: 10.1016/j.aca.2014.11.030)



# Application of pyrolysis–mass spectrometry and pyrolysis–gas chromatography–mass spectrometry with electron-ionization or resonance-enhanced-multi-photon ionization for characterization of crude oils



Stefan Otto<sup>a</sup>, Thorsten Streibel<sup>a,b,\*</sup>, Sabrina Erdmann<sup>a</sup>, Martin Sklorz<sup>a,b</sup>,  
Detlef Schulz-Bull<sup>c</sup>, Ralf Zimmermann<sup>a,b</sup>

<sup>a</sup>Joint Mass Spectrometry Centre, Chair of Analytical Chemistry, Institute of Chemistry, University of Rostock, 18059 Rostock, Germany

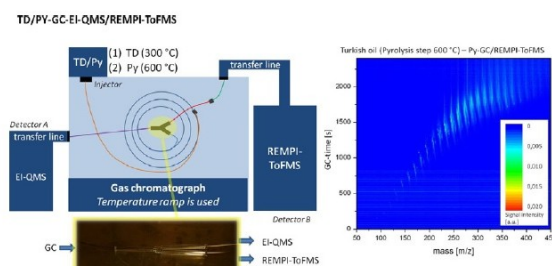
<sup>b</sup>Joint Mass Spectrometry Centre, Cooperation Group Comprehensive Molecular Analytics, Institute of Ecological Chemistry, Helmholtz Zentrum München-German Research Center of Environmental Health (GmbH), Ingolstädter Landstrasse 1, 85764 Neuherberg, Germany

<sup>c</sup>Marine Chemistry, Leibniz Institute for Baltic Sea Research, Warnemünde, Seestrasse 15, 18119 Rostock, Germany

## HIGHLIGHTS

- Gas chromatography setup with two MS detectors applying different ionization methods.
- In parallel structural information and sensitive detection of aromatic species.
- Characterization of setup and application for crude oil samples.
- Detection of polycyclic aromatic hydrocarbons next to sulfur containing aromatics.

## GRAPHICAL ABSTRACT



## ARTICLE INFO

### Article history:

Received 15 September 2014

Received in revised form 20 November 2014

Accepted 23 November 2014

Available online 27 November 2014

### Keywords:

Pyrolysis–GC/MS

Resonance enhanced multi-photon ionization

Electron ionization

Crude oil

Polycyclic aromatic hydrocarbons

## ABSTRACT

A novel analytical system for gas-chromatographic investigation of complex samples has been developed, that combines the advantages of several analytical principles to enhance the analytical information. Decomposition of high molecular weight structures is achieved by pyrolysis and a high separation capacity due to the chromatographic step provides both an universal as well as a selective and sensitive substance detection. The latter is achieved by simultaneously applying electron ionization quadrupole mass spectrometry (EI-QMS) for structural elucidation and [1 + 1]-resonance-enhanced-multi-photon ionization (REMPI) combined with time-of-flight mass spectrometry (ToFMS). The system has been evaluated and tested with polycyclic aromatic hydrocarbon (PAH) standards. It was applied to crude oil samples for the first time. In such highly complex samples several thousands of compounds are present and the identification especially of low concentrated chemical species such as PAH or their polycyclic aromatic sulfur containing heterocyclic (PASH) derivatives is often difficult. Detection of unalkylated and alkylated PAH together with PASH is considerably enhanced by REMPI–ToFMS, at times revealing aromatic structures which are not observable by EI-QMS due to their low abundance. On the other hand, the databased structure proposals of the EI-QMS analysis are needed to confirm structural

\* Corresponding author at: Joint Mass Spectrometry Centre, Chair of Analytical Chemistry, Institute of Chemistry, University of Rostock, 18059 Rostock, Germany.  
Tel.: +49 381 4986 536; fax: +49 381 4986 461.

E-mail address: [thorsten.streibel@uni-rostock.de](mailto:thorsten.streibel@uni-rostock.de) (T. Streibel).



information and isomers distinction. The technique allows a complex structure analysis as well as selective assessment of aromatic substances in one measurement. Information about the content of sulfur containing compounds plays a significant role for the increase of efficiency in the processing of petroleum.

© 2014 Elsevier B.V. All rights reserved.

## 1. Introduction

With the increasing consumption of crude oil and decreasing reserves fractions with higher boiling points will have to be used in the future. They are more complex and composed different than traditional commercial crude oils [1–3]. Aromatic compounds, especially polycyclic aromatic hydrocarbons (PAH) play an important role in fossil fuels and their byproducts. They are considered to be environmental pollutants causing risks to the human health [4,5]. PAH and their alkylated homologues can be persistent and nearly resistant to biodegradation, this holds especially for higher molecular compounds [6,7]. As referred by Mullins et al. [8] in heavy oil feedstock the content of high molecular species as well as the aromaticity increases. The fractions of compounds containing sulfur, often in the form of PAH analogues (polycyclic aromatic sulfur containing heterocycles, PASH) are increasing as well. All this causes problems with the refinery process, desulfurization and storage, which is the reason that these procedures are getting more and more complicated. PASH and PAH are similar in properties and they often have the same nominal mass [9]. The most dominant representatives of PASH in crude oils are thiophene, benzothiophene (BT), dibenzothiophene (DBT) and benzonaphthothiophene (BNT) [10]. In the last years, there has been much research dedicated to the separation and detection of PAH and PASH using GC based techniques [4,9,12,13], but especially for the high molecular fraction new analytical techniques or methods are still needed.

Crude oil is a supercomplex sample [1] of different chemical species. Therefore, the identification and quantification of individual compounds is difficult. As a consequence, there is the need to develop efficient methods to characterize heavy crude oil fractions and to get structural information. Often the low concentrations of many constituents are challenging in this context [14]. The structural diversity is extremely increasing when moving to higher boiling point components. This could be targeted with the help of SARA separation, whereby crude oil is divided into saturated, aromatic, resin and asphaltene fractions [15]. The molecular nature of the latter is still relatively unclear [16]. The main components will be represented by aromatic nuclei, that carry alkyl and alicyclic systems with heteroelements, whereby the aromaticity and the proportion of heteroelements increases over this lower-boiling fraction [17].

It requires a high degree of resolution power and selectivity to analyze crude oil. A variety of analytical systems and methods are available. An overview of chromatographic and mass spectrometric methods is given by Herod et al. [12]. A coupling of high-performance systems is desirable to get as much information as possible with one measurement cycle. It is possible to use selective methods such as high-resolution mass spectrometry (HRMS) in combination with photo ionization (PI) and no chromatographic separation as an intermediate step. Special types of PI have a high selectivity and can be coupled directly to an oven (thermal analysis) or a pyrolysis system [18–21]. Fourier transform ion cyclotron resonance mass spectrometry (FT-ICRMS), which is characterized by achieving a very high mass resolution, can also be applied without prior chromatographic separation, mostly combined with electron ionization (EI) or electrospray ionization (ESI)

[2,3,22,23]. On the other hand, a chromatographic separation is required, if MS with low selectivity and resolution is used. Especially, when multidimensional GC (GC  $\times$  GC) is applied the analytical resolution power increases extremely [21,24–27]. Time-of-flight mass spectrometry (ToFMS) has been employed as detection method for GC  $\times$  GC based investigations of crude oil or oil-like samples [25,27].

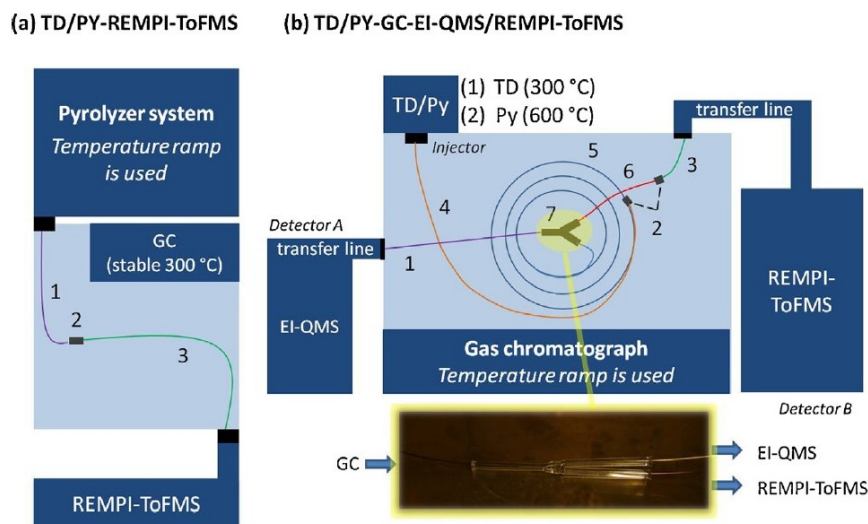
EI ionization in combination with chromatography is nevertheless very powerful and is still used frequently. It is a hard ionization technique, because the kinetic energy of the electrons is typically above the ionization energy of organic molecules, resulting in fragmentation. Albeit the molecular information then often is lost, the fragmentation pattern is characteristic for each chemical compound and available in mass spectrometric libraries for comparative purposes. The lack of the molecular ion signal can be prevented or reduced by soft ionization techniques such as chemical ionization, field ionization and photo ionization (PI). One such PI technique is the resonance-enhanced-multi-photon ionization (REMPI) technique. Especially for the one-dimensional GC coupled with multi-photon ionization mass spectrometry, there are promising developments in terms of selectivity and sensitivity [28–31]. Its selectivity depends on the used photon wavelength and additionally on the UV absorption bands as well as on the ionization energy threshold, since the molecules absorb two photons via an intermediate state [32–35]. REMPI in combination with ToFMS is a useful method for trace analysis and shows a very high selectivity and sensitivity for polycyclic aromatic hydrocarbons [19,29,36–39].

Eschner et al. [27] developed a quasi-simultaneous acquisition of hard EI- and soft single photon ionization mass spectrometry (SPI-MS) for GC/MS analysis by rapid switching between both ionization methods. The system has been successfully applied to diesel fuel, which consists largely of volatile components. It is obvious to transfer this approach to a coupled system utilizing REMPI-MS instead of SPI-MS. Therefore, in this work an analytical system has been developed, that is able to break high molecular weight structures efficiently. With its high separating capacity it provides a universal, but also selective and sensitive substance spectrum. For the sample injection or break down a pyrolyzer is used. This allows both the analysis of solid (e.g., soil samples), as well as viscous (e.g., heavy oil) natural samples and artificial materials. Pyrolysis at certain temperatures is well known in the pyrolysis community [40,41]. Additionally several temperature levels, can be selected, so that a fractionation of heavy oil is imitated. By applying simultaneous detection of the GC separated pyrolysis products with two mass spectrometry units a universal fingerprint of the sample (by EI) as well as an aromatic fingerprint (by REMPI) results. This system was applied to complex crude oil samples for the first time.

## 2. Material and methods

The experimental implementation (Fig. 1) can be divided into the following sections. Firstly, the pyrolyzer is directly connected to the REMPI-ToFMS. A thermogram is obtained to get a first overview of the sample. In the second step, the system is expanded by a GC with an EI-QMS (quadrupole mass spectrometer) as a second detection system.





**Fig. 1.** Samples were introduced by a double-shot-pyrolyzer (Py) that either was (a) directly connected to a mass spectrometer (MS) or (b) was coupled to a gas chromatograph (GC) using two MS for simultaneous detection (REMPI and EI ionisation, respectively). For the connection are used: (1) phenyl/methyl (P/M) deactivated temperature stable polyimide (TSP) standard fused silica (FS) tubing, 250  $\mu\text{m}$  ID, 375  $\mu\text{m}$  OD, 1 m; (2) SS union, 250  $\mu\text{m}$  bore; (3) P/M deactivated TSP standard FS tubing, 200  $\mu\text{m}$  ID, 375  $\mu\text{m}$  OD, 2.5 m; (4) precolumn: P/M deactivated TSP standard FS tubing, 250  $\mu\text{m}$  ID, 375  $\mu\text{m}$  OD, 4 m; (5) separation column: SGB-BPX5, 250  $\mu\text{m}$  ID, 0.25  $\mu\text{m}$  film, 375  $\mu\text{m}$  OD, 30 m; (6) P/M deactivated TSP standard FS tubing, 100  $\mu\text{m}$  ID, 375  $\mu\text{m}$  OD, 0.3 m; (7) deactivated PressFit 3-way Y-Splitter for FS tubing with 0.20–0.75 mm OD.

## 2.1. Thermal analysis/mass spectrometry

The pyrolyzer (Frontier Laboratories, Double-Shot-Pyrolyzer, model: PY-2020iD) was directly coupled to REMPI-ToFMS. For detailed information see Fig. 1a. It allows a thermal desorption under low temperature or a pyrolysis process under high temperature conditions. In addition, temperature ramps are possible as well. The system works oxygen-free, with helium (99,999%, flow rate of 4–6  $\text{mL min}^{-1}$ ) as carrier gas, with a split ratio of 1:10. In this case the integrated gas chromatograph (HP 5890 Series II) is used only as a heat source, operated continuously at 300 °C. Separation is effected only by the temperature ramp of the pyrolyzer. The experiment is more or less a thermogravimetric analysis mass spectrometry (TGA/MS) simulation [17,18]. The pyrolyzer oven was operated as follows: start at 50 °C, increasing by 15 °C  $\text{min}^{-1}$  up to 500 °C, followed by a rise of 10 °C  $\text{min}^{-1}$  up to 600 °C, which was held for 1 min. The released compounds are transported with the carrier gas via a transfer line to the directly connected REMPI-ToFMS.

For REMPI, a Nd:YAG laser (BIG SKY ULTRA, Quantel, Les Uli Cedex, France) with two frequency doubling units at 266 nm was employed, which corresponds to a photon energy of 4.11 eV. The laser is operated with 10 ns pulse width and a 20 Hz repetition rate exhibiting a power density of approximately  $7 \times 10^6 \text{ W cm}^{-2}$ . A reflectron ToFMS (Reflectron CTF10, Kaesdorf Geräte für Forschung und Industrie, Munich, Germany) was utilized for the detection of the molecular ions. The REMPI equipment is described more extensively by Fendt et al. [38]. For calibration and optimization of the REMPI-ToFMS system a gas standard (Linde AG, Pullach, Germany) containing 1 ppm of each benzene, 1,2,4-trimethylbenzene, benzaldehyde and toluene in nitrogen is used.

Five crude oil samples of different countries have been measured varying in their composition (Greek, North Sea Turkish, Californian and Azerbaijan crude oil). The samples were stored at –20 °C. Except for the last one all crude oils have been analyzed by thermal analysis/MS in our working group before [20]. Approximately 0.1 mg of pure crude oil sample was introduced.

## 2.2. Fractionated thermal analysis by TD/Py-GC/MS

The samples first undergo a process of desorption at 300 °C for 1 min. In this step, the present free low molecular weight compounds evaporate into the gas phase and are injected into the direct coupled gas chromatograph, with a split ratio of 1:10 and a carrier gas flow rate of 2  $\text{mL min}^{-1}$ . It is equipped with a non-polar column (SGE-BPX-5; 30 m  $\times$  0.25 mm  $\times$  0.25  $\mu\text{m}$ ). Helium (99,999%) with a head pressure of 100 kPa was the carrier gas. The temperature program was as following: 60 °C (held for 2 min) to 340 °C (held for 10 min) at 10 °C  $\text{min}^{-1}$ . After passing the chromatographic column the gas flow was splitted by a Y-Splitter (deactivated PressFit 3-way Y-Splitter for FS Tubing with 0.20–0.75 mm OD) and transferred simultaneously to an EI-QMS and a REMPI-ToFMS. There was a ratio of mass flow of about 100:1 in favor of the EI-QMS system. This is caused by the different column diameters (Fig. 1b). If the REMPI system gets the same amount of substance as the EI system, the multi channel plate (MCP) would be overloaded and detection of molecular ions would not be possible.

After the thermal desorption process, the same sample was introduced for a second one minute period after the pyrolyzer oven was heated up to 600 °C. The high temperature conditions destroy the macromolecular structure and generate small and evaporable compounds.

For identification of compounds on the one hand comparison with mass spectra libraries (Wiley, Nist) was used. On the other hand a mixture of standard substances was dissolved in a 1:1 solution of dichloromethane (Rotisol, UV/IR-Grade, Carl Roth) and *n*-hexane (HPLC grade, Fisher Scientific) and chromatographed (approximately 100  $\text{mg L}^{-1}$  for each substance). The standard mixture contains ten PAH: Naphthalene (NAP) [ $m/z$  128], phenanthrene (PHE) [ $m/z$  178], pyrene (PYR) [ $m/z$  202] (Aldrich Chemistry), fluorene (FLU) [ $m/z$  166] (Acros Organics), acenaphthylene (ACY) [ $m/z$  152], acenaphthene (ACE) [ $m/z$  154], benzo[*a*]anthracene (BaANT) [ $m/z$  228], benzo[*a*]pyrene (BaPYR) [ $m/z$  252], benzo[*ghi*]perylene (BghiPER) [ $m/z$  276] and dibenz[*ah*]anthracene (DBaHANT) [ $m/z$  278] (PAH Research Institute, D-86926 Greifenberg).



The same crude oils were used as before. Approximately 100 mg of the oil samples were dissolved in a mixture of 1000  $\mu\text{L}$  dichloromethane/*n*-hexane (1:1). 10  $\mu\text{L}$  of the solution was injected into the pyrolysis system.

### 3. Results and discussion

#### 3.1. Thermal analysis: REMPI–ToFMS of crude oils

For a first comparison the crude oil samples were measured in a similar way as in Geissler et al. [20]. The pyrolyzer oven is directly connected to the REMPI–ToFMS system and a temperature ramp from 50 °C up to 600 °C was applied. This is resulting in a thermogram, which shows an aromatic fingerprint of the sample.

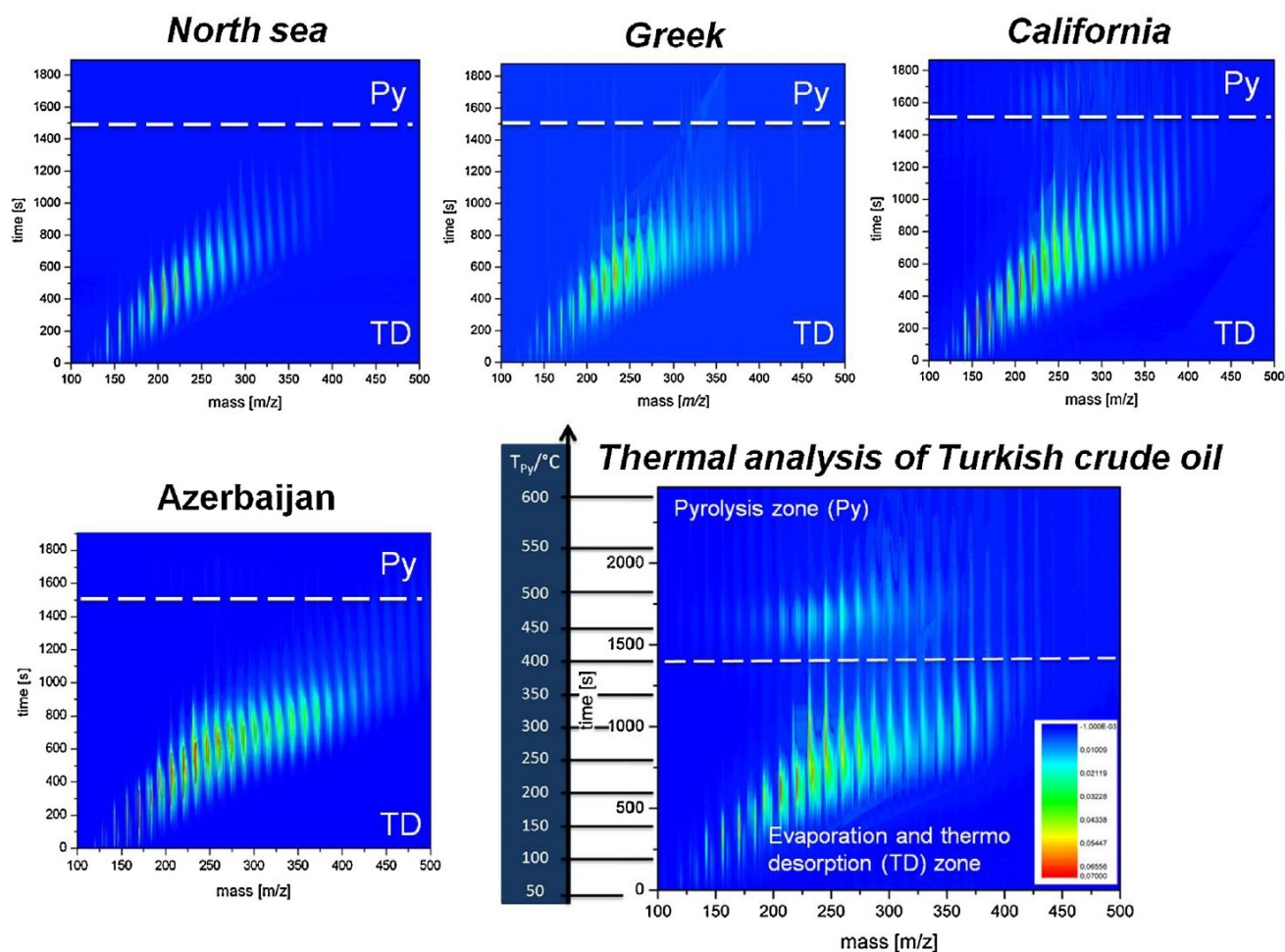
Fig. 2 shows the thermograms of the five crude oils with a different geological origin. The  $m/z$ -value is plotted against time. For the Turkish crude oil the respective heating temperature of the pyrolyzer oven for a given time is displayed additionally. The intensity of the mass signal is depicted as color display.

Even at low temperatures signals are obtained. It indicates that small, free, volatile aromatics are present within the sample. The thermogram can be divided into two distinct areas. The lower section represents a quasi-continuous evaporation process, which ends at a temperature of 350–400 °C. Thus it is corresponding to a classical boiling point separation, similar to crude oil distillation. The pyrolysis step (the upper section) starts at a temperature of 400 °C, where products of a pyrolytic decomposition of non-volatile macromolecular compounds are observed. According to

literature [42], the fractional distillation of crude oil in industrial processes can be separated into several fractions: naphtha (28–191 °C), distillate (191–327 °C), the dominant fraction for aromatic compounds, gas oil (327–566 °C), and residuum fraction (>566 °C). Above 550 °C no evolving species can be detected anymore. The gas–oil class can be split into two temperature ranges, the precracking (327 °C to approximately 400 °C) and cracking (400 °C to nearly 550 °C). For the naphtha fraction of Turkish oil significant signals can be observed only above 140 °C. In contrast to the California crude oil aromatics in the naphtha fraction are clearly represented for the whole temperature range.

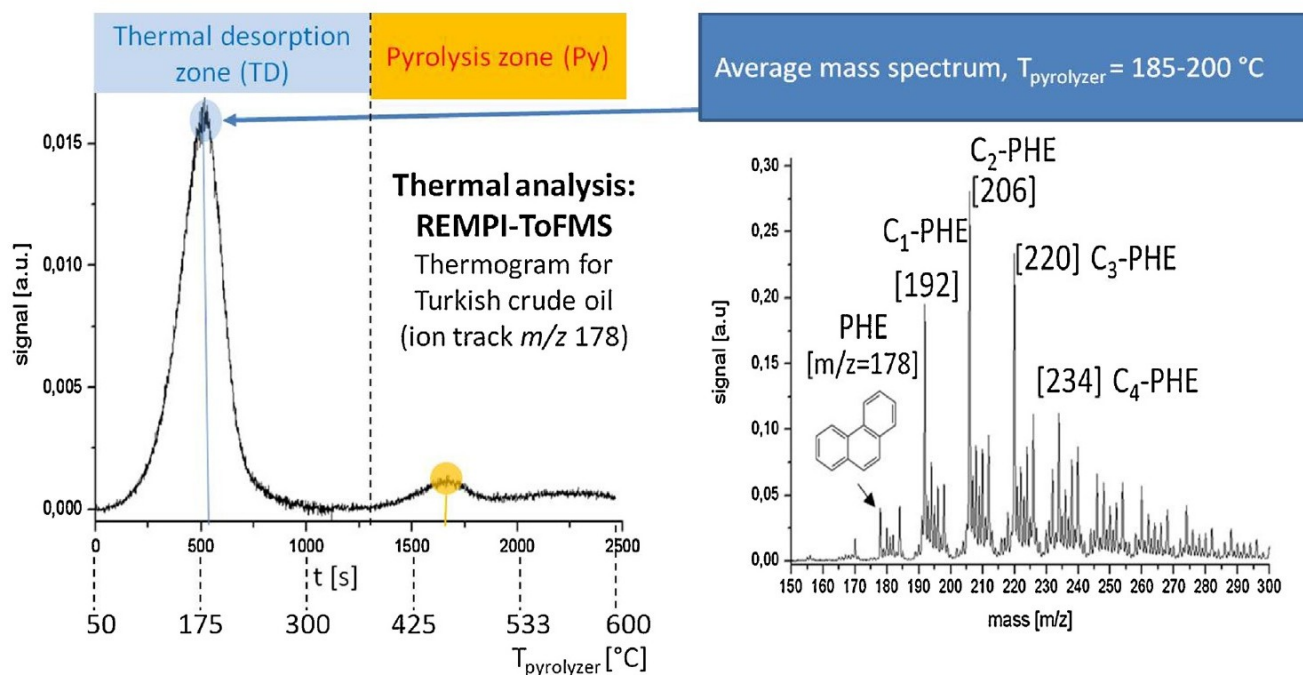
The results are consistent with Geissler et al. [20]. The crude oils show the same trends in the volatile fraction and have a distinct evaporation zone. However, with the exception of the Turkish crude oil decomposition products cannot be detected or the concentrations of the pyrolysis fragments are very low. The highest signal intensities can be found in a mass to charge ratio between 200 and 300, especially for the Greek, Californian and Azerbaijan crude oils. Turkish crude oil seems to contain a larger number of heavier low volatile components than the other four, which in return are richer in (semi) volatile species.

It has to be mentioned that in principle at every single temperature a complete mass spectrum can be derived. Ion traces for individual  $m/z$  values could be pursued as well. The graph for the ion trace of  $m/z$  178 of the thermogram from Turkish oil is seen in Fig. 3, wherein two maxima are observed, one for the thermal desorption zone and one for the pyrolysis zone. Between 500 and 600 s and an oven temperature of approximately 200 °C (thermal



**Fig. 2.** Presentation of five thermograms resulting from Py–REMPI–ToFMS (thermal analysis by direct coupling). Five crude oils were measured: North Sea Greek, California, Azerbaijan and Turkish crude oil. The y-axis shows the course of time, x-axis the  $m/z$  value is plotted. The respective intensity of the mass signal is depicted as color display.



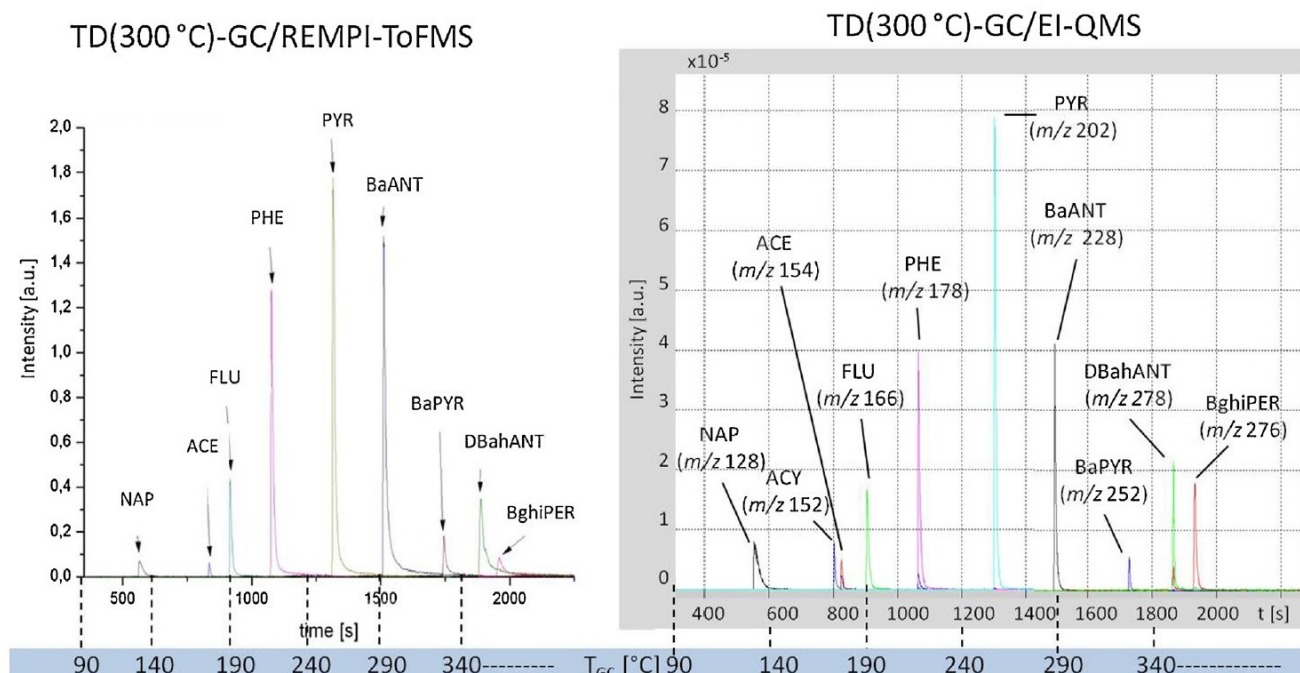


**Fig. 3.** Left: graph for the ion track of 178  $m/z$  from Turkish crude oil, which resulting from the direct coupling pyrolyzer and REMPI-ToFMS. The x-axis represents the time or the temperature of the pyrolyzer. On the y-axis, the signal intensity is shown. Right: the averaged mass spectrum at an oven temperature of about 200 °C (TD step). PHE and alkylated representatives are shown. The x-axis represents the mass-to-charge-ratio the y-axis the signal intensity.

desorption zone) the maximum intensity of substances with the molecular mass of  $m/z$  178 can be detected.

The averaged mass spectrum between 185 and 200 °C, depicted in Fig. 3 as well, shows a periodical distribution of signals, which can be assigned to PHE and its alkylated derivatives. The alkylated compounds are apparently dominant, showing a maximum at the dialkylated PHE isomers. A bell-shape distribution is typical for petrogenic origin [43]. In the Supplementary material (Fig. S1) more spectra of PAH and their alkylated derivatives are depicted.

The intensity in the pyrolytic step is more distinct, especially at the nominal masses  $m/z$  252, 276, 278 and 300. It seems that with increasing size of the PAH its contribution to the pyrolytic step also increases. An increase in the diversity of PAH, including the alkylated compounds, is systematically observed in all studied crude oil samples. This pyrolytic released PAH are mainly derived from high molecular weight aromatic structures. The formation of these PAH from smaller chemically active components (e.g., radicals) under the selected reaction conditions (exclusion of air,



**Fig. 4.** Representation of the measured PAH standard by the coupled pyrolyzer gas chromatograph mass spectrometry system. SIM (single ion monitoring) mode is used. On the left is the chromatogram for the REMPI-ToFMS measurement and on the right the chromatogram for the EI-QMS system. Below the GC timeline and the temperature of the GC program is displayed in direct comparison.



relatively low pyrolysis temperature and pressure) is not probable, but cannot be entirely excluded. This is still the subject of current research [44].

Supplementary material related to this article found, in the online version, at <http://dx.doi.org/10.1016/j.aca.2014.11.030>.

With the employed mass spectrometer no separation between molecules with the same mass is possible. However, there are some selectivity rules that can be exploited for peak assignment in such cases. For instance, the molecular mass  $m/z$  178 can also be assigned to anthracene (ANT). The REMPI ionization effectivity for ANT (relative cross sections  $\sigma_{\text{rel}}$  in comparison to toluene is 3.3) at the utilized wavelength of 266 nm is two orders of magnitude lower than for PHE ( $\sigma_{\text{rel}}=178.9$ ), which could be concluded from own laboratory measurements with standard solutions. Thus the contribution of anthracene to the signal at  $m/z$  178 is negligible. Furthermore, no ANT peak could be detected in the later GC/MS measurements. The reason for this behavior is the drastically decreased absorption efficiency for the irradiated photons in the case of ANT. For other  $m/z$  values the situation may prove more difficult, for instance some alkylated PAH have the same molecular mass than a few PASH, e.g., C4-NAP [ $m/z$  184] and DBT [ $m/z$  184]. There is no possibility to differ between PAH and PASH with direct mass spectrometric detection. However, by using a GC separation before the mass spectrometer, the isomers should be distinguishable.

### 3.2. TD/Py-GC/MS of PAH

The new coupling of pyrolyzer and GC/MS with two distinct ionization methods (Fig. 1b) is checked for functionality. For this purpose a standard mixture with ten different PAH (NAP, ACY, ACE, FLU, PHE, PYR, BaANT, BaPYR, DBahANT, BghiPER) was introduced resulting in two chromatograms shown in Fig. 4. In the chromatogram of the EI-QMS (right) all ten PAH can be recovered. In the chromatogram that is based on REMPI-ToFMS detection nine of these PAH are clearly located. ACY [ $m/z$  152], which is detected by EI-QMS in high abundance, is near the limit of detection when REMPI-ToFMS is used. With nanosecond multiphoton ionization, detection of ACY has been reported to be satisfactory in small quantities [29]. The introduced sample volume of ACY and the theoretically registered quantity at the detector (1 pg) is far below the LOD of Li et al. [29] which is the probable reason why the component cannot be observed here. This is also evidenced in literature by Haeffliger and Zenobi [37]. ACY could be detected there as well, but also with comparatively low signal intensities. The molar absorptivity of this compound in the vicinity of 266 nm is nearly the same as that of NAP. Therefore, the reason could be the short excited-state lifetime of ACY. A femtosecond laser with a pulse width shorter than the excited state lifetime of the analyte molecule can increase the sensitivity extremely [28].

The sensitivity of the two mass selective detectors can be compared directly (Supplementary material (Fig. S2)). It shows how effective the ionization for the two relevant connected mass spectrometric methods is, if the distribution of the substance flow to both systems is the same. The obtained signals were converted accordingly to the respective mass flows (theoretically calculated by using the calculation program Hewlett-Packard FlowCalc 2.0). The representation also demonstrates the respective ionizing efficiency of PAH for the utilized REMPI system. The results correspond with previous measurements conducted in our laboratory. Five of the here listed PAH have been investigated and their relative cross sections ( $\sigma_{\text{rel}}$ ) in comparison to toluene have been calculated. NAP ( $\sigma_{\text{rel}}=25.5$ ) and ACE ( $\sigma_{\text{rel}}=28.5$ ) have a similar low ionization level. In case of BghiPER ( $\sigma_{\text{rel}}=49.8$ ), FLU ( $\sigma_{\text{rel}}=86.8$ ) and DBahANT ( $\sigma_{\text{rel}}=93.1$ ) the effective cross section

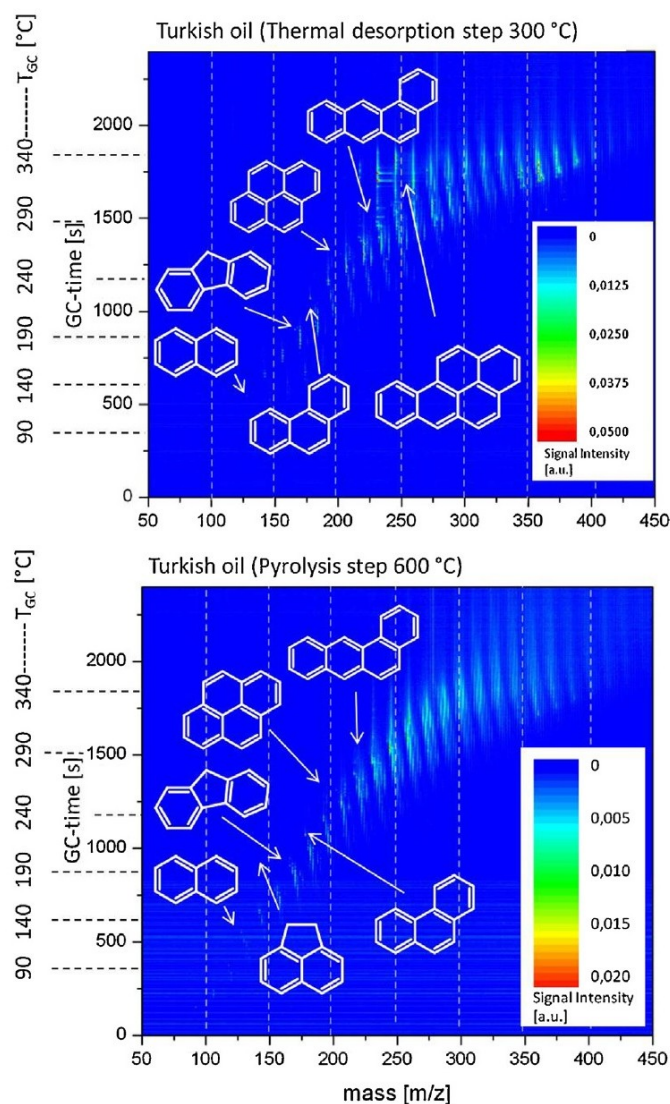
and the ionization efficiency increase. Especially with REMPI, the substances show a large variability, because every compound has its own individual cross section.

Supplementary material related to this article found, in the online version, at <http://dx.doi.org/10.1016/j.aca.2014.11.030>.

All PAH of the standard mixture can be detected with a higher sensitivity by the REMPI system (except ACY [ $m/z$  152]). For NAP [ $m/z$  128], the increase in sensitivity is about a factor of 3. For BaPYR [ $m/z$  252] it shows an increase of 33 when REMPI is compared to EI. Among the PAH FLU, PHE, PYR, BaANT and DBahANT can be ionized very well at a wavelength of 266 nm by REMPI. Compared to the EI-chromatogram the REMPI-chromatogram shows a slight peak widening. The reasons cannot be clearly identified. The significantly longer transfer path between GC and REMPI-ToFMS could be a possible cause.

### 3.3. TD/Py-GC/MS of crude oils

Fig. 5 shows two chromatograms for the Turkish oil from the REMPI-ToFMS measurements under thermal desorption and pyrolysis conditions, respectively. The y-axis displays the retention



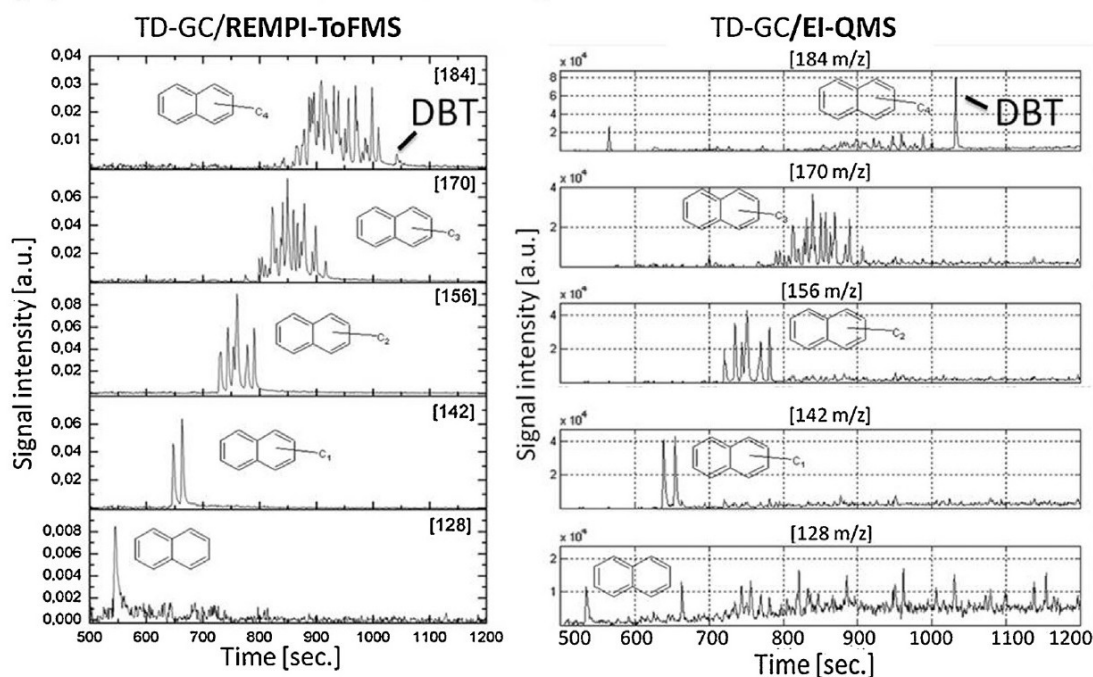
**Fig. 5.** Chromatogram (REMPI-ToFMS) for Turkish crude oil. On the y-axis the GC-time is plotted. On the x-axis the mass-to-charge ratio is shown. Graduated in color are the intensities. The PAH are identified and verified through standard addition. Left: chromatogram of a sample injection temperature of 300 °C. Right: chromatogram of a sample injection temperature of 600 °C.



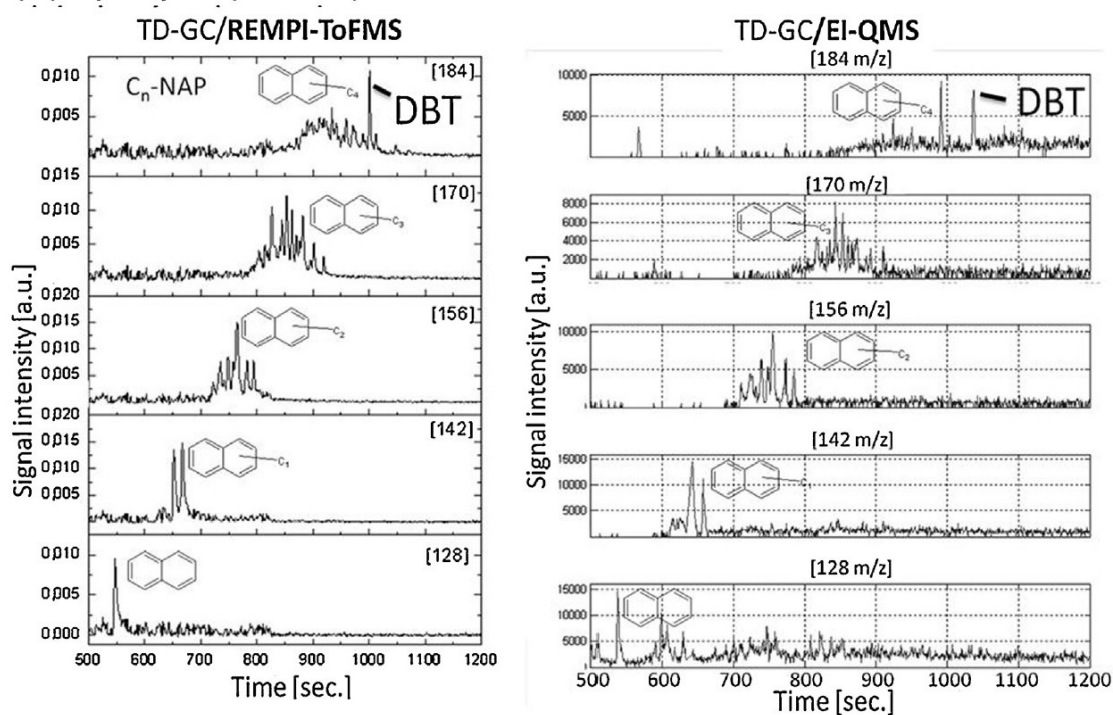
time of the GC. Along the  $x$ -axis the  $m/z$  value is plotted. The respective intensity of the mass signal is depicted as color display. Under thermal desorption conditions a broad substance spectrum is revealed and aromatic compounds are registered in a mass range between  $m/z$  100 and 450. The number of aromatic compounds with the same mass-to-charge-ratio is increasing sharply above a molecular mass of  $m/z$  230. This reflects the increasing variety of alkylated species. The separation process along the column and the

different retention times allow an insight into the different species contributing to one mass-to-charge ratio. However, in the higher mass range above  $m/z$  350, a proper separation is not longer possible, because the compounds get less and less volatile. Some PAH of the standard mixture are identified by their retention time and could also be verified by standard addition. In the pyrolysis step also a broad substance spectrum is visible, but the signal intensities are lower. The aromatic substance spectrum starts with

### (a) Thermal desorption (300 °C) of Turkish oil



### (b) Pyrolysis (600 °C) of Turkish oil



**Fig. 6.** Direct comparison of the chromatograms for specific ion traces of the alkylated NAP series.  $C_0$  corresponds to the unalkylated and  $C_4$  to the four times alkylated NAP and DBT. Above the thermal desorption and below the pyrolysis steps are shown. On the left are the results from the REMPI-ToFMS, and on the right from the EI-QMS measurements.



benzene [ $m/z$  78] and toluene [ $m/z$  92]. Those are pyrolysis fragments and are often observed in pyrolysis processes of natural products [44–46].

The total ion chromatogram of EI-QMS (Supplementary material (Fig. S3)) is mainly dominated by *n*-alkanes and iso-alkanes. The relevant aromatic structures can be found only in small concentrations by using a selective search on the ion tracks. Hence the detection of PAH is made considerably easier with REMPI, enabling a rapid overview of the aromatic pattern of the samples after GC separation.

Supplementary material related to this article found, in the online version, at <http://dx.doi.org/10.1016/j.aca.2014.11.030>.

Fig. 6 shows representatives of all considered PAH compounds of the naphthalene homologue row up to the fourth degree of alkylation. The REMPI-ToFMS data (left) are compared with the EI-QMS data (right), including thermal desorption (top) and pyrolysis conditions (below). On the x-axis the GC-time and on the y-axis the peak intensity is plotted. The REMPI-chromatogram is less complex in the composition compared to the EI-QMS chromatogram. If EI is used, many peaks can be found on the ion track  $m/z$  128. Lots of them can be isomeric structures for nonane (IE 10,2 eV [47]). An assignment is often not possible despite database matching. At a retention time of 550 s, NAP (IE 8,1 eV [48]) is observed in both chromatograms. A peak at about 670 s is only detected with the EI-setup. This will be the molecule ion of a nonane isomer. With increasing GC-time for the ion trace  $m/z$  128 only EI-fragments of possible higher molecular species can be observed in the chromatogram. The curves of ion traces from the first to the third degree of alkylation are very similar in both

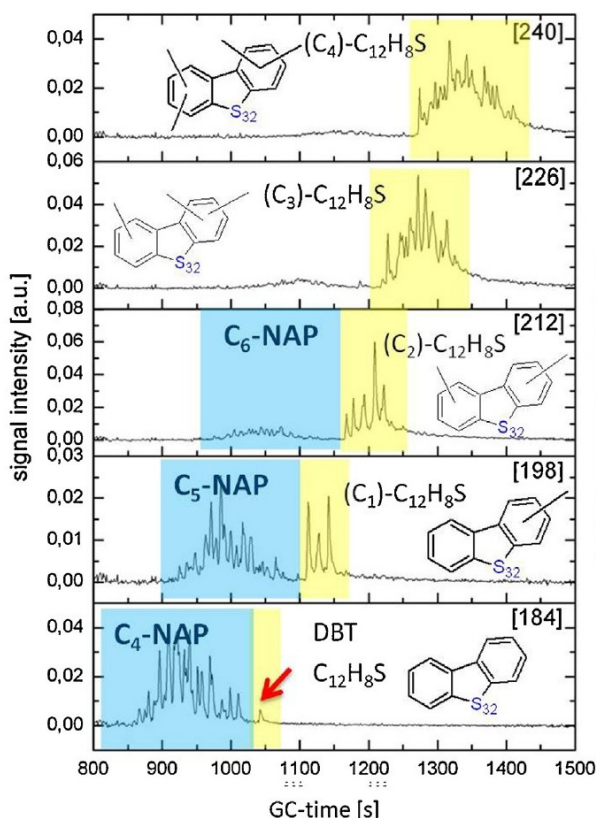
chromatograms. For the fourth degree of alkylation intensities decrease significantly. Only in the REMPI chromatogram high peak intensities are recognized and alkylated NAP species up to the sixth degree of alkylation can be observed. At an approximate retention time of 1030 s, for the fourth degree of alkylation [ $m/z$  184], a peak in the EI chromatogram is apparently much higher than the other peaks of the same ion traces. This is probably DBT, a heterocyclic compound. This class of compounds will be discussed in detail below. A data base matching and especially literature information [49] and results of GC-APCI (atmospheric pressure chemical ionization)-FT-ICRMS measurements in our lab shows the same elution sequence of C4-NAP and DBT. In particular, the advantage to detect PAH and PASH with the same equal mass number side by side [11] verifies the selectivity of the applied mass spectrometer and the coupled system.

In the pyrolysis step, the peak intensities are significantly lower than in the desorption step. Nevertheless, the EI chromatogram is much more complex for the ion tracks  $m/z$  128 and  $m/z$  184, hinting at an augmentation of decomposition products from larger aromatic structures present in the crude oil.

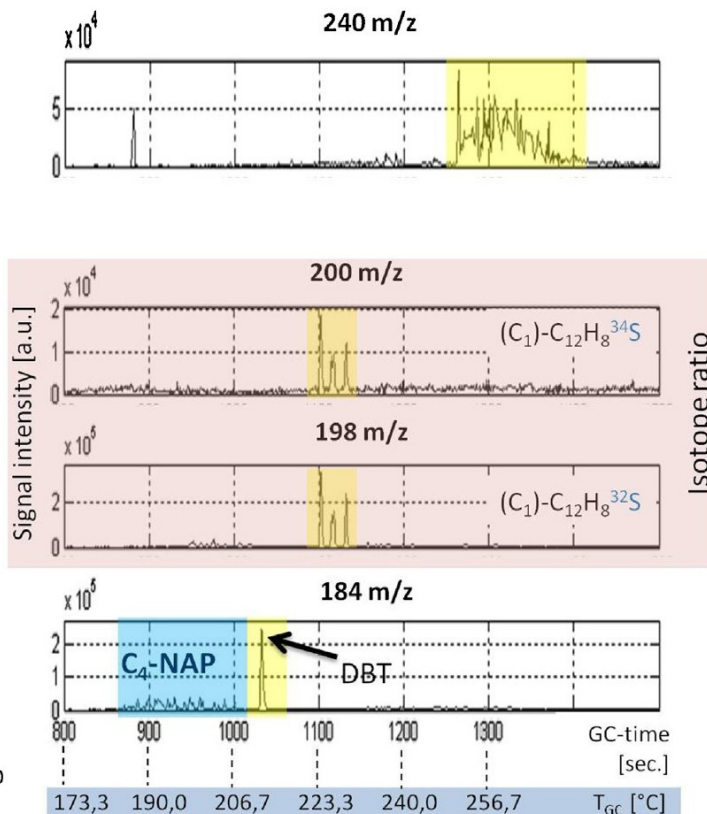
NAP, FLU, PHE and PYR are detected and identified in all of the investigated crude oils along their alkylated homologues. ACE is found only in the Turkish and Azerbaijan crude oil. BaANT and chrysene (CHR) [ $m/z$  228] are rarely evidenced and the peak intensities are low. Also the alkylated species of BaANT and BaPYR are detected in only a very few cases.

Among PASH in crude oils, three representatives are frequently described in the literature: BT [ $m/z$  134], DBT [ $m/z$  184] and BNT [ $m/z$  234] [2,9,50]. Fig. 7 shows DBT in Greek crude oil under TD

(a) TD-GC/REMPI-ToFMS of Greek oil



(b) TD-GC/EI-QMS of Greek oil



**Fig. 7.** DBT and their alkylated representatives ( $C_x$ ) in the Greek crude oil. Direct comparison of the ion traces which resulting from EI-QMS and REMPI-ToFMS measurements. On the x-axis GC-time is plotted (parallel the GC temperature) and on the y-axis the peak intensity is shown. For reason of clarity  $m/z$  212 and  $m/z$  226 of the EI data are eliminated in this analysis.



conditions. Under pyrolysis conditions sulfur aromatics were also detected, but the signal levels were significantly lower. Fig. 7a (REMPI data) shows specific ion traces for DBT and the first up to the fourth degree of alkylation. With the EI-QMS (Fig. 7b) detection, via the databases, an assignment of the peaks is possible. In addition, the isotope ratio of sulfur can be used. Interesting are the isotopes  $^{32}\text{S}$  and  $^{34}\text{S}$ , which are abundant at 95–4%, respectively. The figure shows the occurrence of methyl-DBT with  $^{32}\text{S}$  [ $m/z$  198] in comparison to  $^{34}\text{S}$  [ $m/z$  200]. If the retention times of the two peaks are coinciding, then with high probability it is a sulfur compound. By doing so, one may distinguish between PAH and PASH, which have the same nominal mass.

Comparing EI and REMPI data, the high selectivity and sensitivity with REMPI at a wavelength of 266 nm is obvious. Fig. 7a (REMPI data) shows the fourfold alkylated NAP and DBT for the same nominal mass  $m/z$  184. REMPI-ToFMS is able to detect them separately, without any complex preparation process. It can be assumed that the concentration of DBT is significantly higher than the concentration of the four times alkylated NAP, but REMPI is clearly more sensitive for PAH than for PASH. In the EI chromatogram fourfold alkylated NAP exhibits a significantly lower signal intensity than DBT. In the REMPI chromatogram the conditions are the other way round. It is even possible to see five times and six times alkylated NAP, which are no longer detectable with the EI setup.

Apparently, at a wavelength of 266 nm DBT is obviously not as good ionized as nonalkylated PAH, which refers to an inadequate cross section. Possibly the excited intermediate state is too short-lived. The alkylated species, however, are very easy to recognize. They might be present in a higher concentration or the intermediate state is better stabilized by alkylation. The direct comparison between EI and REMPI shows that in the EI-chromatogram, specifically for the ion traces  $m/z$  184 and  $m/z$  212 concentrations are comparable, because the peak intensities are on the same level. However, in the REMPI chromatogram an approximately tenfold increase in the peak intensity for the doubly alkylated isomer ( $t(R)$  = 1200 s) is obtained. Thus, the hypothesis can be formulated that increased alkylation leads to a better ionization and detection with the used REMPI system (266 nm) for the considered sulfur aromatic compounds.

BT, DBT and BNT were used for the following comparison between the Greek, Turkish, Azerbaijan, North Sea and Californian crude oils. DBT, the overall dominant PASH species, is present in all crude oils, as an unalkylated aromatic as well as an alkylated compound. BT can be found only in Turkish and Greek crude oil, starting with the second degree of alkylation. BNT is present in small concentrations in Azerbaijan and Greek oil, whereby the un- and low-alkylated species are dominant. If one has to evaluate the sulfur load of crude oils based on the three examined PASH, then the Californian and North Sea crude oil are least loaded. In contrast the Greek crude oil has the highest sulfur content. But it is a very rough estimation based on the diversity of the three S-species, which were found and would have to be quantified and confirmed by further measurements.

For PASH, the detection by EI-QMS is even more sensitive than the REMPI-ToFMS system, at least with the measured wavelength of 266 nm. However, the sensitivities and registered peak intensities are more and more on the same level with an increasing degree of alkylation. The use of a different wavelength could provide more sensitive and selective results. The used measuring system is obviously most suitable for PAH, but a good analytical system to analyze PASH for a first approximation. Nevertheless, the adapted setup of REMPI and EI makes a broad spectrum of substances accessible for detection.

## 4. Conclusion

The study focused on the coupled system consisting of a pyrolyzer, a gas chromatograph and two mass selective detectors. It is the first time that pyrolyzer, GC, REMPI- and EI-MS are directly combined. The aim was to demonstrate the largely different selectivity and to make high molecular weight sample components accessible and differentiable. A powerful separation and a combination of universal as well as a selective and sensitive detection are advantageous for an improved description of complex petrochemical mixtures with aromatic contents. The system was firstly successfully tested for PAH standards. A direct comparison of the EI-QMS and REMPI-ToFMS detection for the measured aromatic components was performed. The high selectivity of REMPI for PAH has been accordingly reflected. However, the EI to REMPI (266 nm) ratio is substance-specific and depends on the used wavelength [10,37].

The system was applied to crude oil sample analysis. The Py/TD-GC-EI-QMS/REMPI-ToFMS system has the ability to detect PAH and their alkylated representatives with both mass spectrometric ionization techniques. The analysis of aromatic species with a higher degree of alkylation (dominating in crude oil) is preferably possible by using REMPI-MS. By using EI the general detectable substance class spectrum is significantly increased. The combination of two different ionization techniques gives an improved comprehensiveness of sample characterization. Sulfur compounds are also recognized, despite a relatively uncomplicated sample preparation.

The developed system is ubiquitous applicable. Solid and liquid samples can be introduced, relatively high molecular weight components are accessible and universal and PAH selective detection is possible in parallel. The measuring setup can be further optimized by using a GC  $\times$  GC [26,27] system for a higher separation power. By the use of other wavelengths for REMPI or an increase of the laser frequency [28] more or other substances are accessible.

The obtained information such as distribution of alkyl chain length, size of aromatic structures or the fraction of heteroatomic substances may be important in increasing the efficiency of petroleum processing. Furthermore, the developed system can also be used for other applications, such as environmental studies.

## Acknowledgments

Special thanks go to S. Klingbeil and A. Pommeres for their REMPI response factors, constructive comments and the development of tools for data analysis.

## References

- [1] S.K. Panda, J.T. Andersson, W. Schrader, Characterization of supercomplex crude oil mixtures: what is really in there? *Angew. Chem. Int. Ed.* 48 (10) (2009) 1788–1791.
- [2] S.K. Panda, W. Schrader, J.T. Andersson, Fourier transform ion cyclotron resonance mass spectrometry in the speciation of high molecular weight sulfur heterocycles in vacuum gas oils of different boiling ranges, *Anal. Bioanal. Chem.* 392 (5) (2008) 839–848.
- [3] M.J. Teravainen, J.M.H. Pakarinen, K. Wickström, P. Vainiotalo, Comparison of the composition of Russian and North Sea crude oils and their eight distillation fractions studied by negative-ion electrospray ionization Fourier transform ion cyclotron resonance mass spectrometry: the effect of suppression, *Energy Fuels* 21 (1) (2007) 266–273.
- [4] J.G. Brody, K.B. Moysich, O. Humblet, K.R. Attfield, G.P. Beehler, R.A. Rudel, Environmental pollutants and breast cancer – epidemiologic studies, *Cancer* 109 (12) (2007) 2667–2711.
- [5] K.-H. Kim, S.A. Jahan, E. Kabir, R.J.C. Brown, A review of airborne polycyclic aromatic hydrocarbons (PAHs) and their human health effects, *Environ. Int.* 60 (2013) 71–80.



- [6] S. Thiele-Bruhn, G.W. Brummer, Kinetics of polycyclic aromatic hydrocarbon (PAH) degradation in long-term polluted soils during bioremediation, *Plant Soil* 275 (1–2) (2005) 31–42.
- [7] S. Gagni, D. Cam, Stigmastane and hopanes as conserved biomarkers for estimating oil biodegradation in a former refinery plant-contaminated soil, *Chemosphere* 67 (10) (2007) 1975–1981.
- [8] O.C. Mullins, E.Y. Sheu, A. Hammami, A.G. Marshall, *Asphaltenes, Heavy Oils, and Petrochemicals*, Springer Science + Business Media, New York, 2007.
- [9] M. Nocun, J.T. Andersson, Argentation chromatography for the separation of polycyclic aromatic compounds according to ring number, *J. Chromatogr. A* 1219 (2012) 47–53.
- [10] H. Muller, F.M. Adam, S.K. Panda, H.H. Al-Jawad, A.A. Al-Hajji, Evaluation of quantitative sulfur speciation in gas oils by Fourier transform ion cyclotron resonance mass spectrometry: validation by comprehensive two-dimensional gas chromatography, *J. Am. Soc. Mass Spectrom.* 23 (5) (2012) 806–815.
- [11] C. Zeigler, N. Wilton, A. Robbat Jr., Toward the accurate analysis of C1–C4 polycyclic aromatic sulfur heterocycles, *Anal. Chem.* 84 (5) (2012) 2245–2252.
- [12] A.A. Herod, K.D. Bartle, R. Kandiyoti, Characterization of heavy hydrocarbons by chromatographic and mass spectrometric methods: an overview, *Energy Fuels* 21 (4) (2007) 2176–2203.
- [13] M.S. Eschner, T.M. Groger, T. Horvath, M. Gonin, R. Zimmermann, Quasi-simultaneous acquisition of hard electron ionization and soft single-photon ionization mass spectra during GC/MS analysis by rapid switching between both ionization methods: analytical concept, setup, and application on diesel fuel, *Anal. Chem.* 83 (10) (2011) 3865–3872.
- [14] A.H. Hegazi, J.T. Andersson, Limitations to GC–MS determination of sulfur-containing polycyclic aromatic compounds in geochemical, petroleum, and environmental investigations, *Energy Fuels* 21 (6) (2007) 3375–3384.
- [15] T.G. Fan, J.S. Buckley, Rapid and accurate SARA analysis of medium gravity crude oils, *Energy Fuels* 16 (6) (2002) 1571–1575.
- [16] H. Groenzin, O.C. Mullins, Molecular size and structure of asphaltenes from various sources, *Energy Fuels* 14 (3) (2000) 677–684.
- [17] J.G. Speight, S.E. Moschopedis, On the molecular nature of petroleum asphaltenes, *Adv. Chem. Ser.* 195 (1981) 1–15.
- [18] T.W. Adam, M. Clairotte, T. Streibel, M. Elsasser, A. Pommeres, U. Manfredi, M. Carriero, G. Martini, M. Sklorz, A. Krasenbrink, C. Astorga, R. Zimmermann, Real-time analysis of aromatics in combustion engine exhaust by resonance-enhanced multiphoton ionization time-of-flight mass spectrometry (REMPI-TOF-MS): a robust tool for chassis dynamometer testing, *Anal. Bioanal. Chem.* 404 (1) (2012) 273–276.
- [19] R. Geissler, M.R. Saraji-Bozorgzad, T. Groger, A. Fendt, T. Streibel, M. Sklorz, B.M. Krooss, K. Fuhrer, M. Gonin, E. Kaisersberger, T. Denner, R. Zimmermann, Single photon ionization orthogonal acceleration time-of-flight mass spectrometry and resonance enhanced multiphoton ionization time-of-flight mass spectrometry for evolved gas analysis in thermogravimetry: comparative analysis of crude oils, *Anal. Chem.* 81 (15) (2009) 6038–6048.
- [20] R. Geissler, M. Saraji-Bozorgzad, T. Streibel, E. Kaisersberger, T. Denner, R. Zimmermann, Investigation of different crude oils applying thermal analysis/mass spectrometry with soft photoionisation, *J. Therm. Anal. Calorim.* 96 (3) (2009) 813–820.
- [21] A. Fendt, T. Streibel, M. Sklorz, D. Richter, N. Dahmen, R. Zimmermann, On-line process analysis of biomass flash pyrolysis gases enabled by soft photoionization mass spectrometry, *Energy Fuels* 26 (1) (2011) 701–711.
- [22] K. Miyabayashi, Y. Naito, M. Miyake, Characterization of heavy oil by FT-ICR MS coupled with various ionization techniques, *J. Jpn. Petrol. Inst.* 52 (4) (2009) 159–171.
- [23] D.F. Smith, R.P. Rodgers, P. Rahimi, A. Teclemariam, A.G. Marshall, Effect of thermal treatment on acidic organic species from athabasca bitumen heavy vacuum gas oil analyzed by negative-ion electrospray fourier transform ion cyclotron resonance (FT-ICR) mass spectrometry, *Energy Fuels* 23 (1) (2009) 314–319.
- [24] R. Edam, J. Blomberg, H.G. Janssen, P.J. Schoenmakers, Comprehensive multi-dimensional chromatographic studies on the separation of saturated hydrocarbon ring structures in petrochemical samples, *J. Chromatogr. A* 1086 (1–2) (2005) 12–20.
- [25] C.Y. Hao, J.V. Headley, K.A. Peru, R. Frank, P. Yang, K.R. Solomon, Characterization and pattern recognition of oil–sand naphthenic acids using comprehensive two-dimensional gas chromatography/time-of-flight mass spectrometry, *J. Chromatogr. A* 1067 (1–2) (2005) 277–284.
- [26] W. Welthagen, S. Mitschke, F. Muhlberger, R. Zimmermann, One-dimensional and comprehensive two-dimensional gas chromatography coupled to soft photo ionization time-of-flight mass spectrometry: a two- and three-dimensional separation approach, *J. Chromatogr. A* 1150 (1–2) (2007) 54–61.
- [27] M.S. Eschner, W. Welthagen, T.M. Groger, M. Gonin, K. Fuhrer, R. Zimmermann, Comprehensive multidimensional separation methods by hyphenation of single-photon ionization time-of-flight mass spectrometry (SPI-TOF-MS) with GC and GC × GC, *Anal. Bioanal. Chem.* 398 (3) (2010) 1435–1445.
- [28] T. Imasaka, Gas chromatography/multiphoton ionization/time-of-flight mass spectrometry using a femtosecond laser, *Anal. Bioanal. Chem.* 405 (22) (2013) 6907–6912.
- [29] A. Li, T. Uchimura, H. Tsukatani, T. Imasaka, Trace analysis of polycyclic aromatic hydrocarbons using gas chromatography–mass spectrometry based on nanosecond multiphoton ionization, *Anal. Sci.* 26 (8) (2010) 841–846.
- [30] A. Li, T. Uchimura, Y. Watanabe-Ezoe, T. Imasaka, Analysis of dioxins by gas chromatography/resonance-enhanced multiphoton ionization/mass spectrometry using nanosecond and picosecond lasers, *Anal. Chem.* 83 (1) (2011) 60–66.
- [31] A. Li, T. Imasaka, T. Uchimura, Analysis of pesticides by gas chromatography/multiphoton ionization/mass spectrometry using a femtosecond laser, *Anal. Chim. Acta* 701 (1) (2011) 52–59.
- [32] U. Boesl, H.J. Neusser, E.W. Schlag, Multiphoton ionization in the mass-spectrometry of polyaromatic-molecules-cross-sections, *Chem. Phys.* 55 (2) (1981) 193–204.
- [33] U. Boesl, Multiphoton excitation and mass selective ion detection for neutral and ion spectroscopy, *J. Phys. Chem.* 95 (8) (1991) 2949–2962.
- [34] R. Zimmermann, U. Boesl, C. Weickhardt, D. Lenoir, K.W. Schramm, A. Kettrup, E.W. Schlag, Isomer-selective ionization of chlorinated aromatics with LASERS for analytical time-of-flight mass-spectrometry – first results for polychlorinated dibenzo-*p*-dioxins (PCDD), biphenyls (PCB) and benzenes (PCBz), *Chemosphere* 29 (9–11) (1994) 1877–1888.
- [35] S. Mitschke, W. Welthagen, R. Zimmermann, Comprehensive gas chromatography–time-of-flight mass spectrometry using soft and selective photoionization techniques, *Anal. Chem.* 78 (18) (2006) 6364–6375.
- [36] R. Zimmermann, C. Lermer, K.W. Schramm, A. Kettrup, U. Boesl, 3-dimensional trace analysis-combination of gas-chromatography, supersonic beam UV spectroscopy and time-of-flight mass-spectrometry, *Eur. Mass Spectrom.* 1 (4) (1995) 341–351.
- [37] O.P. Haefliger, R. Zenobi, Laser mass spectrometric analysis of polycyclic aromatic hydrocarbons with wide wavelength range laser multiphoton ionization spectroscopy, *Anal. Chem.* 70 (13) (1998) 2660–2665.
- [38] A. Fendt, R. Geissler, T. Streibel, M. Sklorz, R. Zimmermann, Hyphenation of two simultaneously employed soft photo ionization mass spectrometers with thermal analysis of biomass and biochar, *Thermochim. Acta* 551 (2012) 155–163.
- [39] C. Stader, F.T. Beer, C. Achten, Environmental PAH analysis by gas chromatography–atmospheric pressure laser ionization–time-of-flight-mass spectrometry (GC–APLI-MS), *Anal. Bioanal. Chem.* 405 (22) (2013) 7041–7052.
- [40] F. Behar, M. Vandenbroucke, Y. Tang, F. Marquis, J. Espitalie, Thermal cracking of kerogen in open and closed systems: determination of kinetic parameters and stoichiometric coefficients for oil and gas generation, *Org. Geochem.* 26 (5–6) (1997) 321–339.
- [41] N. Ozbay, B.B. Uzun, E.A. Varol, A.E. Putun, Comparative analysis of pyrolysis oils and its subfractions under different atmospheric conditions, *Fuel Process. Technol.* 87 (11) (2006) 1013–1019.
- [42] Strategic Petroleum Reserve, *Gilesh Crude Oil Assay Manual*, United States Department of Energy, Washington, D.C., 2008.
- [43] C.D. Zeigler, A. Robbat, Comprehensive profiling of coal tar and crude oil to obtain mass spectra and retention indices for alkylated pah shows why current methods err, *Environ. Sci. Technol.* 46 (7) (2012) 3935–3942.
- [44] O. Faix, D. Meier, I. Fortmann, Thermal-degradation products of wood – a collection of electron-impact (EI) mass-spectrometry of monomeric lignin derived products, *Holz als Roh- und Werkstoff* 48 (9) (1990) 351–354.
- [45] B. Shukla, M. Koshi, A highly efficient growth mechanism of polycyclic aromatic hydrocarbons, *Phys. Chem. Chem. Phys.* 12 (10) (2010) 2427–2437.
- [46] K. Kiersch, J. Kruse, K.U. Eckhardt, A. Fendt, T. Streibel, R. Zimmermann, G. Broll, P. Leinweber, Impact of grassland burning on soil organic matter as revealed by a synchrotron- and pyrolysis-mass spectrometry-based multi-methodological approach, *Org. Geochem.* 44 (2012) 8–20.
- [47] P. Potzinger, G. Vonbunau, Empirical considerations of excess energy in assay of appearance potentials, *Berich. Bunsen. Gesell.* 73 (5) (1969) 466.
- [48] Y. Gotkis, M. Oleinikova, M. Naor, C. Lifshitz, Time-dependent mass-spectra and breakdown graphs. 17. Naphthalene and phenanthrene, *J. Phys. Chem.* 97 (47) (1993) 12282–12290.
- [49] J.T. Andersson, A.H. Hegazi, B. Roberz, Polycyclic aromatic sulfur heterocycles as information carriers in environmental studies, *Anal. Bioanal. Chem.* 386 (4) (2006) 891–905.
- [50] T.K. Green, P. Whitley, K. Wu, W.G. Lloyd, L.Z. Gan, Structural characterization of sulfur-compounds in petroleum by S-methylation and C-13 NMR-spectroscopy, *Energy Fuels* 8 (3) (1994) 814.

## Publikation 2

Otto, S.; Erdmann, S.; Streibel, T.; Herlemann, PR D.; Schulz-Bull, D.; Zimmermann, R., 2016. Pyrolysis-gas chromatography-mass spectrometry with electron-ionization and resonance-enhanced-multi-photon-ionization for characterization of terrestrial dissolved organic matter in the Baltic Sea. *Analytical Methods* 8: 2592-2603.  
(DOI: 10.1039/C5AY01292A)





Cite this: DOI: 10.1039/c5ay01292a

# Pyrolysis-gas chromatography-mass spectrometry with electron-ionization and resonance-enhanced-multi-photon-ionization for the characterization of terrestrial dissolved organic matter in the Baltic Sea†

Stefan Otto,<sup>a</sup> Sabrina Erdmann,<sup>a</sup> Thorsten Streibel,<sup>\*ab</sup> Daniel P. R. Herlemann,<sup>c</sup> Detlef Schulz-Bull<sup>d</sup> and Ralf Zimmermann<sup>ab</sup>

With the effects of global warming the input of terrigenous material into the oceans is increasing, with unknown consequences for the ecosystem. The Baltic Sea is an ideal research object and observed effects can be transferred to the oceans. This paper combines the influence of biotic and abiotic factors especially for terrigenous dissolved organic matter (tDOM). The study is focused on specific lignin target molecules and reflects the influence of salinity and microbial activity. Samples were taken along the salt gradient. In addition, an incubation experiment, mixing of tDOM-rich river water with Baltic Sea water from three different stations, was carried out. A newly developed pyrolysis gas chromatography mass spectrometry (Py-GC/MS) method using two different mass selective analyzers in one measurement cycle was established for the analysis of tDOM species. It enables the characterization of natural samples by a universal (electron ionization quadrupole MS) as well as an aromatic fingerprint (resonance-enhanced-multi-photon-ionization time-of-flight MS). By thermal desorption (TD) and subsequent pyrolysis the free volatile and high molecular weight structures are accessible. A huge part of the chemical species exists as high molecular structures. The salt content has a high influence on the composition of DOM. Generally, under TD conditions greater changes were observed, especially for the incubation experiment. Under pyrolysis and the chosen experimental conditions, the lignin apparently is hardly degraded by microorganisms.

Received 19th May 2015  
Accepted 12th February 2016

DOI: 10.1039/c5ay01292a

www.rsc.org/methods

## 1. Introduction

The climate change and the associated negative consequences for many ecosystems, particularly the oceans, are discussed worldwide. As a result of the global warming, the temperature in arctic regions increases and the rivers located there have shown trends of a higher water discharge.<sup>1</sup> With the enhanced inflow by Nordic rivers, the input of terrigenous material in the oceans

risers as well. The structural characterization of this material such as dissolved organic matter (DOM) and the understanding of its alterations while being transported to the oceans has been an increasing area of research over the past few decades.<sup>2</sup> Large fractions of terrigenous dissolved organic matter (tDOM) are removed from the river inflow areas towards the open oceans. Possible reasons are abiotic as well as microbial degradation.<sup>3–5</sup> While abiotic factors such as salinity or solar radiation are studied in detail,<sup>6–10</sup> the microbial degradation is poorly understood and previous experiments showed contrasting results.<sup>1,4,11–14</sup>

Terrestrial DOM is a ubiquitous and dynamic mixture with a characteristic organic chemical signature for every individual region.<sup>15,16</sup> A distinction between particulate organic matter (POM) and DOM is operationally defined. The latter is assumed to pass a 0.45 µm filter pore whereas POM is retarded. It is also a combination of refractory and labile marine and terrigenous compounds. The riverine organic matter can be soil-derived and mostly has a terrigenous origin.<sup>6</sup> The input of tDOM by freshwater is considerably high,<sup>8,17</sup> but only a small fraction (0.7–2.4%) of this introduced total DOM in the oceans is detectable.<sup>18</sup>

<sup>a</sup>Joint Mass Spectrometry Centre, Chair of Analytical Chemistry, Institute of Chemistry, University of Rostock, 18059 Rostock, Germany. E-mail: thorsten.streibel@uni-rostock.de; Tel: +49 381 498 6536

<sup>b</sup>Joint Mass Spectrometry Centre, Cooperation Group Comprehensive Molecular Analytics (CMA), Helmholtz Zentrum München-German Research Center of Environmental Health (GmbH), Ingolstädter Landstrasse 1, 85764 Neuherberg, Germany

<sup>c</sup>Biological Oceanography, Leibniz Institute for Baltic Sea Research, 18119 Warnemünde-Rostock, Germany

<sup>d</sup>Marine Chemistry, Leibniz Institute for Baltic Sea Research, 18119 Warnemünde-Rostock, Germany

† Electronic supplementary information (ESI) available. See DOI: 10.1039/c5ay01292a



The reason for this could be various elimination processes that are still unclear in detail. This is remarkable, because arctic tDOM seems to be relatively stable over time.<sup>19,20</sup>

Lignin, as a part of tDOM, is a tracer for terrestrial organic matter, since it is source specific and produced only by vascular plants.<sup>2,13,16</sup> The degradation products of lignin are phenolic monomers, which can be divided into four different structural families: *p*-hydroxy (H building block), syringyl (S building block), vanillyl and cinnamyl family.<sup>21</sup> For simplification the last two are taken together as V building blocks, because they have the same aromatic base bodies. The S/V value is often used to distinguish between gymnosperm (non-flowering vascular plants) and angiosperm (flowering vascular plants) sources.<sup>13,21</sup> A high amount of H building blocks often represents grass lignins,<sup>4</sup> but the free forms can also have a marine origin.<sup>22</sup>

The influence of an increasing salinity on high-molecular-weight-DOM and the alterations by flocculation, adsorption to suspended matter,<sup>23</sup> photochemical transformation<sup>7,9,24</sup> and microbial decomposition<sup>10</sup> are important removal mechanisms for tDOM on its way from the freshwater input to the oceans. Often a combination of biotic and abiotic factors is responsible for the degradation of DOM. Salinity can play an important role in enhancing the decomposition rate by bacterial communities.<sup>4,5,10</sup> In general, the degradation rates of DOM vary tremendously, between 6 and 70%,<sup>1,14,25,26</sup> depending on the experimental approach. Moreover, the temperature has a significant influence on the degradation of DOM.<sup>27</sup> It is claimed, that colloidal, high-molecular-weight-DOM is more biological and chemical reactive than under low temperature conditions.<sup>28</sup>

In order to describe the role of tDOM, especially of lignin, its input, transformation and degradation, specific methods are needed to get more detailed information on the structure at a molecular level. In the ocean the concentration of DOM is extremely low with <1 mg L<sup>-1</sup>.<sup>29</sup> Therefore the isolation and purification of DOM is important and often linked to the subsequent analysis. Retention-based methods are enriching the DOM and remove inorganic material (*i.e.* salt),<sup>28,30</sup> which is essential for chromatographic methods. Generally gas chromatography (GC) in combination with alkaline cupric oxidation to yield specific lignin monomers<sup>11,13,21</sup> or conversational pyrolytic degradation<sup>28,31</sup> are established for characterizing lignin-deriving organics. By using a derivatisation reagent the number of compounds that are identifiable can be increased.<sup>4,8,21,32</sup>

In this study, a GC separation followed by two distinct MS-methods in parallel was applied for the characterization of tDOM for the first time. The analytical system consists of a quadrupole and a time-of-flight MS (QMS and ToFMS) in combination with electron ionization (EI) and photo ionization (PI), respectively. EI, a hard ionization technique, leads to high fragmentation of the organic molecules. Despite the fact that the characteristic fragmentation pattern can be used for substance identification, sometimes the loss of the molecular ion aggravates the identification. The lack of the molecular ion signal can be prevented by using photo ionization such as

resonance-enhanced-multi-photon-ionization (REMPI), a soft ionization method. For a successful ionization *via* an intermediate state two photons have to be absorbed.<sup>33–35</sup> REMPI has a high selectivity and sensitivity for aromatic hydrocarbons, depending on the used photon wavelength and additionally on the ionization energy threshold.<sup>36–38</sup> The developed Py-GC/MS method with two different mass selective analyzers combined in one measurement cycle, enables the characterization of natural samples by a universal (EI) as well as an aromatic fingerprint (REMPI) and was successfully applied by Otto *et al.* (2015) to crude oil samples.<sup>39</sup> Therefore the aim of the present study was to characterize riverine DOM by the newly developed Py-GC/MS combination<sup>39</sup> and its structural and semi-quantitative compositional changes along the gradient of salinity and during decomposition by marine bacterial communities.

## 2. Experimental section

The experimental part is roughly divided into the sampling along the salt gradient of the Baltic Sea and the incubation experiment on three different stations.

### 2.1. Sample size and sampling

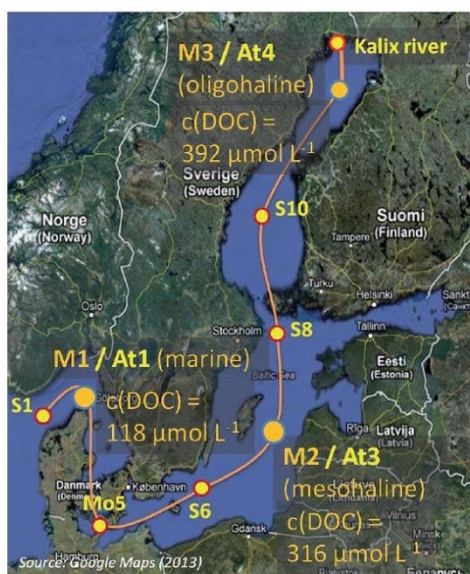
Samples were collected on a research cruise with the Meteor (M87/3a) between Skagerrak (S1 station) and the Gulf of Bothnia (At4 station) in May/June 2012. One part of the sampled water was taken for the salinity gradient measurements (see Fig. 1a).

Another important part of the study was the incubation experiment at three representative salinities. The stations are labeled with M1, M2 and M3 (identical with At1, At3 and At4). The selection of the relevant stations was based on the publication of Herlemann *et al.* (2011), where three suitable bacterial communities in the Baltic Sea, a marine/brackish group (salinity 8–32), brackish group (salinity 3–8) and a freshwater-brackish group (salinity < 3) were identified.<sup>40</sup> The microorganisms are able to use tDOM as the carbon source. In order to investigate the degradation of tDOM by microorganisms, tank experiments were conceived.

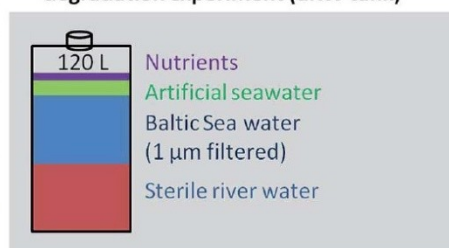
Kalix river water (located in North Sweden), which is rich in terrigenous dissolved organic material, was mixed with the sampled Baltic Sea water. The river water was sampled during the spring flood in May 2011 (see Herlemann *et al.* (2014) for detailed information), sterile-filtered and stored at –20 °C. For each sampling station, the river water was at first mixed with artificial seawater to reach the salt content of the current sample station, in order to limit the stress for the microorganisms. Finally, it was filled up with 50% surface water of the current station. This mixing tank contains 120 L water volume and is abbreviated as uRW-tank. In this study the mixed uRW tanks as well as a control tanks (cBS, Baltic Sea water only) were examined for three representative salinities. The reason for utilizing the cBS tank is the fact that Baltic Sea water contains natural DOM and microbial processes are still running. The composition of DOM is also changed. Therefore, the investigation of such changes by added artificial DOM through river water becomes necessary. Three biological replicates from each



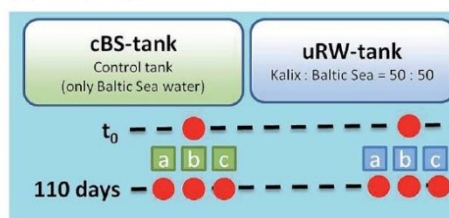
(a) Line of salinity (summer 2012)



(b) Experimental set up for DOM degradation experiment (uRW tank)



(c) Sampling



(d) Details for important sample stations

Station	Date of sampling	GPS-position	Depth [m]	Temperature [°C]	Salinity [PSU]
S1	2012-05-30	57 00.0995N 006 55.1060E	2.85	11.61	32.06
At1	2012-06-01	58 07.9991N 010 00.0005E	1.70	12.16	30.38
Mo5	2012-05-31	54 42.0068N 010 56.0121E	1.59	12.88	11.68
S6	2012-06-01	55 33.9834N 016 22.0539E	2.70	9.83	7.47
At3	2012-06-02	57 18.3467N 020 04.6968E	3.75	9.07	7.19
S8	2012-06-04	59 21.4864N 020 06.0728E	1.35	6.93	6.31
S10	2012-06-06	61 46.9808N 19 17.6021E	2.33	5.77	5.47
At4	2012-06-05	65 26.7066N 023 17.9074E	1.79	4.32	2.66

Fig. 1 (a) Map of the Baltic Sea displaying the sample stations for the line of salinity and the three sampling sites for the incubation experiment. The sampling of Kalix river water is described in detail by Herlemann *et al.* (2014).<sup>3</sup> The dissolved organic carbon (DOC) concentration on At1, At3 and At4 is shown. (b) Experimental design of the tDOM decomposition culture experiment, (c) the tank setup and the time line for sampling and (d) location sites in detail.

selected station were stored for 110 days at 10 °C. Sampling was carried out at the beginning and after 110 days. The experimental set up for DOM degradation experiments is illustrated in Fig. 1b and c.

## 2.2. Sample preparation

All water samples taken along the gradient of salinity and for the degradation experiment were treated in the same way. 1 L was immediately filtered through pre-combusted (400 °C, 6 h) Whatman GF/F filters upon collection and the DOM fraction was concentrated by solid phase extraction (SPE) using reverse phase cartridges according to the protocol of Dittmar *et al.* (2008). A recovery rate of the reverse phase extraction for DOM is approximately 65 percent.<sup>30</sup> The water was acidified with HCl (37%, Carl ROTH, Karlsruhe) to pH = 2 and pumped through the cartridges at a low flow rate of ~30 mL min<sup>-1</sup> by a membrane pump. Then the cartridges were purged twice with 6 mL Milli-Q water (pH = 2) to remove salt residues. The cartridge adsorber material was dried under a stream of N<sub>2</sub>,

extracted with 6 mL of methanol (ultra LC-MS, Carl ROTH, Karlsruhe) and rapidly stored at -20 °C after the extraction. All glassware used was acid-washed (0.1 M HCl) and pre-combusted at 350 °C for 6 h.

## 2.3. Measurement system and sample injection

For the chemical analysis of tDOM, a pyrolysis-gas chromatography/mass spectrometry (Py-GC/MS) system enabling simultaneous application of hard and soft ionization techniques was used (for details see ESI† S1), which had been successfully applied for the investigation of crude oil samples.<sup>39</sup>

Before sample injection, the methanolic extract was pre-concentrated under N<sub>2</sub> (2 mL to 60 μL approximately), so that 0.5 to 1.0 mg of organic material is present. 10 μL of this extract were injected into the pyrolyzer (Frontier Laboratories, Double-Shot-Pyrolyzer, model: PY-2020iD), which is working with helium as carrier gas (head pressure 1 bar). The samples first undergo a thermal desorption (TD) process at 250 °C for one minute. After the TD process, the same sample is introduced for



a second time after the oven was heated up to 500 °C. For analysis of the elevated chemical compounds, the pyrolyzer is coupled directly to a gas chromatograph (HP 5890 Series II), split 1 : 10, equipped with a non-polar column (SGE-BPX-5; 30 m × 0.25 mm × 0.25 µm). The temperature program was conducted as follows: 60 °C (held for 2 min) to 320 °C (held for 12 min) with 10 °C min<sup>-1</sup>. After the separation process the gas flow was split (by a deactivated press fit 3-way Y-Splitter for FS tubing with 0.20 to 0.75 mm OD) and transferred simultaneously to two different mass spectrometers. One MS system is a QMS using EI with 70 eV. The other one is a ToFMS using [1 + 1]-REMPI (266 nm). The split ratio was 1 : 100 in favor of the EI-QMS. This is caused by the different column diameters. If the REMPI system gets the same amount of substance as the EI system, the multi channel plate (MCP) would be overloaded and detection of molecular ions would not be possible.

For calibration and optimization of the REMPI-ToFMS system a gas standard (Linde AG, Pullach, Germany) containing 1 ppm of each benzene, 1,2,4-trimethylbenzene, benzaldehyde and toluene in N<sub>2</sub> was applied. For generating REMPI, a Nd:YAG laser (BIG SKY ULTRA, Quantel, Les Ulis Cedex, France) with two frequency doubling units yielding 266 nm photons was employed, which corresponds to a photon energy of 4.11 eV. The laser is operated with 10 ns pulse width and a 20 Hz repetition rate exhibiting a power density of approximately 7 × 10<sup>6</sup> W cm<sup>-2</sup>. A reflectron ToF-MS (Reflectron CTF10, Kaesdorf Geräte für Forschung und Industrie, Munich, Germany) is utilized for the detection of the molecular ions. Details about the coupling and more specific device parameters are given in Otto *et al.* (2015) and Fendt *et al.* (2012).<sup>36,39</sup> The coupling of pyrolyzer and GC/MS with two distinct ionization methods was checked for functionality with an IHSS (International Humic Substances Society) reference sample (Nordic Reservoir NOM). The reference material was dissolved in Milli-Q water and the sample preparation was carried out in the same way as for the water samples. The samples were measured in a mass-to-charge-ratio (*m/z*) range from 10 to 400. On the one hand the total ion chromatograms (TIC) of EI-QMS were consulted to identify compounds with the help of different MS tools (NIST spectral library, mass spectral interpretation). On the other hand, if the data base information was inaccurate, then standard substances were dissolved (approximately 100 mg L<sup>-1</sup>) and subjected to chromatographic analysis or a tentative assignment was performed, based only on analysis of the fragmentation patterns. For semi quantitative statements the peak intensity of molecular ions of the REMPI-ToFMS measurements was used.

### 3. Results and discussion

The high complexity of DOM in Baltic Sea water is evident from Fig. 2. It shows an aromatic fingerprint (detection by REMPI-ToFMS) of the sample under TD and pyrolysis conditions, respectively. The *m/z* ratio is plotted against GC retention time. The intensity of the mass signal is depicted as color display. The surface water of the northernmost station (At4) was analyzed. It has a much higher concentration of DOM in comparison to

stations of lower latitudes due to many boreal and subarctic rivers, which drain in the Gulf of Bothnia and influence the water chemistry *via* a high tDOM input, especially in spring time.<sup>15</sup> The TD step shows a less complex spectrum of substances with low signal intensities. Aromatic compounds are present in a mass range between *m/z* 70 and 250. In the pyrolysis step a broad substance spectrum with higher signal intensities is visible. The aromatic substance spectrum starts with an *m/z*-value of approximately 60 going up to 330.

Fig. 2 illustrates that free evaporable molecular structures are barely present. In contrast, a lot of components are accessible only in the pyrolysis step. Hence, DOM mainly consists of large high molecular complex structures. Many of these are aromatic, especially phenolic compounds, hinting at lignin degradation products.<sup>32</sup>

With the help of EI-QMS, referring to the fragmentation pattern and database matching, (Wiley, Nist) a classification was successful. Some representatives of possible lignin derivatives are shown in Fig. 3. The GC retention time is displayed against the signal intensity for specific molecular ion tracks. Guaiacol (*m/z* 124, *t*(R) = 468 s), *p*-hydroxyacetophenone (*m/z* 136, *t*(R) = 698 s), 2,6-dimethoxyphenol (*m/z* 154, *t*(R) = 800 s) and vanillin (*m/z* 152, *t*(R) = 152 s) are typical degradation products of lignin. Phenol (*m/z* 94, *t*(R) = 370 s) could be a pyrolysis fragment of *p*-hydroxybenzoic acid, an H-building block of the lignin structure (Fendt *et al.*, 2011; van Heemst *et al.*, 2000).<sup>32,41</sup> The direct comparison of the two ionization techniques shows that with EI nearly all structures are detectable, but the chromatograms get very complex. Moreover, fragmentation makes peak evaluation even more difficult, which is obvious for the traces *m/z* 152 (vanillin) and 154 (2,6-dimethoxyphenol), respectively, where the relevant peaks are difficult to detect. The simultaneously recorded REMPI-ToFMS spectrum depicts only the molecular ions of aromatic structures. The chromatograms become less complex. REMPI shows clear peak intensities for the aromatic structures vanillin (*m/z* 152) and 2,6-dimethoxyphenol (*m/z* 154). Therefore REMPI data are used for the subsequent statistical analysis (see below), whereas the EI data are still consulted for structural identification.

#### 3.1. Trends with salinity

The changes of DOM with salinity as well as during the incubation experiments are discussed in the following on the basis of selected and frequently observed species representing the H- (phenol, vinyl phenol, *p*-hydroxyacetophenone), V- (guaiacol, 4-vinyl-2-methoxyphenol, vanillin) and S-building blocks (2,6-dimethoxyphenol, 4-vinyl-2,6-dimethoxyphenol, acetosyringone), respectively.<sup>2,16,21</sup>

For data analysis and to obtain semi-quantitative results, the peak intensity from the REMPI-chromatogram of a molecule with a characteristic retention time is used. That was conducted for all stations from the Kalix river (tDOM source, lowest salinity) to the S1 station (highest salinity). On every station three replicates of the surface water samples were measured. The relative peak intensities were calculated and are illustrated



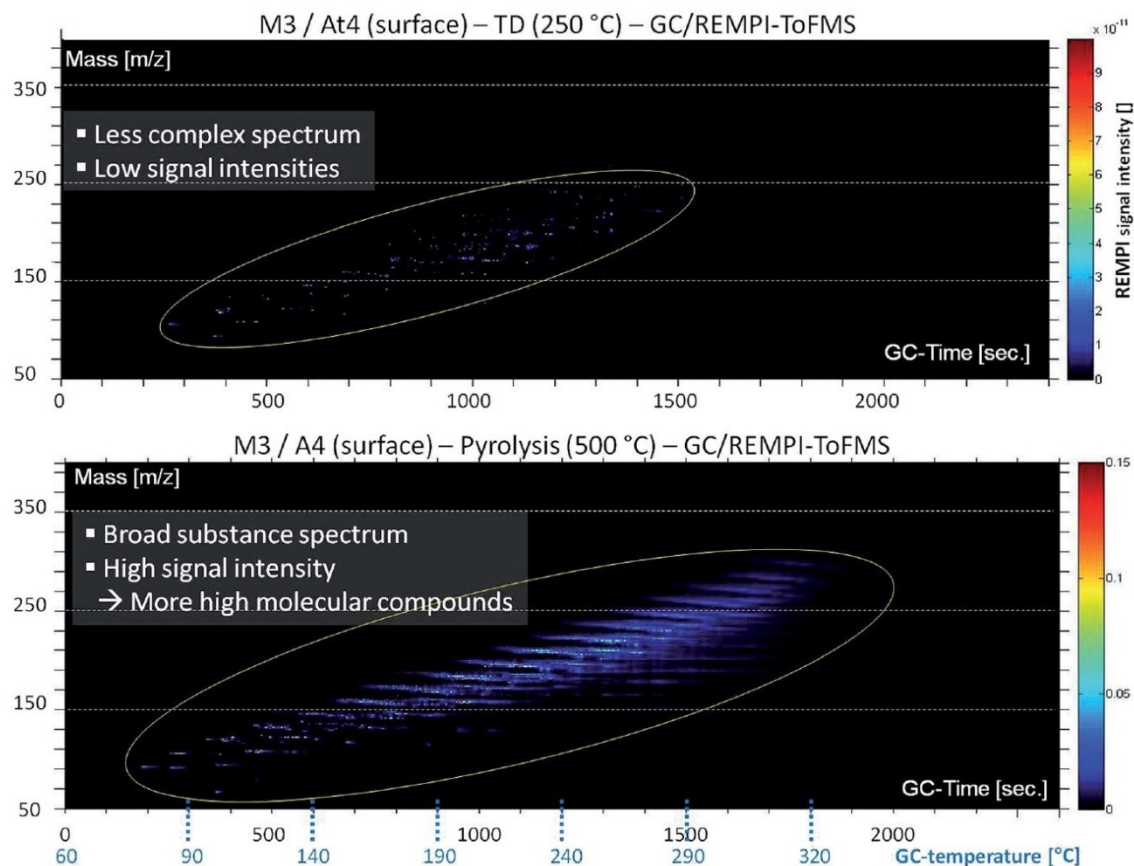


Fig. 2 Image plot (GC retention time vs. mass-to-charge-ratio vs. signal intensity) of At4 surface water (rich in tDOM) under TD (top) and Py (bottom) conditions resulting from the use of REMPI-ToFMS detection.

in Fig. 4–6. For this, the peak intensity of the REMPI chromatogram of a molecular ion was divided by the total intensities for all nominal masses from 90 to 450  $m/z$  in a certain time window. Under the additional assumption that the North Sea input (*via* Skagerrak) constitutes no source for the components of tDOM its influence is not considered.<sup>18</sup>

Phenol ( $m/z$  94,  $t(R)$  = 370 s) is observed to show a decreasing trend from the river mouth to the S1 station (under TD conditions). It is feasible that it was released by biotic or abiotic processes from high molecular weight structures (*e.g.* lignin). To decide about this, incubation experiments were carried out, the results of which are discussed later. Under pyrolysis conditions phenol is also observed, with a slightly falling trend towards the higher salinity. The main origin of pyrolytic phenol is lignin. Similar courses are obtained for other H building block species such as vinylphenol ( $m/z$  120,  $t(R)$  = 610 s).

In contrast, *p*-hydroxyacetophenone ( $m/z$  136,  $t(R)$  = 698 s) shows a different pattern. The concentration of the free component clearly increases up to the S6 station and then decreases towards the salt water inflow. However, under pyrolysis conditions, its content remains almost unchanged. This suggests that the free substance (registered under TD conditions) is additionally formed by an alternative mechanism,

which superimposes the general mechanisms forming other H-building blocks such as phenol. However, this only holds down to the latitude of the S6 station. The V-building blocks (Fig. 5), under TD as well as pyrolysis conditions, depict a similar decreasing trend along the Baltic Sea transect as the H-building blocks.

The S building blocks were taken into consideration (Fig. 6), although their input sources into the Baltic Sea should be very low, because there is mainly a freshwater surplus from Scandinavian rivers<sup>15</sup> with typical vegetation of non-flowering vascular plants.<sup>13,21</sup> Therefore, according to a signal-to-noise  $\geq 3$ , the representatives 2,6-dimethoxyphenol and 4-vinyl-2,6-dimethoxyphenol could not be analyzed semi-quantitatively under TD conditions. Acetosyringone as the only detectable relevant substance under TD is represented graphically and shows a constant distribution along the transect. Under pyrolysis conditions the concentration of S-building blocks is generally higher. For 2,6-dimethoxyphenol and 4-vinyl-2,6-dimethoxyphenol a slightly rising trend is visible with increasing salinity. A possible explanation is that lignin components are introduced *via* the river systems, having their origin in angiosperm tissues. In general, the relative distribution pattern of the S-building blocks along the line of salinity does not change.



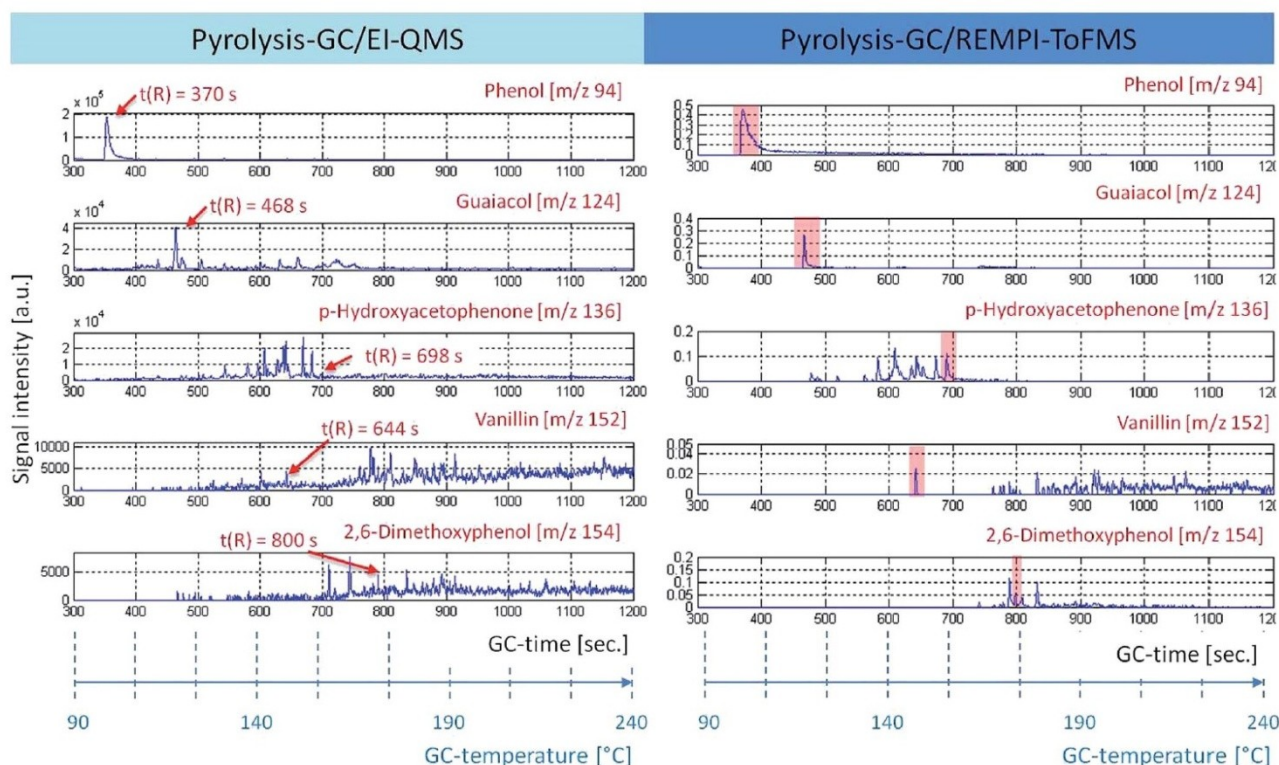


Fig. 3 The time course of ion traces under pyrolysis conditions (retention time or GC temperature vs. signal intensity). It allows a direct composition between the two mass-selective detectors, EI-QMS (left) and REMPI-ToFMS (right). In particular,  $m/z$  94, 124, 136, 152 and 154 can be related to possible lignin degradation products, which can be used as tracers for tDOM.<sup>32</sup>

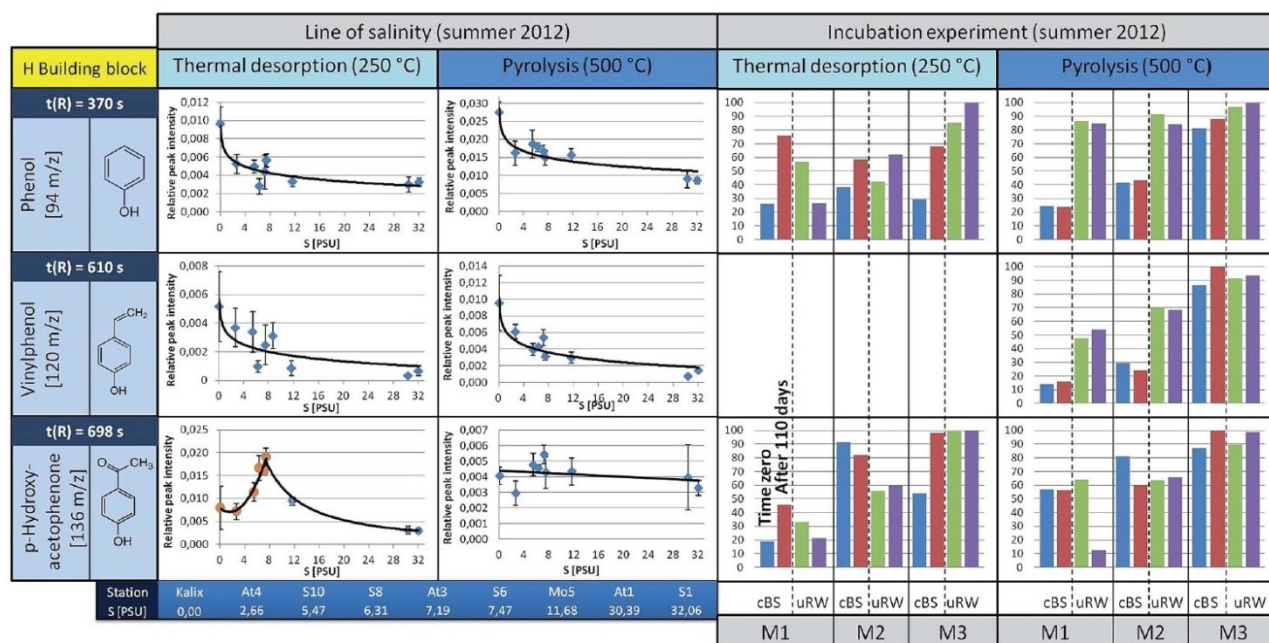


Fig. 4 Summary of three representatives of the H building blocks is shown (left: the curves along the transect of the Baltic Sea, right: the results of the incubation experiments, under TD and pyrolysis conditions). In the diagrams for the line of salinity the relative peak intensities are given for each compound vs. the salinity  $S$ . The error bars being the standard derivation of the three measurements. The black lines are the trend curves for the compound concentration. The latter of the respective stations is noted below. For the incubation experiments, the relative peak intensities are shown for a component (specific retention time). The control cBS (pure Baltic Sea water) at time zero (blue) and after 110 days (red) and the mixing tank uRW (Baltic Sea water + river water) at time zero (green) and after 110 days (purple) were compared for every station M1-3. For M1 surface water of At1 station were used, for M2 water of At3 and for M3 water of At4. Only REMPI-ToFMS data were used for the images.



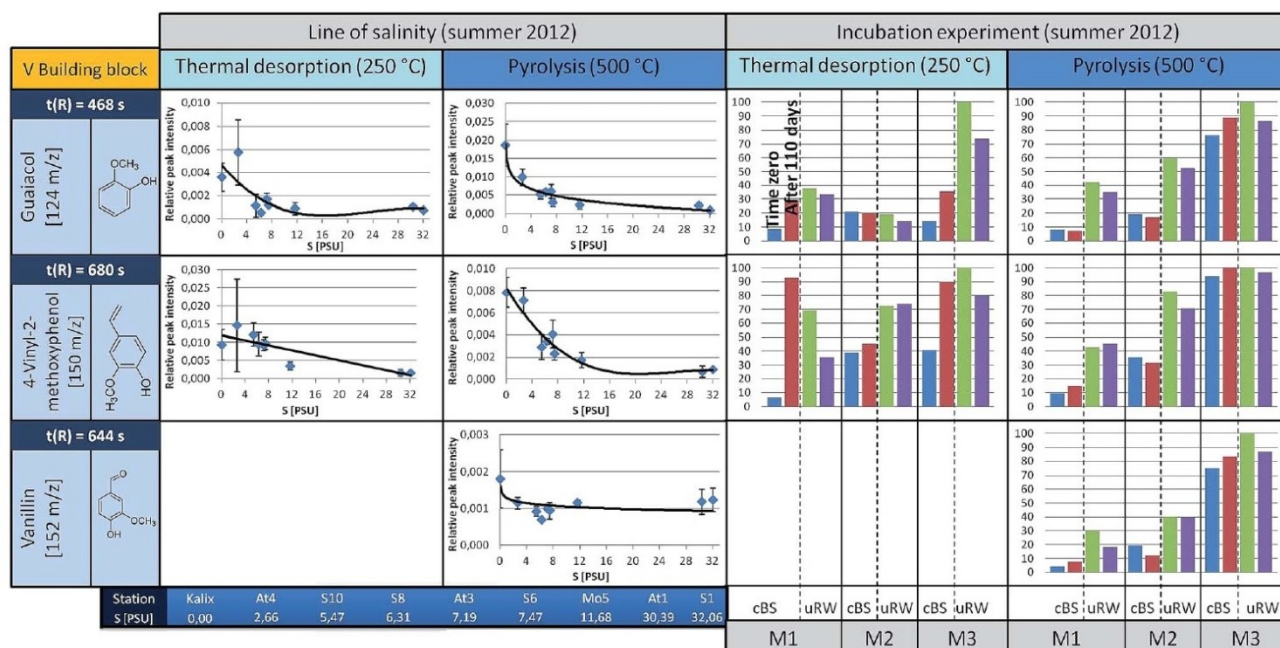


Fig. 5 A summary for three representatives of the V building blocks is given (left: the courses along the line of salinity, right: the results of the incubation experiments, under TD and pyrolysis conditions). For detailed information see Fig. 4. In the free areas (the incubation experiment at 250 °C, component  $m/z$  120) no insufficient data for a clean presentation was available.

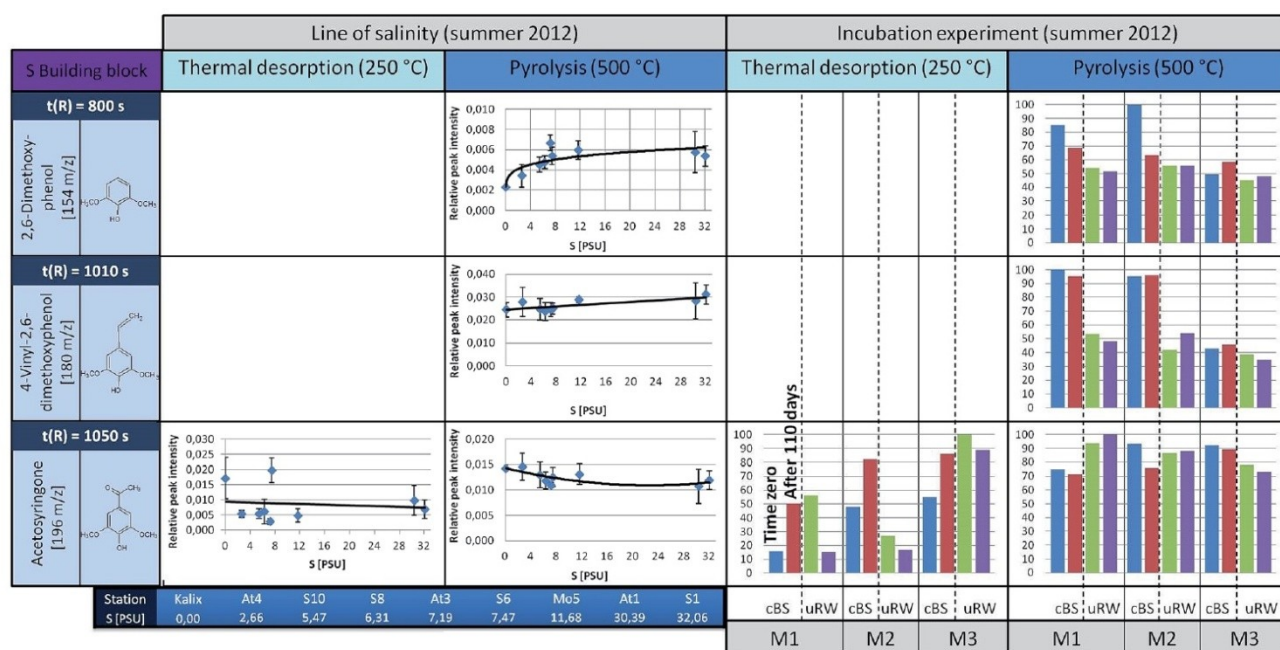


Fig. 6 A summary for four representatives of the S building blocks is illustrated (left: the courses along the line of salinity, right: the results of the incubation experiments, under TD and pyrolysis conditions). For detailed information see Fig. 4 and 5.

### 3.2. Incubation experiments

But what are the reasons that phenol and vinylphenol (free or macromolecular pyrolysis fragment) tend to decline with higher salt content? In addition to the degradation by sunlight or flocculation,<sup>9,23</sup> microorganisms are possibly able to affect the

compound concentration along the transect. This hypothesis was studied in the already mentioned tank experiments carried out for three stations, designated as M1, M2 and M3, corresponding to salinities of approximately  $S = 32$ , 7, and 3, respectively.



The results for selected H-building blocks are also given in Fig. 4. The bars in the diagram represent the relative peak intensity of a molecule at the compound-specific retention time. For each station a control tank (cBS) and a mixing tank (uRW) are compared, both for time zero (blue or green bar) and after approximately 110 days of incubation, equivalent to the end of the experiment (red or purple bars).

The direct comparison between cBS- and uRW-tank at time zero shows that the phenolic fraction (under TD) increases significantly due to the addition of river water. This is obvious at all three stations. Comparing the cBS tank at time zero (cBS<sub>0</sub>) with the state at the end of the experiment (cBS<sub>End</sub>) illustrates that the proportion of phenol increases. A similar trend is evident for the mixing tanks uRW (M2 and M3). The differing behavior of the uRW tank cannot be explained with the available data. Nevertheless, the free phenol content shows the tendency to be higher after 110 days. A possible source for this increase could be phenol previously bonded within the lignin structure, which is then released by microbial degradation. In order to prove this hypothesis, pyrolysis measurements were performed. If lignin was indeed degraded during the incubation experiment, the released pyrolytic phenol should decrease significantly after 110 days of incubation time, because it has already been microbially degraded. However, the phenol content between the start and the end time of incubation in all tanks stays nearly the same. This implies that the lignin in the tDOM is not degraded by microbial processes after all. Another source for the increase of the free phenol concentration in the TD step of the sBS and uRW tanks cannot be clearly assigned. For *p*-hydroxyacetophenone, it is difficult to give a reliable statement. In tendency, there hardly occurs a change under TD and pyrolysis conditions in the tank between time zero and 110 days.

The incubation experiment measurements of the V-building blocks under TD conditions show no clear trend. Vanillin was not detected, because its concentration at all stations is below the limit of detection (LOD) for the TD setup. For guaiacol and 4-vinyl-2-methoxyphenol with the exception of the M2 station a significant increase in concentration is observed in the cBS-tank after 110 days. With the M1 and M3 tanks an opposite trend between cBS and uRW samples is observed. For unraveling these contradicting findings, a broader data basis from additional experiments will be needed. In general, the V-building blocks behave similar to the H-building blocks, especially the absence of significant changes in the pyrolytic experiments is striking, corroborating the findings of the H-building blocks.

In the incubation experiments of the S-building blocks samples under TD conditions exhibited too low peak intensities. Under pyrolysis conditions no clear significant changes are observed between the start and end point of sampling for both the cBS and the uRW tank.

The biggest effect on the chemical composition of the tDOM is caused by the added, salinated river water (see ESI,† S2) in the incubation. In order to take a closer look on these effects, in the next section PCA is applied, which can be a helpful tool for data interpretation.

### 3.3. Principal component analysis (PCA)

Principal component analysis on the basis of the REMPI-ToFMS data was used as a statistical tool in order to detect structural changes along the salt gradient. In addition, PCA is utilized to evaluate the repeatability of technical replicates. The peak intensities of nominal masses between 50 and 350 *m/z* of a GC run were taken. For the three technical replicates of each station and between each station the retention times for the peak have to be matched. For this a self-developed specific software routine (in Matlab) is used that allows an automatic correction of the time shifts between the GC runs. Finally, the performed PCAs are resulting in a matrix of 27 measurements (3 replicates  $\times$  9 stations), the nominal masses 50–350 *m/z* and the maxima peak intensities for every ion trace. The data were normalized by the sum peak intensities in the window of the observed mass-to-charge ratio. The reduction to one peak per nominal mass leads to a loss of information, but is necessary for handling and interpreting the huge amount of data.

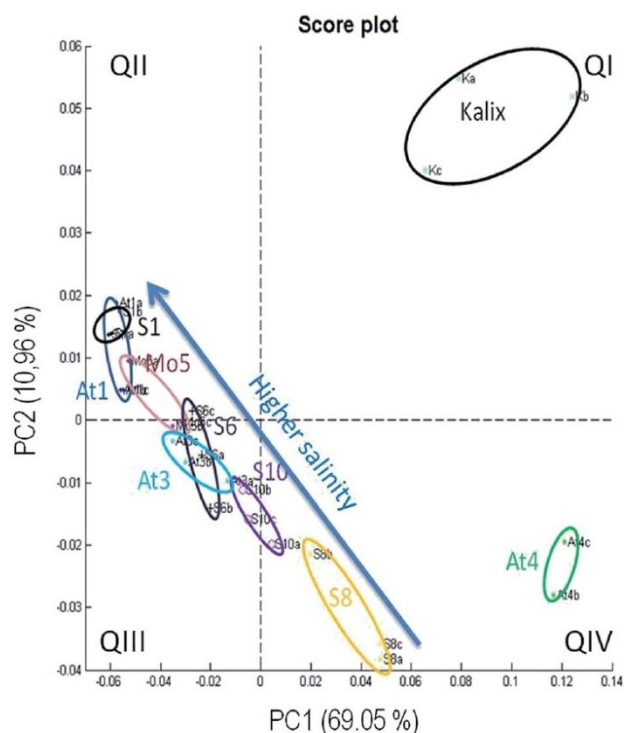
The results are displayed in Fig. 7. The repeatability of technical replicates is quite recognizable, the three measurements from each station are grouped together. An axis assignment for PC1 and PC2 is not clearly possible. Both reflect the trend of salinity as well as of temperature. These parameters decrease accordingly from the southwest to the northeast of the Baltic Sea. This would explain the apparent diagonal course in the diagram. In the TD step the stations extend in a line from the QII to the QIV sector, according to the salinity or temperature pattern. Apparently, except for the stations S8 and S10, a straight relationship between the molecular structure and abiotic parameters exists. In this context, the separation of the stations is not linear and logically grouped with the salinity gradient. The reasons are unclear and difficult to explain by one parameter. The At4 replicates are located in sector IV, but not in line with the other stations. The replicates of Kalix even significantly differ and have an outstanding position in the plot. Roughly the PCA can be divided in two different areas, the Kalix/At4 and the remaining line of salinity from S1 to S10.

The appropriate loadings plot shows some significant *m/z* values under TD conditions. Those nominal masses are situated in sector QIV, which are present at a lower salinity, for example *m/z* 136 as a possible lignin building block. In addition *m/z* 146, 192, 196 and 206 are significant for the location of At4 in this sector, however, a structural characterization for these *m/z* values was not possible. In sector QII nominal masses are located, which are linked to higher salinities, for example *m/z* 128 (naphthalene) or 166 (fluorene). They represent typical markers for polycyclic aromatic hydrocarbons (PAH) as a possible result of massive ship traffic in the Kattegat/Skagerrak area.<sup>42</sup> These two *m/z*-ratios and *m/z* 180 (unknown structure) strongly influence the course. The *m/z* values 156, 170, 172, 206 and 213 are detected in the Kalix river, which are responsible for the location of the replicates in QI. A structural characterization is difficult, but a contamination by a plasticizer cannot be excluded.

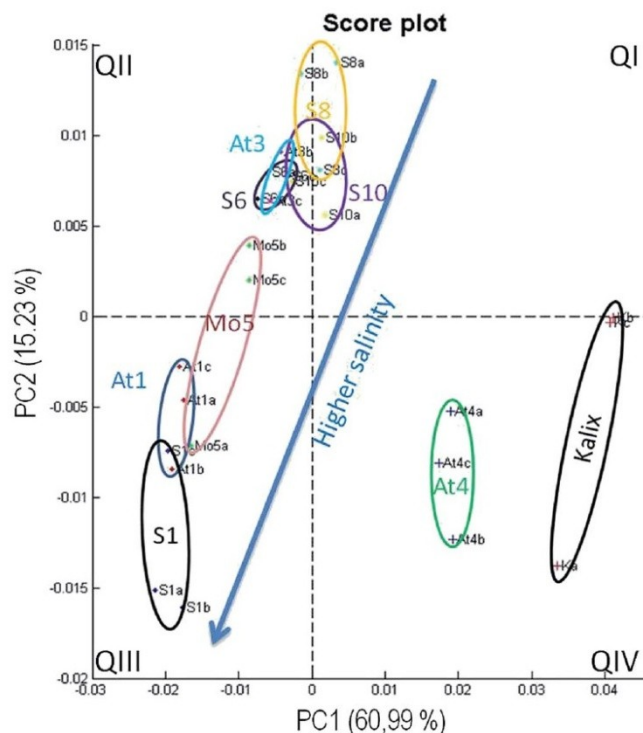
The PCA under pyrolysis conditions shows a curve from sector 3 up to 1 along the line of decreasing salinity. Under high



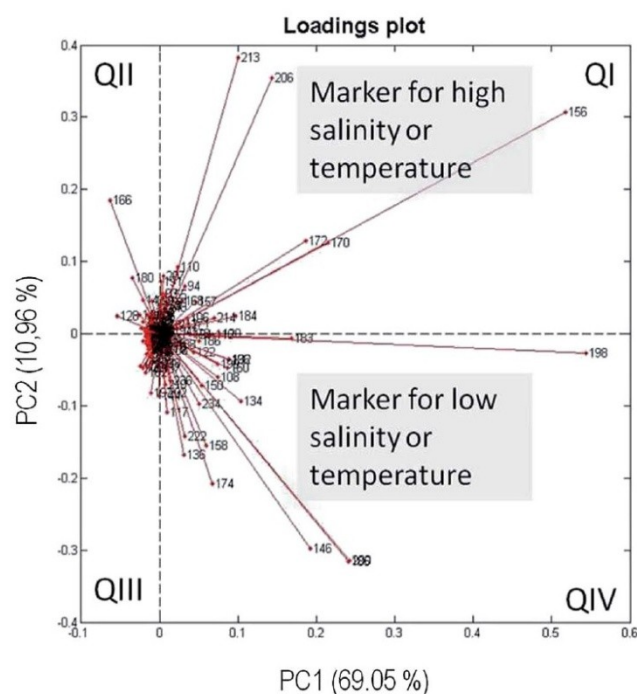
Thermal desorption (250 °C)



Pyrolysis (500 °C)



Thermal desorption (250 °C)



Pyrolysis (500 °C)

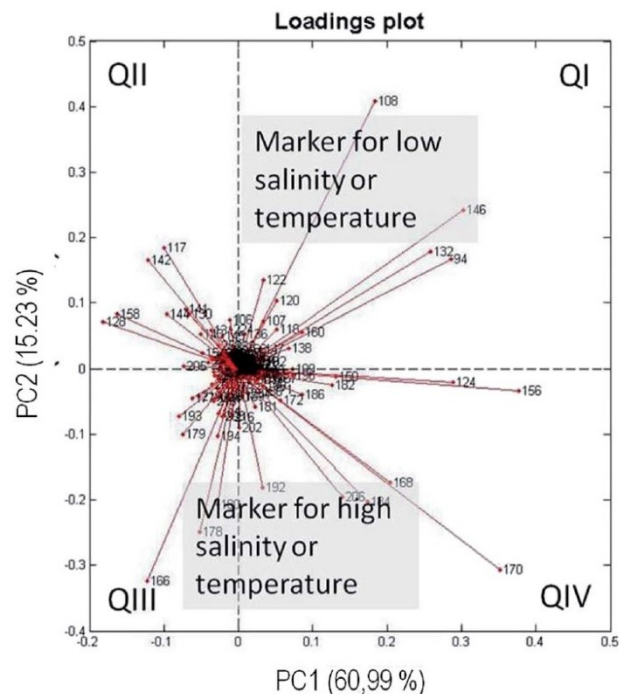


Fig. 7 Top: The score plot of the Principal Component Analysis (PCA) for the line of salinity for three technical replicates per station (grouped together in one cycle) under TD conditions (left) and pyrolysis conditions (right). PC1 and PC2 represent the salinity or the temperature gradient respectively. The trend arrow shows the gradient of salinity. Bottom: Loading plots for the score plots with nominal masses between 50 and 350  $m/z$ .



salinity conditions, again PAH representatives are responsible for the shift. The loadings plot illustrates that  $m/z$  166 (fluorene) or 178 (phenanthrene) are dominant at a high salinity (QIII). In QI (low salinity) mainly the nominal masses  $m/z$  94, 108, 124, 132, 146, 156 and 170 – all of them representing lignin moieties – are responsible for the At4 and Kalix replicates having high positive PC1 scores and that is the reason why these two stations are differing from the others.

As a summary, the results of the PCA are consistent with those from the trend charts before. The abiotic factor salinity has a high influence on the DOM composition. A further important factor for the separation of sampling stations with respect to DOM mixture is the content of lignin derived species and PAH, indicating the influence of terrestrial material and anthropogenic input.

## 4. Conclusion

The compositional changes of DOM in the Baltic Sea were studied with respect to two different aspects: first, along a Baltic Sea surface water transect and secondly with a focus on the microbial degradation under various special salinity conditions. The chemical analysis of the water samples were carried out by a new coupled system, which has already been successfully tested on crude oil samples.<sup>39</sup>

Generally along the salinity gradient, referring to the semi-quantitative measurements, a decrease of free and bonded lignin compounds was observed. The PCA underlines that, additionally showing a correlation between salt content and DOM composition. This trend of lignin along salinity is well described in the literature,<sup>43</sup> but the used method of TD and pyrolysis in combination with REMPI was applied for the first time for DOM characterization and allows the analysis of aromatic and macromolecular species in a relatively easy way.

Salinity has a crucial influence on DOM concentration and especially on the lignin derived structures. Other compound classes such as PAH are also affected, which is the subject of currently conducted additional analyses. In contrast, microorganisms are hardly breaking the lignin structure. This follows from the semi-quantitative analysis under pyrolysis conditions. Compared to this, under TD conditions changes are quite visible but difficult to interpret. It cannot be ruled out that on different conditions and longer time scales microorganisms would break the lignin structure. Especially several abiotic factors such as wind (continuous mixing, fresh air supply) and UV radiation were excluded in the current setup.

Nonetheless, the coupled system, consisting of a pyrolyzer, a gas chromatograph and two mass selective mass analyzers, has been proven useful to analyze water samples with respect to their DOM content. A sample separation and a combination of universal as well as selective and sensitive detection are advantageous for the characterization of the complex DOM. In particular trace levels of low molecular weight substances (free components or pyrolytic degradation products) can be detected. The analytical method enables a closer look at the molecular composition of natural samples.

The measuring setup could be optimized further by using varying GC columns or a GC  $\times$  GC system for a higher separation power.<sup>44,45</sup> By the use of other relevant wavelengths for REMPI other substances should be accessible. Moving to higher wavelengths, larger aromatic species are ionized more efficiently.<sup>37</sup> By an increase of the pulse frequency (femtosecond LASER) short-lived intermediate states of molecules are better stabilized and the sensitivity thus increases.<sup>46</sup>

## Acknowledgements

Leibniz-Gemeinschaft is acknowledged for financial support of the ATKiM project. A special thanks goes to S. Klingbeil for the development of tools for data analysis and I. Hand for the support by planning our cruise. Many thanks goes to V. Trommer for his constructive comments and opinions.

## References

- 1 T. S. Bianchi, The role of terrestrially derived organic carbon in the coastal ocean: a changing paradigm and the priming effect, *Proc. Natl. Acad. Sci. U. S. A.*, 2011, **108**(49), 19473–19481.
- 2 A. Nebbioso and A. Piccolo, Molecular characterization of dissolved organic matter (DOM): a critical review, *Anal. Bioanal. Chem.*, 2013, **405**(1), 109–124.
- 3 D. P. R. Herlemann, M. Manecki, C. Meeske, F. Pollehne, M. Labrenz, D. Schulz-Bull, T. Dittmar and K. Juergens, Uncoupling of bacterial and terrigenous dissolved organic matter dynamics in decomposition experiments, *PLoS One*, 2014, **9**(4), e93945.
- 4 V. Kisand, S. Gebhardt, J. Rullkotter and M. Simon, Significant bacterial transformation of riverine humic matter detected by pyrolysis GC-MS in serial chemostat experiments, *Mar. Chem.*, 2013, **149**, 23–31.
- 5 V. Kisand, D. Rocker and M. Simon, Significant decomposition of riverine humic-rich DOC by marine but not estuarine bacteria assessed in sequential chemostat experiments, *Aquat. Microb. Ecol.*, 2008, **53**, 151–160.
- 6 T. Dittmar and G. Kattner, The biogeochemistry of the river and shelf ecosystem of the Arctic Ocean: a review, *Mar. Chem.*, 2003, **83**(3–4), 103–120.
- 7 S. Opsahl and R. Benner, Photochemical reactivity of dissolved lignin in river and ocean waters, *Limnol. Oceanogr.*, 1998, **43**(6), 1297–1304.
- 8 D. Rocker, V. Kisand, B. Scholz-Böttcher, T. Kneib, A. Lemke, J. Rullkötter and M. Simon, Differential decomposition of humic acids by marine and estuarine bacterial communities at varying salinities, *Biogeochemistry*, 2012b, **111**(1–3), 331–346.
- 9 B. Rosenstock, W. Zwisler and M. Simon, Bacterial consumption of humic and non-humic low and high molecular weight DOM and the effect of solar irradiation on the turnover of labile DOM in the Southern Ocean, *Microb. Ecol.*, 2005, **50**(1), 90–101.
- 10 J. Wikner, R. Cuadros and M. Jansson, Differences in consumption of allochthonous DOC under limnic and



- estuarine conditions in a watershed, *Aquat. Microb. Ecol.*, 1999, **17**(3), 289–299.
- 11 P. J. Hernes and R. Benner, Terrigenous organic matter sources and reactivity in the North Atlantic Ocean and a comparison to the Arctic and Pacific oceans, *Mar. Chem.*, 2006, **100**(1–2), 66–79.
  - 12 E. B. Kujawinski, The impact of microbial metabolism on marine dissolved organic matter, *Annual Review of Marine Science*, 2011, **3**, 567–599.
  - 13 A. Miltner and K. C. Emeis, Terrestrial organic matter in surface sediments of the Baltic Sea, Northwest Europe, as determined by CuO oxidation, *Geochim. Cosmochim. Acta*, 2001, **65**(8), 1285–1299.
  - 14 D. Rocker, T. Brinkhoff, N. Gruener, M. Dogs and M. Simon, Composition of humic acid-degrading estuarine and marine bacterial communities, *FEMS Microbiol. Ecol.*, 2012, **80**(1), 45–63.
  - 15 C. Humborg, E. Smedberg, S. Blomqvist, C. M. Morth, J. Brink, L. Rahm, A. Danielsson and J. Sahlberg, Nutrient variations in boreal and subarctic Swedish rivers: landscape control of land-sea fluxes, *Limnol. Oceanogr.*, 2004, **49**(5), 1871–1883.
  - 16 J. R. Ertel, J. I. Hedges and E. M. Perdue, Lignin signature of aquatic humic substances, *Science*, 1984, **223**(4635), 485–487.
  - 17 R. L. Sleighter and P. G. Hatcher, Molecular characterization of dissolved organic matter (DOM) along a river to ocean transect of the lower Chesapeake Bay by ultrahigh resolution electrospray ionization Fourier transform ion cyclotron resonance mass spectrometry, *Mar. Chem.*, 2008, **110**(3–4), 140–152.
  - 18 S. Opsahl and R. Benner, Distribution and cycling of terrigenous dissolved organic matter in the ocean, *Nature*, 1997, **386**(6624), 480–482.
  - 19 R. M. W. Amon and H. P. Fitznar, Linkages among the bioreactivity, chemical composition, and diagenetic state of marine dissolved organic matter, *Limnol. Oceanogr.*, 2001, **46**(2), 287–297.
  - 20 T. Dittmar, H. P. Fitznar and G. Kattner, Origin and biogeochemical cycling of organic nitrogen in the Eastern Arctic ocean as evident from D- and L-amino acids, *Geochim. Cosmochim. Acta*, 2001, **65**(22), 4103–4114.
  - 21 J. I. Hedges and J. R. Ertel, Characterisation of lignin by gas capillary chromatography of cupric oxide oxidation-products, *Anal. Chem.*, 1982, **54**(2), 174–178.
  - 22 M. A. Goni and J. I. Hedges, Sources and reactivities of marine-derived organic-matter in coastal sediments as determined by alkaline CuO oxidation, *Geochim. Cosmochim. Acta*, 1995, **59**(14), 2965–2981.
  - 23 E. R. Sholkovitz, Flocculation of dissolved organic and inorganic matter during mixing of river water and sea water, *Geochim. Cosmochim. Acta*, 1976, **40**(7), 831–845.
  - 24 T. Dittmar, K. Whitehead, E. C. Minor and B. P. Koch, Tracing terrigenous dissolved organic matter and its photochemical decay in the ocean by using liquid chromatography/mass spectrometry, *Mar. Chem.*, 2007, **107**(3), 378–387.
  - 25 R. Benner and K. Kaiser, Biological and photochemical transformations of amino acids and lignin phenols in riverine dissolved organic matter, *Biogeochemistry*, 2011, **102**(1–3), 209–222.
  - 26 J. B. Fellman, R. G. M. Spencer, P. J. Hernes, R. T. Edwards, D. V. D'Amore and E. Hood, The impact of glacier runoff on the biodegradability and biochemical composition of terrigenous dissolved organic matter in near-shore marine ecosystems, *Mar. Chem.*, 2010, **121**(1–4), 112–122.
  - 27 F. Shiah and H. W. Ducklow, Multiscale variability in bacterioplankton abundance, production, and specific growth rate in a temperate salt-marsh tidal creek, *Limnol. Oceanogr.*, 1995, **40**(1), 55–66.
  - 28 L. D. Guo, D. M. White, C. Xu and P. H. Santschi, Chemical and isotopic composition of high-molecular-weight dissolved organic matter from the Mississippi River plume, *Mar. Chem.*, 2009, **114**(3–4), 63–71.
  - 29 K. J. Meyersschulte and J. I. Hedges, Molecular evidence for a terrestrial component of organic-matter dissolved in ocean water, *Nature*, 1986, **321**, 61–63.
  - 30 T. Dittmar, B. Koch, N. Hertkorn and G. Kattner, A simple and efficient method for the solid-phase extraction of dissolved organic matter (SPE-DOM) from seawater, *Limnol. Oceanogr.: Methods*, 2008, **6**, 230–235.
  - 31 H. R. Schulten and G. Gleixner, Analytical pyrolysis of humic substances and dissolved organic matter in aquatic systems: structure and origin, *Water Res.*, 1999, **33**(11), 2489–2498.
  - 32 J. D. H. van Heemst, J. C. del Rio, P. G. Hatcher and J. W. de Leeuw, Characterization of estuarine and fluvial dissolved organic matter by thermochemolysis using tetramethylammonium hydroxide, *Acta Hydrochim. Hydrobiol.*, 2000, **28**(2), 69–76.
  - 33 U. Boesl, H. J. Neusser and E. W. Schlag, Multiphoton ionization in the mass-spectrometry of polyaromatic-molecules-cross-sections, *Chem. Phys.*, 1981, **55**(2), 193–204.
  - 34 U. Boesl, Multiphoton excitation and mass selective ion detection for neutral and ion spectroscopy, *J. Phys. Chem.*, 1991, **95**(8), 2949–2962.
  - 35 R. Zimmermann, U. Boesl, C. Weickhardt, D. Lenoir, K. W. Schramm, A. Kettrup and E. W. Schlag, Isomer-selective ionization of chlorinated aromatics with LASERS for analytical time-of-flight mass-spectrometry – first results for polychlorinated dibenzo-p-dioxins (PCDD), biphenyls (PCB) and benzenes (PCBZ), *Chemosphere*, 1994, **29**(9–11), 1877–1888.
  - 36 A. Fendt, R. Geissler, T. Streibel, M. Sklorz and R. Zimmermann, Hyphenation of two simultaneously employed soft photo ionization mass spectrometers with thermal analysis of biomass and biochar, *Thermochim. Acta*, 2012, **551**, 155–163.
  - 37 O. P. Haefliger and R. Zenobi, Laser mass spectrometric analysis of polycyclic aromatic hydrocarbons with wide wavelength range laser multiphoton ionization spectroscopy, *Anal. Chem.*, 1998, **70**(13), 2660–2665.
  - 38 R. Zimmermann, C. Lermer, K. W. Schramm, A. Kettrup and U. Boesl, 3-Dimensional trace analysis-combination of gas-chromatography, supersonic beam UV spectroscopy and



- time-of-flight mass-spectrometry, *Eur. Mass Spectrom.*, 1995, **1**(4), 341–351.
- 39 S. Otto, T. Streibel, S. Erdmann, M. Sklorz, D. Schulz-Bull and R. Zimmermann, Application of pyrolysis-mass spectrometry and pyrolysis-gas chromatography-mass spectrometry with electron-ionization or resonance-enhanced-multi-photon ionization for characterization of crude oils, *Anal. Chim. Acta*, 2015, **855**, 60–69.
- 40 D. P. R. Herlemann, M. Labrenz, K. Juergens, S. Bertilsson, J. J. Waniek and A. F. Andersson, Transitions in bacterial communities along the 2000 km salinity gradient of the Baltic Sea, *ISME J.*, 2011, **5**(10), 1571–1579.
- 41 A. Fendt, T. Streibel, M. Sklorz, D. Richter, N. Dahmen and R. Zimmermann, On-Line Process Analysis of Biomass Flash Pyrolysis Gases Enabled by Soft Photoionization Mass Spectrometry, *Energy Fuels*, 2011, **26**(1), 701–711.
- 42 HELCOM, Report on Shipping Accidents in the Baltic Sea Area for the Year, 2010.
- 43 L. Hoikkala, P. Kortelainen, H. Soinne and H. Kuosa, Dissolved organic matter in the Baltic Sea, *J. Mar. Syst.*, 2015, **142**, 47–61.
- 44 M. S. Eschner, W. Welthagen, T. M. Groger, M. Gonin, K. Fuhrer and R. Zimmermann, Comprehensive multidimensional separation methods by hyphenation of single-photon ionization time-of-flight mass spectrometry (SPI-TOF-MS) with GC and GC  $\times$  GC, *Anal. Bioanal. Chem.*, 2010, **398**(3), 1435–1445.
- 45 W. Welthagen, S. Mitschke, F. Muhlberger and R. Zimmermann, One-dimensional and comprehensive two-dimensional gas chromatography coupled to soft photo ionization time-of-flight mass spectrometry: a two- and three-dimensional separation approach, *J. Chromatogr. A*, 2007, **1150**(1–2), 54–61.
- 46 A. Li, T. Imasaka and T. Uchimura, Analysis of pesticides by gas chromatography/multiphoton ionization/mass spectrometry using a femtosecond laser, *Anal. Chim. Acta*, 2011, **701**(1), 52–59.

## Publikation 3

Otto, S.; Streibel, T.; Erdmann, S.; Klingbeil, S.; Schulz-Bull, D.; Zimmermann, R., 2015. Pyrolysis-gas chromatography-mass spectrometry with electron-ionization or resonance-enhanced-multi-photon-ionization for characterization of polycyclic aromatic hydrocarbons in the Baltic Sea. *Marine Pollution Bulletin* 99: 35-42.  
(DOI:10.1016/j.marpolbul.2015.08.001)



# Pyrolysis–gas chromatography–mass spectrometry with electron-ionization or resonance-enhanced-multi-photon-ionization for characterization of polycyclic aromatic hydrocarbons in the Baltic Sea



Stefan Otto<sup>a</sup>, Thorsten Streibel<sup>a,b,\*</sup>, Sabrina Erdmann<sup>a</sup>, Sophie Klingbeil<sup>a</sup>, Detlef Schulz-Bull<sup>c</sup>, Ralf Zimmermann<sup>a,b</sup>

<sup>a</sup>Joint Mass Spectrometry Centre, Chair of Analytical Chemistry, Institute of Chemistry, University of Rostock, 18059 Rostock, Germany

<sup>b</sup>Joint Mass Spectrometry Centre, Cooperation Group Comprehensive Molecular Analytics, Institute of Ecological Chemistry, Helmholtz Zentrum München-German Research Center of Environmental Health (GmbH), Ingolstädter Landstrasse 1, 85764 Neuherberg, Germany

<sup>c</sup>Marine Chemistry, Leibniz Institute for Baltic Sea Research, Seestrasse 15, 18119 Warnemünde, Rostock, Germany

## ARTICLE INFO

### Article history:

Received 27 March 2015

Revised 31 July 2015

Accepted 2 August 2015

Available online 14 August 2015

### Keywords:

Baltic Sea

Dissolved organic matter

Mass spectrometry

Resonance-enhanced-multi-photon-ionization

Polycyclic aromatic hydrocarbons

Pyrolysis

## ABSTRACT

Polycyclic aromatic hydrocarbons (PAH), as a part of dissolved organic matter (DOM), are environmental pollutants of the marine compartment. This study investigates the origin of PAH, which is supposed to derive mainly from anthropogenic activities, and their alteration along the salinity gradient of the Baltic Sea. Pyrolysis in combination with gas chromatography and two mass selective detectors in one measurement cycle are utilized as a tool for an efficient trace analysis of such complex samples, by which it is possible to detect degradation products of high molecular structures. Along the north–south transect of the Baltic Sea a slightly rising trend for PAH is visible. Their concentration profiles correspond to the ship traffic as a known anthropogenic source, underlined by the value of special isomer ratios such as phenanthrene and anthracene (0.31–0.45) or pyrene and fluoranthene (0.44–0.53). The detection of naphthalene and the distribution of its alkylated representatives support this statement.

© 2015 Elsevier Ltd. All rights reserved.

## 1. Introduction

Aromatic compounds, especially polycyclic aromatic hydrocarbons (PAH) are widespread pollutants in various compartments of the environment (e.g. Baumard et al., 1999; Broman et al., 1991; Lipiatou et al., 1997; Witt, 1995). They can originate from anthropogenic sources as well as from natural processes (Neff, 1979) and have received increasing scientific interest during the last years (e.g. Motelay-Massei et al., 2006; Pazdro, 2004; Rogowska et al., 2010; Ruczyńska et al., 2011; Stader et al., 2013; Witt et al., 2009; Wu et al., 2011). PAH in the marine environment rapidly become associated with particulate matter (Chiou et al., 1998), due to their hydrophobic nature. They are poorly water soluble and in this context their detection by analytical systems is challenging. PAH can be a risk to human health (Ruczyńska et al., 2011) and especially the higher molecular-weight aromatics often act carcinogenic and mutagenic (Brody et al., 2007; Shor et al.,

2004). Together with their alkylated homologues they show persistence and are nearly resistant to biodegradation (Reunamo et al., 2013). As a general trend it can be observed that smaller PAHs exhibit better biodegradability than larger ones (Thiele-Bruhn and Brummer, 2005). Nevertheless, a high accumulation level of PAH compounds in the sediment (Neff, 1979) results and the global oceans constitutes a large sink for these contaminants (Wang et al., 2007).

PAHs are interacting with dissolved organic matter (DOM) constituents. DOM is defined as organic matter that passes a filter with a pore size near 1 µm including a wide range of constituents (Schwarzenbach et al., 2003). The structural characterization of high molecular PAH as associated DOM constituents, the understanding of its origin and its alteration while being transported to the oceans have hardly been researched yet. PAH can be formed and introduced into the marine environment by various processes, mostly caused by anthropogenic effects, as by-products of chemical processes such as incomplete combustion and pyrolysis of fossil fuel as well as the release into the environment by petroleum spilling or from ships (Pazdro, 2004; Witt, 1995). Natural processes such as oil seeps, plant debris and forest fires have an influence,

\* Corresponding author at: Joint Mass Spectrometry Centre, Chair of Analytical Chemistry, Institute of Chemistry, University of Rostock, 18059 Rostock, Germany.

E-mail address: [thorsten.streibel@uni-rostock.de](mailto:thorsten.streibel@uni-rostock.de) (T. Streibel).



too (Wu et al., 2011). In general, a distinction between pyrolytic, diagenetic and petrogenic origin is possible (Lubecki and Kowalewska, 2012).

It is difficult to distinguish between the different PAH sources. The molecular ratios of such compounds as anthracene (ANT) and phenanthrene (PHE) as well as fluoranthene (FLU) and pyrene (PYR) with mass-to-charge-ratios ( $m/z$ ) of 178 or 202, can provide useful information of the origin of PAH and have the best potential to distinguish between combustion and petroleum sources. For  $m/z$  178, an ANT to ANT plus PHE ratio  $<0.10$  usually is taken as an indicator for petroleum and a higher ratio than 0.10 indicates combustion processes (Yunker et al., 2002). Because of its thermodynamic stability petroleum often contains more PHE than ANT. With the FLU/(FLU + PYR)-value a source evaluation between petroleum, fossil fuel combustion or wood and coal combustion is feasible (Tam et al., 2001; Yunker et al., 2002). On the other hand naphthalene (NAP) is a reliable tracer for contamination by petroleum (Sporstol et al., 1983). In addition, alkyl homologue series of PAH with a maximum at  $C_1$  (monoalkylated) or substances with a higher degree of alkylation are indicator compounds for petroleum, too (Yunker et al., 2002).

The Baltic Sea is an ideal research object, covering a salinity gradient from 2 in the northern area to 25–32 in the southwest (Miltner and Emeis, 2001). Moreover, a large freshwater surplus, mainly from Scandinavian rivers, an only moderate water discharge via North Sea (removal processes) as well as industrial hot-spots strongly influence the distribution of PAH compounds. Due to the high residence time (Opsahl and Benner, 1997) its concentration is often 2–10 times higher than the concentration in the North Sea (Witt, 1995). In addition their semi-closed nature surrounded by well developed countries (variety of industry, modern agriculture and high traffic shipping areas) leads to a high environmental load (HELCOM, 2010a; Ruczynska et al., 2011). Riverine runoff and atmospheric input are the two most important vectors of transportation into the marine environments (Lipiatou et al., 1997; Motelay-Massei et al., 2006), whereby the highest concentrations are observed in coastal areas. In addition, a seasonal variation is known, with lowest PAH concentrations in summer and higher concentrations in late autumn (Witt, 1995).

It requires a high degree of resolution power and selectivity to analyze DOM, especially to detect the low concentrated PAH. A variety of analytical systems and methods are available for PAH characterization in water. Often chromatographic techniques such as high performance liquid chromatography (HPLC) in combination with fluorescence detection are used (Ruczynska et al., 2011; Witt, 1995). Gas chromatography (GC) in combination with mass spectrometry (MS) is widespread (e.g. Broman et al., 1991; Baumard et al., 1999). Only sample preconcentration and injection methods such as solid phase extraction (e.g. Witt et al., 2009; Wu et al., 2011) or soxhlet-extraction (Wang et al., 2007) do vary. For a further increase in selectivity and sensitivity for specific tracer molecules in complex samples LASER based methods in MS are indispensable (Li et al., 2010; Stader et al., 2013).

In this study, a chromatographic analysis followed by two different types of mass spectrometers, an electron ionization quadrupole MS (EI-QMS) and resonance-enhanced-multi-photon-ionization time-of-flight MS (REMPI-ToFMS) in combination with the pyrolysis technique was applied to characterize associated PAHs in DOM for the first time in this context. EI is a hard and universal method, by which the identification of compounds is possible through specific fragmentation patterns of the organic molecules, unfortunately it often results in a loss of molecular information. The lack of the molecular ion signal can be prevented by soft ionization techniques such as photo ionization (PI). One such PI technique is Resonance-Enhanced-Multi-Photon-Ionization (REMPI). Especially in combination with GC there are promising

developments in terms of selectivity and sensitivity for aromatic hydrocarbons (Fendt et al., 2012; Haeffliger and Zenobi, 1998; Imasaka, 2013; Li et al., 2010, 2011; Zimmermann et al., 1995). REMPI selectivity depends on the used photon wavelength as well as on the ionization energy threshold, since the molecules absorb two photons via an intermediate state (Boesl et al., 1981; Boesl, 1991; Mitschke et al., 2006; Zimmermann et al., 1994).

Under pyrolysis conditions high weight molecular species are indirectly accessible as fragments (e.g. regarding heavy crude oil components), which have rarely been analyzed yet. In combination with GC and two mass selective detectors in one measurement cycle, an universal (EI) as well as an aromatic fingerprint (REMPI) result. This system was already successfully applied by Otto et al. (2015a) for crude oil samples. Semi-quantitative compositional changes along the Baltic Sea transect from the north to the southwest by using NAP, FLO, PHE and PYR are described in the literature (Broman et al., 1991). An assignment to anthropogenic sources is possible. In addition, the here used extraction method (Dittmar et al., 2008) was tested for suitability to retain PAH components.

## 2. Material and methods

This study presents data on the occurrence and distribution of PAH in surface water samples from river Kalix (located in North Sweden) and the Baltic Sea. The river water was sampled during the spring flood in May 2011 (see Herlemann et al. (2014) for detailed information). Marine samples were taken from the Skagerrak (S1) to Bothnian Bay (At4) along salinity gradient (Fig. 1a), while a cruise with the research vessel Meteor (M87/3a) in May and June 2012. The sampling sites and collection methods are described in detail in Otto et al. (submitted for publication) and therefore only a brief description is presented here. Specific sampling dates, depths, salinities and temperatures are listed in Fig. 1b.

### 2.1. Sample preparation and extraction

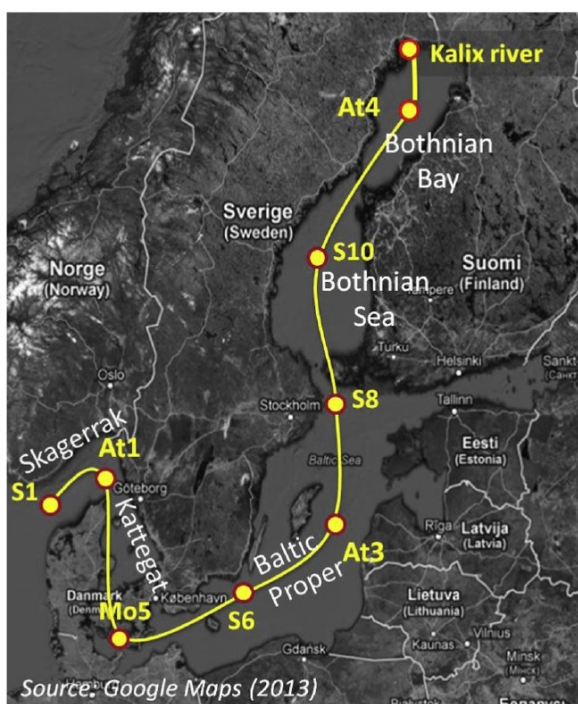
Each water sample was collected into a 1 l pre-cleaned glass bottle and separated into dissolved and particulate phase (using 400 °C for 6 h burned glass filters; Whatman, GF/F, diameter 47.0 mm, retention 0.7 µm). The filtered water did undergo a solid phase extraction (SPE) according to the protocol of Dittmar et al. (2008). The cartridges (reverse phase polymeric bond elute PPL cartridges; Agilent) were first conditioned with methanol followed by Milli-Q water acidified with HCl (37 %, Carl ROTH, Karlsruhe) to a pH of 2. One liter Baltic Sea water was extracted with a flow rate of  $\sim 30 \text{ mL min}^{-1}$  by using a vacuum pump. Afterwards the cartridges were washed with 12 mL Milli-Q water ( $\text{pH} = 2$ ) to remove salt residues. Immediately the adsorber material was dried under pure nitrogen and extracted with 6 mL methanol (ultra LC-MS, Carl ROTH, Karlsruhe). Afterwards the methanolic extract was stored at  $-20^\circ\text{C}$ . All glassware used was acid-washed (0.1 M HCl) and dried immediately at  $350^\circ\text{C}$  (except the Schott bottles) for 6 h.

### 2.2. Measurement system and sample injection

For the analysis, 2 mL of the methanolic extract were preconcentrated to approximately 60 µL under a stream of pure nitrogen. 10 µL were introduced via a quartz vessel in the pyrolysator system (Frontier Laboratories, Double-Shot-Pyrolyzer, model: PY-2020iD), resulting in about 1 mg of organic material. The pyrolyzer is mounted on a gas chromatograph (HP 5890 Series II), which was coupled to two mass spectrometers for simultaneous application of hard and soft ionization techniques.



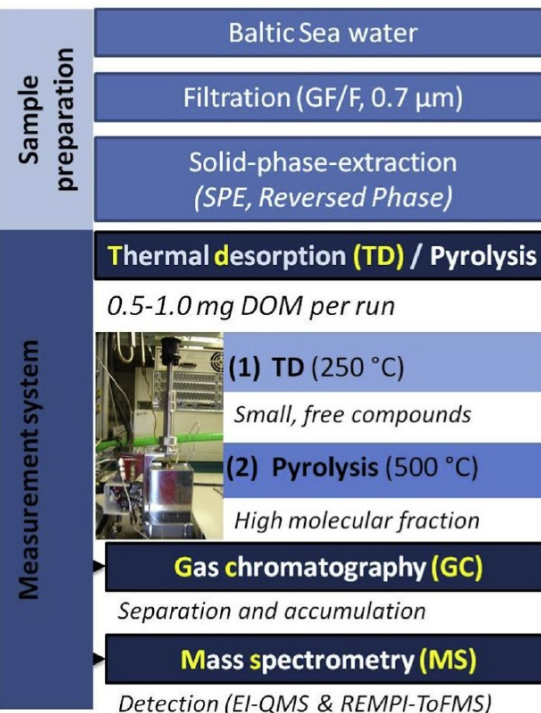
## (a) Line of salinity



## (b) Details for the salinity gradient

Station	Date of sampling	GPS-position		Depth [m]	Temperature [°C]	Salinity [PSU]
S1	2012-05-30	57 00.0995N	006 55.1060E	2.85	11.61	32.06
At1	2012-06-01	58 07.9991N	010 00.0005E	1.70	12.16	30.38
Mo5	2012-05-31	54 42.0068N	010 56.0121E	1.59	12.88	11.68
S6	2012-06-01	55 33.9834N	016 22.0539E	2.70	9.83	7.47
At3	2012-06-02	57 18.3467N	020 04.6968E	3.75	9.07	7.19
S8	2012-06-04	59 21.4864N	020 06.0728E	1.35	6.93	6.31
S10	2012-06-06	61 46.9808N	19 17.6021E	2.33	5.77	5.47
At4	2012-06-05	65 26.7066N	023 17.9074E	1.79	4.32	2.66

## (c) Measurement System



**Fig. 1.** (a) “Meteor” cruise route in summer 2012, with stations of sampling in the Baltic Sea. (b) Location sites in detail. (c) Overview diagram for sample preparation and measurement system.

For the conditioning of the system and the evaporation of the solvent, the sample was flushed with helium in the cooling zone of the pyrolyzer. Helium was also used as carrier gas, with a head pressure of 1 bar. At first the pyrolyzer oven heated up to 250 °C and the sample was pushed into the heating zone for one minute (desorption time). Immediately, a GC/MS measurement followed. Then, the same sample was introduced for a second time, after the oven heated up to 500 °C (pyrolysis step) and the GC/MS cycle started again.

The vaporized chemical compounds in the respective TD and pyrolysis step are separated by the coupled GC system (split mode 1:10; 30 m × 0.25 mm × 0.25 µm non-polar column, SGE-BPX-5). The column temperature was programmed for 60 °C (held for two minute) to 320 °C (held for 12 min) at a rate of 10 °C/min. After the separation process the gas flow was split by a deactivated press fit 3-way Y-Splitter for FS tubing (0.20–0.75 mm OD) and transferred simultaneously to both connected mass spectrometers. One MS system ionizes via EI, where mass fragments are generated in the positive EI mode with an electron voltage of 70 eV, followed by a quadrupole for separation. The total ion chromatograms (TIC) of EI-QMS are used to characterize compounds with the help of

different MS tools (NIST spectral library). If the data base information was inaccurate, standard substances NAP, PHE, PYR (Aldrich Chemistry) and FLO (Acro Organics) were chromatographed. Approximately 100 mg L<sup>-1</sup> substance were solved in a 1:1 mixture of dichloromethane and *n*-hexane (described in Otto et al., 2015a). For an aromatic fingerprint and an additional proof of relevant PAH compounds a [1+1]-REMPI-ToFMS system was used (Boesl et al., 1981; Boesl, 1991; Zimmermann et al., 1994). For generating REMPI, a Nd:YAG laser (BIG SKY ULTRA, Quantel, Les Uli Cedex, France) with two frequency doubling units yielding 266 nm photons was employed, which corresponds to a photon energy of 4.11 eV. The laser is operated with 10 ns pulse width and a 20 Hz repetition rate exhibiting a power density of approximately 7 × 10<sup>6</sup> W cm<sup>-2</sup>. A reflectron ToF-MS (Reflectron CTF10, Kaesdorf Geräte für Forschung und Industrie, Munich, Germany) is utilized for the detection of the molecular ions. More specific device parameters for the REMPI equipment are given in Fendt et al. (2012).

The split ratio after the chromatographic separation at the Y-splitter was 1:100 in favor of the EI-QMS. For calibration and optimization of the REMPI-ToFMS setup a gas standard (Linde



AG, Pullach, Germany) containing 1 ppm benzene, 1,2,4-trimethylbenzene, benzaldehyde and toluene in nitrogen was used.

### 3. Results and discussion

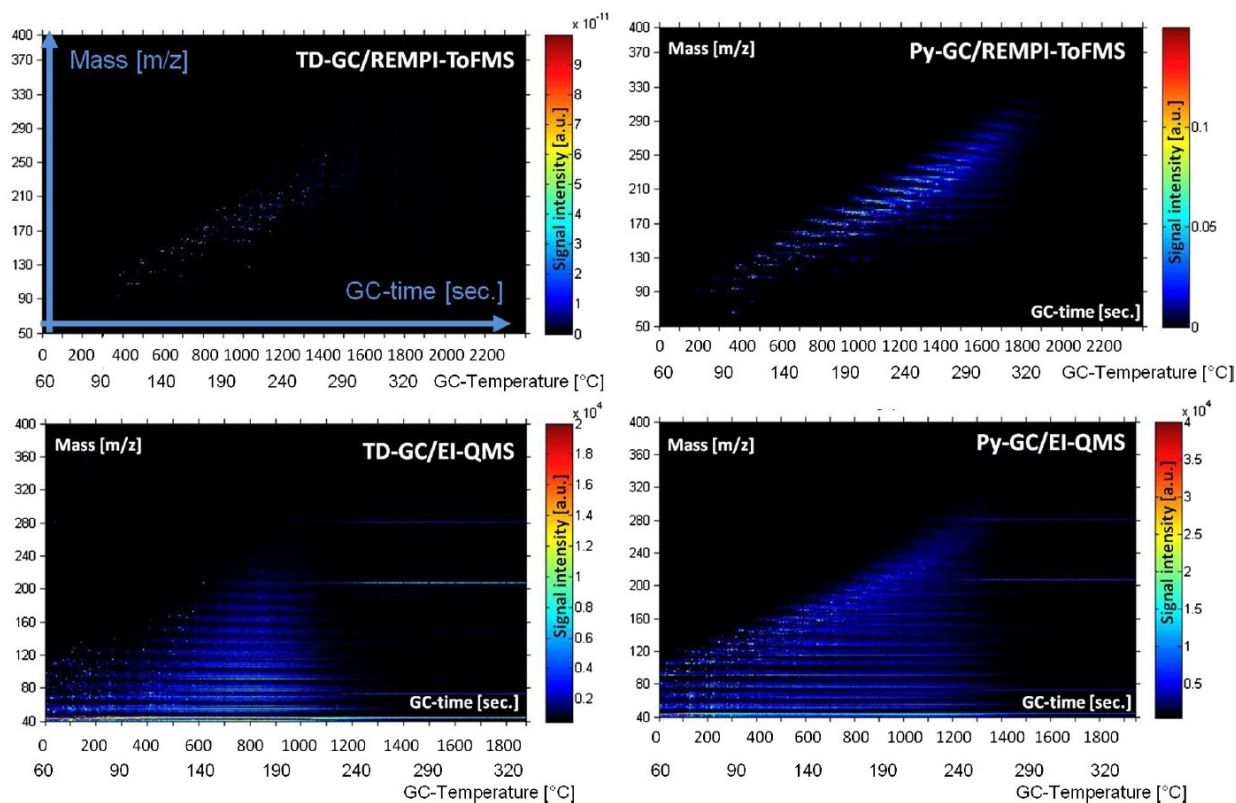
The high complexity of DOM is illustrated in Fig. 2 for the northernmost station At4. It allows a first overview through comparison between EI-QMS and REMPI-ToFMS (above and below) as well as TD and pyrolysis (left and right). The abscissa displays the retention time of the GC. Along the ordinate the  $m/z$  value is plotted. The respective intensity of the mass signal is depicted as color bar. The EI-substance spectrum is very complex and superimposed under TD and pyrolysis conditions. The compounds are detected in a mass range between  $m/z$  40 and 270 for TD. In the pyrolysis step the substance spectrum is expanded and higher signal intensities are visible, with an  $m/z$ -value of approximately 60 up to 320. The ion traces  $m/z$  73, 207 and 281 become more relevant as a permanent signal at higher GC temperatures (above 250 °C), because these represent siloxane fragments, originating from the column coating. Despite the high complexity of the sample, the EI data can provide reliable information about the structural composition. Furthermore, with regard to aromatic compounds and their alkylated representatives the REMPI-ToFMS data do assist, because the fragmentation is suppressed. It shows an aromatic fingerprint of the sample. A small range of substances is detected with high sensitivity and less complex chromatograms result. If one looks at the measurements under TD conditions in a time window of approximately 400 and 1200 s, with EI a cloud of non-delimitable signals is observed and with REMPI clear signals result. Generally in REMPI, under TD conditions, an aromatic substance spectrum is revealed in a mass range between  $m/z$  90 and 270. In the pyrolysis step a broader substance spectrum with higher signal

intensities between  $m/z$  60 and 330 is depicted. The aromatic substance spectrum increases significantly toward larger  $m/z$ -values, reflecting a growing number of alkylated species. Taking the At3 (central Baltic Sea) and At1 station (Skagerrak) into consideration (see supplemental material S1), a decrease in signal intensity under TD condition is obvious. Under pyrolysis condition no significant changes are visible.

In the following the semi-quantitative changes of PAH as function of industrial pollution hotspots, (HELCOM, 2014) roughly corresponding with the salinity gradient, is discussed on the basis of selected species: NAP [ $m/z$  128], FLO [ $m/z$  166], PHE [ $m/z$  178] and PYR [ $m/z$  202]. They were identified by standards and their GC profile is illustrated in Fig. 3a under pyrolysis conditions for the At4 station. These are the most dominant PAH compounds in previous studies (Tam et al., 2001).

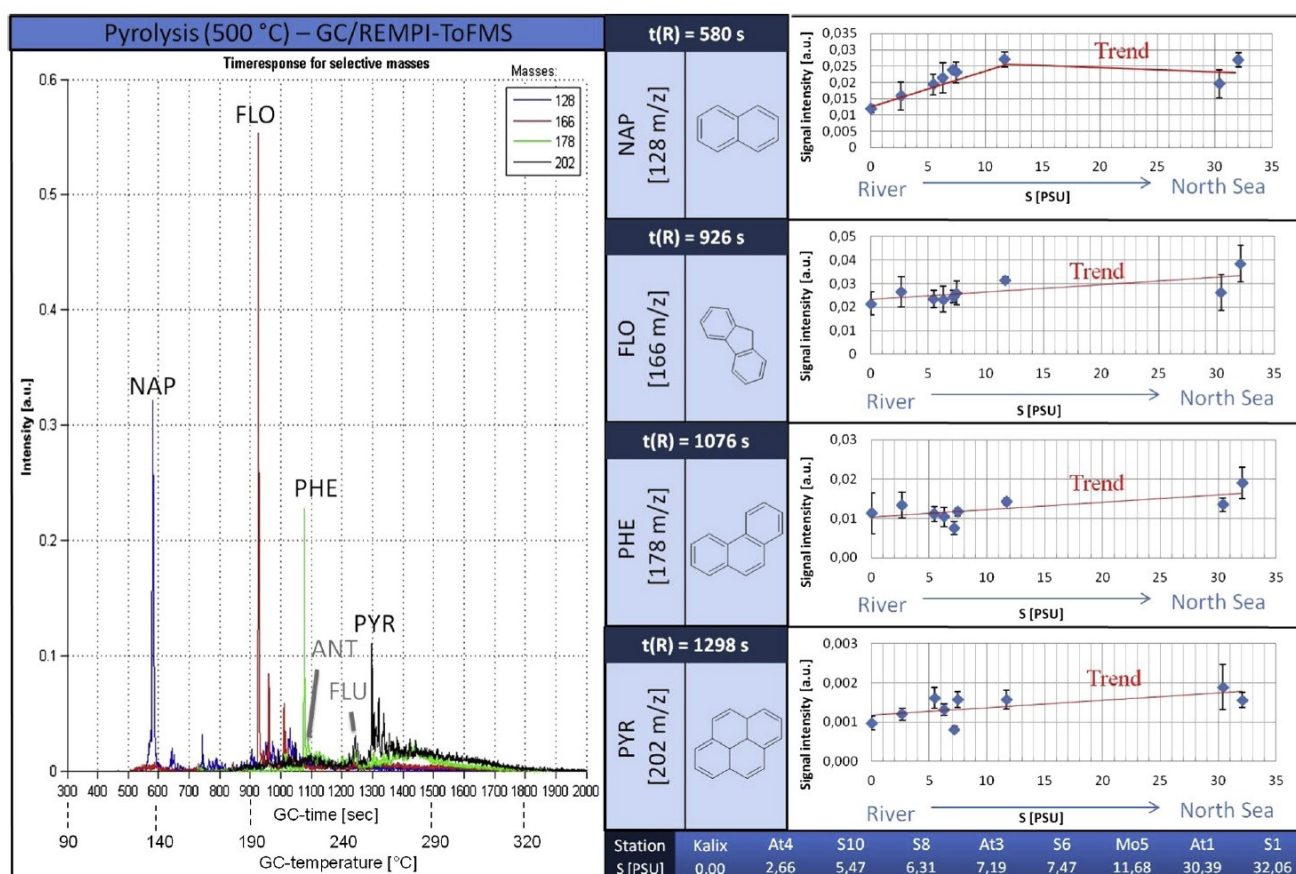
Generally, under TD conditions the detectable concentration decreases considerably with increasing salinity due to the dilution of North Sea inflow. In this context the low concentrations of dissolved PAH are challenging. In the pyrolysis step sufficient concentrations for every relevant PAH species are obtained to represent semi-quantitative statements along the Baltic Sea transect from the north to the southwestern station S1. The pyrolysis results are providing adequate peak intensities for all stations.

In different regions of the Baltic Sea different levels of contamination exist. The distribution of PAH is described by Broman et al. (1991). Some stations are almost analogous to the sampling sites described here (SB ~ S6, SA ~ S8, BS ~ S10, BB ~ At4). However, in this study the area of the Skagerrak and Kattegat, which is often neglected, was also taken into consideration. Near the North Sea inflow the salinity change in the surface water of the stations S1 (32 PSU) to Mo5 (12 PSU) and the freshwater inflow is extreme. It will likely have a strong influence on the DOM composition



**Fig. 2.** Direct comparison of the chromatograms resulting from the REMPI-ToFMS (above) and EI-QMS (below) detection for At4 station (Bothnian Bay). The TD step is shown on the left and the pyrolysis step on the right. On the ordinate the GC-time and -temperature is plotted. On the abscissa the mass-to-charge ratio is depicted. Graduated in color are the intensities. (For interpretation of the references to color in this figure legend, the reader is referred to the web version of this article.)





**Fig. 3.** (a) Chromatogram of At4 surface water samples under pyrolysis conditions, for the ion traces 128, 166, 178 and 202, resulting from the use of REMPI-ToFMS detection. In addition to NAP, FLO, PHE and PYR the time position of ANT and FLU is located in the REMPI-Chromatogram. (b) In the diagrams for the line of salinity the relative peak intensities are given vs. the salinity  $S$ . The latter of the respective stations is noted below.

and distribution, as it is well known for the sum parameter of DOM (Sholkovitz, 1976). The impact on the PAH composition is difficult to predict. The aqueous solubility of PAHs has been found to be dependent in most cases on the concentration and type of salt present in solution (Ni and Yalkowsky, 2003). Moreover the Baltic Sea is characterized by high ship traffic, which represents an anthropogenic source for PAH (HELCOM, 2010b).

For data analysis and to obtain particular semi-quantitative results, the peak intensities from the REMPI-chromatograms of the individual molecule ions are used for all stations from the river Kalix (lowest salinity) to the S1 station (highest salinity). Three technical replicates per station for each surface water sample were measured. The relative peak intensities were calculated and are illustrated in Fig. 3b. Therefore, the peak intensity of the REMPI chromatogram for the molecular ion was divided by the total intensities for all nominal masses (90–450  $m/z$ ) in a certain time window including the retention time. For NAP ( $m/z$  128,  $t(R)$  = 580 s) an increasing trend from the river mouth to the Mo5 station (southernmost point of sampling) is observed. After passing Mo5 to S1 station the trend is nearly constant. In general for FLO, PHE and PYR a stagnating to slightly rising trend along the salinity gradient, from the river inflow up to the North Sea is visible. This may be linked to increasing industrial pollution coming along with the gradient of salinity. Although considering pyrolysis fragments of higher aromatic structures in this work, the results show a good agreement to the publication of Broman et al. (1991), where the total concentrations of 11 unbonded PAH was summarized.

Under the assumption that the North Sea input constitutes no relevant source for the PAH components, a slight increase of the PAH content is visible. In the northern Baltic Sea the input of

terrestrial organic material by rivers is high (Humborg et al., 2004; Otto et al., submitted for publication), but the industrial development and shipping are low (HELCOM, 2014), explaining the low PAH content. In contrast, in the Baltic Proper and the North Sea channel, higher PAH concentrations are registered. The reason may be the increased ship traffic (HELCOM, 2010b), the higher number of industrialized cities as well as the rivers, partly contaminated by industrial waste, which drain into the southern Baltic Sea.

Linking main sources of PAH in different compartments (northern, central and south-western Baltic Sea) of the marine environment to natural processes and human activities is difficult. The anthropogenic PAH are classified as pyrolytic and petrogenic PAH (Wu et al., 2011). According to Tam et al. (2001) and Yunker et al. (2002) isomer ratios have a good potential to distinguish between natural and anthropogenic sources as well as pyrolytic and petrogenic anthropogenic sources. In this context the ANT/(ANT + PHE)-value and FLU/(FLU + PYR)-ratio were applied. The retention sequence was characterized by measurements of standard solutions. Additionally, the PAH retention indices of Lee (1979) support the evaluation for these substances. There are some selectivity rules that are exploited for peak assignment. The relative cross sections ( $\sigma_{rel}$ ) of ANT ( $\sigma_{rel}$  = 3.3) in comparison to toluene at the utilized wavelength of 266 nm is two orders of magnitude lower than for PHE ( $\sigma_{rel}$  = 178.9) displayed in Fig. 3a. The same applies to the ratio between FLU ( $\sigma_{rel}$  = 5.8) and PYR ( $\sigma_{rel}$  = 196.2) (Otto et al., 2015a). The resulting differences in ionization, in particular of ANT and FLU, are the reason why the EI chromatograms under pyrolysis conditions are used to calculate the isomer ratios. The formation and isomerisation of PAH, if they are released from



higher molecular structures or build up from smaller, chemically active components (e.g. radicals) under the selected reaction conditions (low pyrolysis temperature, exclusion of air, low pressure) is not probable and can be entirely excluded (Faix et al., 1990). The results for heavy crude oils support the statement, because under pyrolysis conditions next to PHE no peak for ANT was visible (Otto et al., 2015a).

In Kalix river and for At4 (northern Baltic Sea, Bothnian Bay) results an ANT/(ANT + PHE) value between 0.45 and 0.41 and for FLU/(FLU + PYR) a ratio of approximately 0.45 is visible. In the central Baltic (S8, At3) the values are constant by 0.41 or 0.44. Near the North Sea (Mo5, At1, S1) a slight decreasing trend to a value of 0.31 for ANT/(ANT + PHE) was achieved. This corresponds to Yunker et al. (2002) and Tam et al. (2001) suggesting pyrolytic sources over the whole salt gradient. In contrast the FLU/(FLU + PYR) value is nearly constant with a slightly increasing trend toward the North Sea. The range for the line of salinity is 0.4–0.5 and indicating incomplete fossil fuel combustion (Wu et al., 2011). The isomer ratios along the salinity gradient are presented in Fig. 4.

Alkylated PAH can also be used as indicator for an anthropogenic source (Wang et al., 2007). Especially, NAP and its homologues derive mainly from petrogenic inputs (Tam et al., 2001) and constitute a significant fraction of crude oils and petroleum products (Mullins et al., 2007; Otto et al., 2015a). Fig. 5 shows representatives of the NAP homologue row up to the fourth degree of alkylation under pyrolysis conditions. The REMPI-ToFMS chromatograms (right) are compared with the EI-QMS chromatograms (left) for relevant ion traces. On the abscissa the GC-time (-temperature) is plotted and on the y-axis the peak intensity is shown. In the EI chromatogram many peaks can be found on the ion track  $m/z$  128. Lots of them were only detected by the EI setup and can originate from compound fragmentation of e.g. alkanes. An

assignment is often not possible despite database matching due to the complexity of signals, which complicates the identification of components. In contrast the REMPI chromatogram for  $m/z$  128 is less complex. The dominant NAP peak is visible with a retention time of 580 s. The intensity of ion traces from the first and the second degree of alkylation are increased in both chromatograms. Afterwards for the third and fourth degree of alkylation the intensities decrease significantly, while the product variety is increasing continuously. Similar results are observed for the larger PAH FLO, PHE and PYR.

Using the REMPI setup, high peak intensities for PAH are detected for alkylated species up to the sixth degree of alkylation (Otto et al., 2015a). NAP and its alkylated representatives were found in the chromatograms resulting from the TD step (supplemental material S2), but with low signal intensities. The free evaporable PAH are barely present. Hence, the investigated organic material mainly consists of large molecular aromatic structures. Alkylated homologues of PAH with maxima at  $C_1$  and higher usually indicate mature organic matter or petroleum. For diesel and oil combustion the maxima shift to  $C_1$  and higher alkylation degrees (Yunker et al., 2002). For general combustion processes the maximum is mainly located at  $C_0$  (Sporstol et al., 1983). In combination with the previously calculated isomer ratios (ANT/PHE and FLU/PYR) a pyrolytic source by incomplete combustion of fossil fuel over the whole salt gradient is probable. This trend is increasing toward the southern and western Baltic Sea, which is in good agreement with the industrial development (HELCOM, 2014) and the more and more densifying shipping routes toward the North Sea (HELCOM, 2010b). The combustion and pyrolytic products of fuels, released into the atmosphere (Pazdro, 2004), are probably the dominant input for PAH to the aquatic environment (Motelay-Massei et al., 2006).

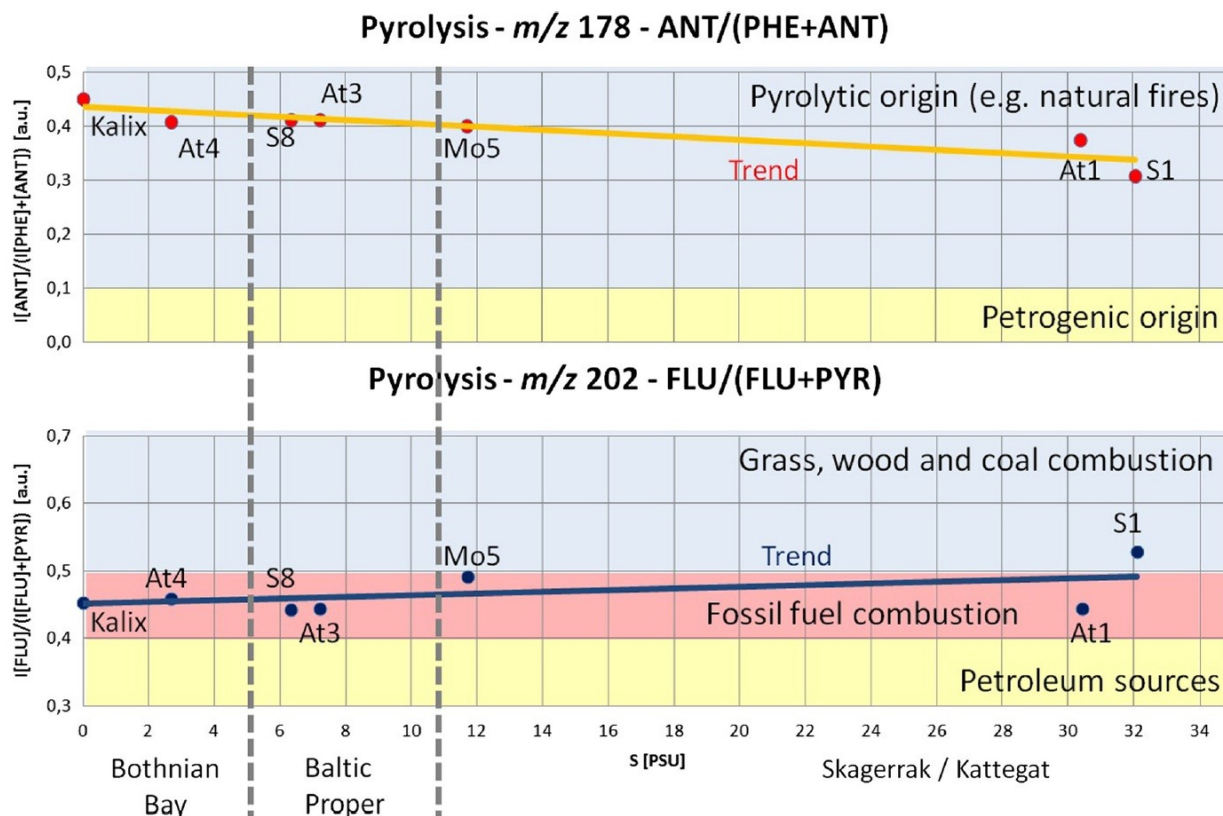


Fig. 4. The isomer ratios ANT/(PHE + ANT) and FLU/(PYR + FLU) are given (ordinate) along the transect (abscissa) of the Baltic Sea under pyrolysis conditions. Each colored area marks a specific source origin. This corresponds with the literature (Yunker et al., 2002; Tam et al., 2001). The trend curve is displayed for semi qualitative statement. (For interpretation of the references to color in this figure legend, the reader is referred to the web version of this article.)



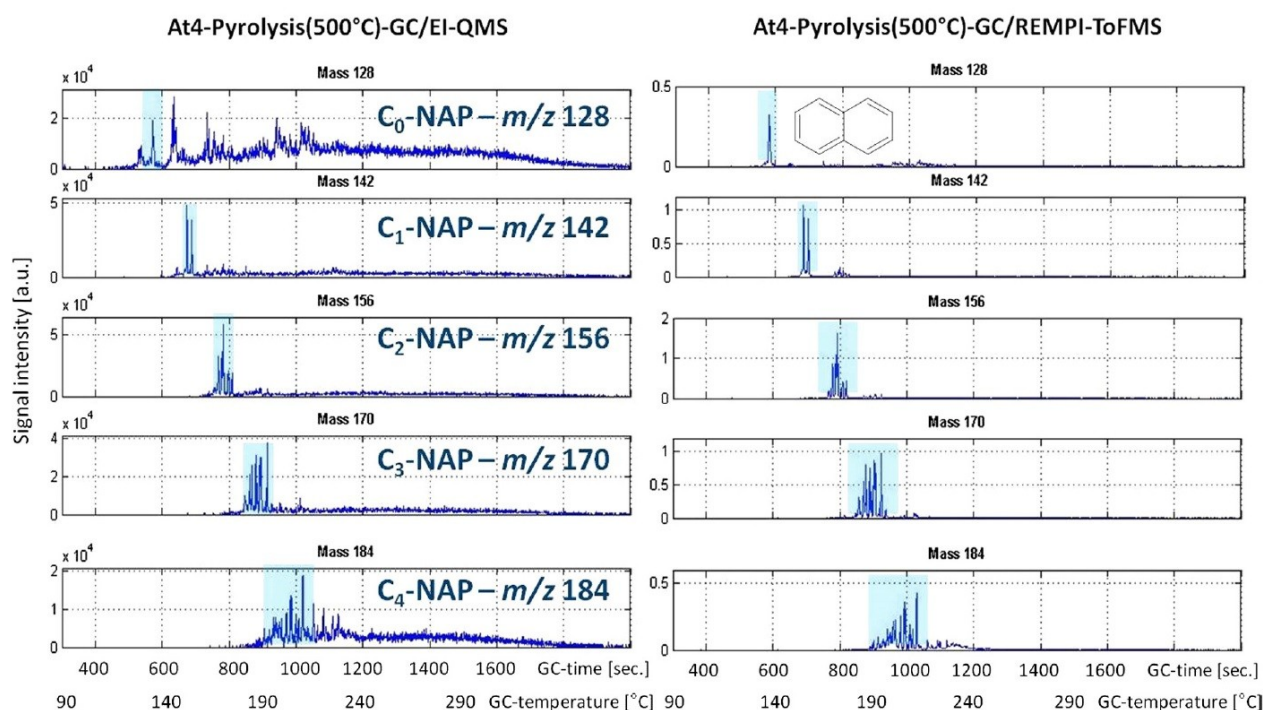


Fig. 5. NAP and its alkylated representatives ( $C_x$ ) up to the fourth degree of alkylation on the At4 station (Bothnian Bay). Direct comparison of the ion traces which result from EI-QMS (left) and REMPI-ToFMS (right) measurements under pyrolysis conditions. On the abscissa GC-time (parallel the GC temperature) and on the ordinate the peak intensity are plotted.

#### 4. Conclusion

The described Py-GC/MS method with two simultaneous measuring detection units allows an innovative chemical analysis of DOM, which was applied for the first time to investigate PAH compounds in aquatic environments. In addition to the TD step for analysis of the well-studied small PAH components (e.g. Baumard et al., 1999; Broman et al., 1991; Witt, 1995; Witt et al., 2009), a pyrolysis step is necessary to enable the detection of higher molecular degradation products. This field of research is largely unexplored and this study offers an opportunity to gain a first look at the topic.

Referring to the semi-quantitative measurements, a stagnating or slightly rising trend for selected PAH components along the Baltic Sea transect from the north to the southwestern area was visible. Corresponding to the concentration profiles of NAP, FLO, PHE and PYR, their distribution is contrary to the previously investigated lignin degradation products (Otto et al., submitted for publication). This could indicate an anthropogenic input by increasing shipping traffic. That is underlined by the ANT/(PHE + ANT)-value (0.31–0.45) as well as the FLU/(PYR + FLU)-value (0.44–0.53), which is indicative for a release of fossil fuels to the environment by incomplete combustion or pyrolytic processes. The detection of naphthalene and the distribution of its alkylated representatives also support this statement.

The riverine runoff and particularly the atmosphere are the two most important vectors of PAH transportation into the marine systems (Lipiatou et al., 1997; Motelay-Massei et al., 2006). To support this statement, future research should deal with the investigation of all marine environmental compartments of sediment, water and air. For one station in the Baltic Sea the sediment, water column and aerosol should be sampled at the same time. A direct comparison could help to understand exchange processes in more detail. In addition to DOM also the particulate matter should be investigated, because PAH do rapidly adsorb on particles (Neff, 1979). All these types of samples could be measured without time

consuming sample preparation by the presented TD/Py-GC-EI-QMS/REMPI-ToFMS system. The separation and a combination of an universal as well as a PAH selective and sensitive detection are useful for a closer look at the high molecular composition of natural samples.

The system could be optimized further by the application of GCxGC systems for a higher separation power (Eschner et al., 2010; Welthagen et al., 2007). Using other wavelengths or increasing LASER repetition frequency (Haeffliger and Zenobi, 1998; Li et al., 2011) could expand the substance spectrum and other compounds should be accessible. In summary, the obtained information such as size of aromatic structures, especially under pyrolysis conditions, provides a new access to the research topic of DOM.

#### Acknowledgments

Leibniz-Gemeinschaft is acknowledged for financial support of the ATKiM project. Special thanks go to V. Trommer for his constructive comments and opinions.

#### Appendix A. Supplementary material

Supplementary data associated with this article can be found, in the online version, at <http://dx.doi.org/10.1016/j.marpolbul.2015.08.001>.

#### References

- Baumard, P., Budzinski, H., Garrigues, P., Narbonne, J.F., Burgeot, T., Michel, X., Bellocq, J., 1999. Polycyclic aromatic hydrocarbon (PAH) burden of mussels (*Mytilus* sp.) in different marine environments in relation with sediment PAH contamination, and bioavailability. *Mar. Environ. Res.* 47 (5), 415–439.
- Boesl, U., 1991. Multiphoton excitation and mass selective ion detection for neutral and ion spectroscopy. *J. Phys. Chem.* 95 (8), 2949–2962.
- Boesl, U., Neusser, H.J., Schlag, E.W., 1981. Multiphoton ionization in the mass-spectrometry of polyaromatic-molecules-cross-sections. *Chem. Phys.* 55 (2), 193–204.



- Brody, J.G., Moysich, K.B., Humblet, O., Attfield, K.R., Beehler, G.P., Rudel, R.A., 2007. Environmental pollutants and breast cancer – epidemiologic studies. *Cancer* 109 (12), 2667–2711.
- Broman, D., Naf, C., Rolff, C., Zebuhr, Y., 1991. Occurrence and dynamics of polychlorinated dibenzo-para-dioxins and dibenzofurans and polycyclic aromatic-hydrocarbons in the mixed surface-layer of remote coastal and offshore waters of the Baltic. *Environ. Sci. Technol.* 25 (11), 1850–1864.
- Chiou, C.T., McGroddy, S.E., Kile, D.E., 1998. Partition characteristics of polycyclic aromatic hydrocarbons on soils and sediments. *Environ. Sci. Technol.* 32 (2), 264–269.
- Dittmar, T., Koch, B., Hertkorn, N., Kattner, G., 2008. A simple and efficient method for the solid-phase extraction of dissolved organic matter (SPE-DOM) from seawater. *Limnol. Oceanogr.-Methods* 6, 230–235.
- Eschner, M.S., Welthagen, W., Groger, T.M., Gonin, M., Fuhrer, K., Zimmermann, R., 2010. Comprehensive multidimensional separation methods by hyphenation of single-photon ionization time-of-flight mass spectrometry (SPI-TOF-MS) with GC and GCxGC. *Anal. Bioanal. Chem.* 398 (3), 1435–1445.
- Faix, O., Meier, D., Fortmann, I., 1990. Thermal-degradation products of wood – a collection of electron-impact (EI) mass-spectrometry of monomeric lignin derived products. *Holz als Roh- und Werkstoff* 48 (9), 351–354.
- Fendt, A., Geissler, R., Streibel, T., Sklorz, M., Zimmermann, R., 2012. Hyphenation of two simultaneously employed soft photo ionization mass spectrometers with thermal analysis of biomass and biochar. *Thermochim. Acta* 551, 155–163.
- Haefliger, O.P., Zenobi, R., 1998. Laser mass spectrometric analysis of polycyclic aromatic hydrocarbons with wide wavelength range laser multiphoton ionization spectroscopy. *Anal. Chem.* 70 (13), 2660–2665.
- Helcom, 2010a. Hazardous substances in the Baltic Sea: an integrated thematic assessment of hazardous substances in the Baltic Sea. *Baltic Sea Environ. Proc.* 120B, 1–116.
- HELCOM, 2010b. Report on Shipping Accidents in the Baltic Sea Area for the Year. HELCOM, 2014. List of JCP Hot Spots in the Baltic Sea Catchment Area.
- Herlemann, D.P.R. et al., 2014. Uncoupling of bacterial and terrigenous dissolved organic matter dynamics in decomposition experiments. *PLoS ONE* 9 (4), e93945.
- Humborg, C., Smedberg, E., Blomqvist, S., Mörtz, C.M., Brink, J., Rahm, L., Danielsson, S., Sahlberg, J., 2004. Nutrient variations in boreal and subarctic Swedish rivers: landscape control of land-sea fluxes. *Limnol. Oceanogr.* 49 (5), 1871–1883.
- Imasaka, T., 2013. Gas chromatography/multiphoton ionization/time-of-flight mass spectrometry using a femtosecond laser. *Anal. Bioanal. Chem.* 405 (22), 6907–6912.
- Lee, M.L., 1979. Retention indices for programmed-temperature capillary-column gas chromatography of polycyclic aromatic hydrocarbons. *Anal. Chem.* 51 (6), 768–774.
- Li, A., Uchimura, T., Tsukutani, H., Imasaka, T., 2010. Trace analysis of polycyclic aromatic hydrocarbons using gas chromatography-mass spectrometry based on nanosecond multiphoton ionization. *Anal. Sci.* 26 (8), 841–846.
- Li, A., Imasaka, T., Uchimura, T., 2011. Analysis of pesticides by gas chromatography/multiphoton ionization/mass spectrometry using a femtosecond laser. *Anal. Chim. Acta* 701 (1), 52–59.
- Lipiatou, E., Tolosa, I., Simó, R., Bouloubassi, I., Dachs, J., Marti, S., Sicre, M.-A., Bayona, J.M., Grimalt, J.O., Salot, A., Albaigés, J., 1997. Mass budget and dynamics of polycyclic aromatic hydrocarbons in the Mediterranean Sea. *Deep-Sea Res. Part II: Top. Stud. Oceanogr.* 44 (3–4), 881–905.
- Lubecki, L., Kowalewska, G., 2012. Indices of PAH origin – a case study of the Gulf of Gdansk (SE Baltic) sediments. *Polycyclic Aromat. Compd.* 32 (3), 335–363.
- Miltner, A., Emeis, K.C., 2001. Terrestrial organic matter in surface sediments of the Baltic Sea, Northwest Europe, as determined by CuO oxidation. *Geochim. Cosmochim. Acta* 65 (8), 1285–1299.
- Mitschke, S., Welthagen, W., Zimmermann, R., 2006. Comprehensive gas chromatography-time-of-flight mass spectrometry using soft and selective photoionization techniques. *Anal. Chem.* 78 (18), 6364–6375.
- Motelay-Massei, A., Garban, B., Tiphagne-larcher, K., Chevreuil, M., Ollivon, D., 2006. Mass balance for polycyclic aromatic hydrocarbons in the urban watershed of Le Havre (France): transport and fate of PAHs from the atmosphere to the outlet. *Water Res.* 40 (10), 1995–2006.
- Mullins, O.C., Sheu, E.Y., Hammami, A., Marshall, A.G., 2007. *Asphaltenes, Heavy Oils, and Petroeconomics*. Springer Science and Business Media, New York.
- Neff, J.M., 1979. *Polycyclic Aromatic Hydrocarbons in the Aquatic Environment*. Applied Science Publishers Ltd., London.
- Ni, N., Yalkowsky, S.H., 2003. Prediction of Setschenow constants. *Int. J. Pharm.* 254 (2), 167–172.
- Opsahl, S., Benner, R., 1997. Distribution and cycling of terrigenous dissolved organic matter in the ocean. *Nature* 386 (6624), 480–482.
- Otto, S., Streibel, T., Erdmann, S., Sklorz, M., Schulz-Bull, D., Zimmermann, R., 2015a. Application of pyrolysis-mass spectrometry and pyrolysis-gas chromatography-mass spectrometry with electron-ionization or resonance-enhanced-multi-photon-ionization for characterization of crude oils. *Anal. Chim. Acta* 855, 60–69.
- Otto, S., Erdmann, S., Streibel, T., Herlemann, D., Schulz-Bull, D., Zimmermann, R., 2015b. Pyrolysis-gas chromatography-mass spectrometry with electron-ionization or resonance-enhanced-multi-photon-ionization for characterization of terrestrial dissolved organic matter in the Baltic Sea. *Anal. Methods* (submitted for publication).
- Pazdro, K., 2004. Persistent organic pollutants in sediments from the Gulf of Gdansk. *Ann. Set Environ. Prot.* 6, 63–76.
- Reunamo, A., Riemann, L., Leskinen, P., Jorgensen, K.S., 2013. Dominant petroleum hydrocarbon-degrading bacteria in the Archipelago Sea in South-West Finland (Baltic Sea) belong to different taxonomic groups than hydrocarbon degraders in the oceans. *Mar. Pollut. Bull.* 72 (1), 174–180.
- Rogowska, J., Wolska, L., Namiesnik, J., 2010. Impacts of pollution derived from ship wrecks on the marine environment on the basis of s/s “Stuttgart” (Polish coast, Europe). *Sci. Total Environ.* 408 (23), 5775–5783.
- Ruczynska, W.M., Szlinder-Richert, J., Malesa-Ciecwierz, M., Warzocha, J., 2011. Assessment of PAH pollution in the southern Baltic Sea through the analysis of sediment, mussels and fish bile. *J. Environ. Monit.* 13 (9), 2535–2542.
- Schwarzenbach, R.P., Gschwend, P.M., Imboden, D.M., 2003. Sorption of natural compounds to “Dissolved” Organic Matter (DOM). *Environ. Org. Chem. (second edition)* 9 (4), 314–321.
- Sholkovitz, E.R., 1976. Flocculation of dissolved organic and inorganic matter during mixing of river water and sea water. *Geochim. Cosmochim. Acta* 40 (7), 831–845.
- Shor, L.M., Kosson, D.S., Rockne, K.J., Young, L.Y., Taghon, G.L., 2004. Combined effects of contaminant desorption and toxicity on risk from PAH contaminated sediments. *Risk Anal.* 24 (5), 1109–1120.
- Sporstol, S., Gjøs, N., Lichtenthaler, R.G., Gustavsen, K.O., Urdal, K., Orelid, F., Skel, J., 1983. Source identification of aromatic-hydrocarbons in sediments using GC/MS. *Environ. Sci. Technol.* 17 (5), 282–286.
- Stader, C., Beer, F.T., Achten, C., 2013. Environmental PAH analysis by gas chromatography-atmospheric pressure laser ionization-time-of-flight-mass spectrometry (GC-APLI-MS). *Anal. Bioanal. Chem.* 405 (22), 7041–7052.
- Tam, N.F.Y., Ke, L., Wang, X.H., Wong, Y.S., 2001. Contamination of polycyclic aromatic hydrocarbons in surface sediments of mangrove swamps. *Environ. Pollut.* 114 (2), 255–263.
- Thiele-Bruhn, S., Brummer, G.W., 2005. Kinetics of polycyclic aromatic hydrocarbon (PAH) degradation in long-term polluted soils during bioremediation. *Plant Soil* 275 (1–2), 31–42.
- Wang, J.Z., Guan, Y.F., Ni, H.G., Luo, X.L., Zeng, E.Y., 2007. Polycyclic aromatic hydrocarbons in riverine runoff of the pearl river delta (China): concentrations, fluxes, and fate. *Environ. Sci. Technol.* 41 (16), 5614–5619.
- Welthagen, W., Mitschke, S., Muhlberger, F., Zimmermann, R., 2007. One-dimensional and comprehensive two-dimensional gas chromatography coupled to soft photo ionization time-of-flight mass spectrometry: a two- and three-dimensional separation approach. *J. Chromatogr. A* 1150 (1–2), 54–61.
- Witt, G., 1995. Polycyclic aromatic hydrocarbons in water and sediment of the Baltic Sea. *Mar. Pollut. Bull.* 31 (4–12), 237–248.
- Witt, G., Liehr, G.A., Borck, D., Mayer, P., 2009. Matrix solid-phase microextraction for measuring freely dissolved concentrations and chemical activities of PAHs in sediment cores from the western Baltic Sea. *Chemosphere* 74 (4), 522–529.
- Wu, Y.-L., Wang, X.-H., Li, Y.-Y., Hong, H.-S., 2011. Occurrence of polycyclic aromatic hydrocarbons (PAHs) in seawater from the Western Taiwan Strait, China. *Mar. Pollut. Bull.* 63 (5–12), 459–463.
- Yunker, M.B., Macdonald, R.W., Vingarzan, R., Mitchell, R.H., Goyette, D., Sylvestre, S., 2002. PAHs in the Fraser River basin: a critical appraisal of PAH ratios as indicators of PAH source and composition. *Org. Geochem.* 33 (4), 489–515.
- Zimmermann, R., Boesl, U., Weickhardt, C., Lenoir, D., Schramm, K.W., Kettrup, A., Schlag, E.W., 1994. Isomer-selective ionization of chlorinated aromatics with LASERS for analytical Time-of-Flight mass-spectrometry – first results for polychlorinated dibenzo-p-dioxins (PCDD), biphenyls (PCB) and Benzenes (PCBZ). *Chemosphere* 29 (9–11), 1877–1888.
- Zimmermann, R., Lermer, C., Schramm, K.W., Kettrup, A., Boesl, U., 1995. 3-dimensional trace analysis-combination of gas-chromatography, supersonic beam UV spectroscopy and Time-of-Flight mass-spectrometry. *Eur. Mass Spectrom.* 1 (4), 341–351.

## V. Wissenschaftlicher Lebenslauf

### Persönliches:

Name: Stefan Otto

Geburtstag / -ort: 22. Februar 1983, Ostseebad Kühlungsborn

Staatsangehörigkeit: deutsch

### Berufserfahrung:

seit 06/15 Chemieingenieur / Leibniz Institut für Ostseeforschung Warnemünde, Abt. Meereschemie (Spurengase), Arbeitskreis Prof. Dr. G. Rehder

01/15 – 03/15 Wissenschaftlicher Mitarbeiter an der Universität Rostock / Institut für  
und Chemie, Abt. Analytische Chemie, Arbeitskreis Prof. Dr. R.  
10/09 – 03/14: Zimmermann

### Ausbildung:

10/2009 – heute: Promotionsstudium an der Universität Rostock / Institut für Chemie, Abt. Analytische Chemie, Arbeitskreis Prof. Dr. R. Zimmermann

10/2004 – 09/2009 Diplomstudiengang Chemie / Institut für Chemie / Universität Rostock (Diplom-Abschluss)

09/1999 – 06/2003 Heinrich-Schliemann-Gymnasium \ Neubukow

09/1993 – 08/1999 Verbundene Haupt- und Realschule \ Kröpelin



